ENCLOSURE 5
SPECIAL REPORT 04-02

FRAMATOME-ANP REPORT 51-5046570-01
"EXAMINATION OF DIABLO CANYON UNIT 1 STEAM GENERATOR TUBE NO. R20C54, FINAL REPORT, AUGUST 2004"

Examination of Diablo Canyon Unit 1 Steam Generator Tube No. R20C54

51-5046570-01
Final Report, August 2004

Prepared for Pacific Gas & Electric Company

AREVA

AREVA

ENGINEERING INFORMATION RECORD

Document Identifier 51 - 5046570 - 01

Title EXAMINATION OF DIABLO CANYON UNIT 1 STEAM GENERATOR TUBE NO. R20C54

PREPARED BY:		REVIEWED BY:	
Name	P.A. SHERBURNE	Name	C.E. MARTIN/JR.
Signature	[signature] Date 8/30/2004	Signature	[signature] Date 9/1/2004

Technical Manager Statement: Initials [initials]

Reviewer is Independent. L. S. Lamanna

Remarks:

Sections of steam generator (SG) tube no. R20C54 were removed from Diablo Canyon Power Plant Unit 1 (DCPP-1) during the 1R12 outage in April 2004. This tube was removed from SG 11 to meet the three-cycle frequency requirement of EPRI Report No. 1006255. Tube no. R20C54 had 3 eddy current (EC) indications representative of axially oriented OD stress corrosion cracks (ODSCC) at the 1st TSP (1H) intersection.

Laboratory examination of the pulled tube was subsequently conducted in support of NRC GL 95-05 requirements for voltage-based alternate repair criteria (ARC) for axial ODSCC. The primary objectives of the examination were the following:

- To physically characterize the tube degradation for correlation with field NDE results and to verify that the degradation morphology is consistent with the assumptions made in NRC GL 95-05.
- To determine the effect of degradation on the burst strength of the tubing and the leak rate under main steam line break (MSLB) conditions.

These examinations included receipt inspection and verification of identity, eddy current testing, dimensional measurements, ambient temperature leak rate and burst testing, visual and stereovisual inspections and photography, scanning electron microscopy (SEM) including energy dispersive spectroscopy (EDS) and wavelength dispersive spectroscopy (WDS), fractography, metallography, and tensile testing.

Results of the laboratory examinations are described in this report.

RECORD OF REVISION

DATE	REV.	SECTION	DESCRIPTION
8/03/2004	00	All	Original Release
8/30/2004	01	Footnote, p.13	The report date was corrected.
		Section 2.2, p.16	The +Point coil voltage for the largest indication was changed to 4.00V from 3.99V to be consistent with the value reported in the Framatome Data Management System (FDMS).
		Section 2.8, p.20	In the 2H TSP discussion, the axial extent of corrosion was changed from 0.86 inches to 0.795 inches to reflect axial length data adjusted for curvature of the burst fracture face.
		Section 2.9, p.21	Discussion was added to the paragraphs for R20C54-5B3 (2H TSP) to explain the curvature adjustment made to measured lengths for the axial corrosion profile. Reference 8 was added.
		Section 3, p.25	The summary of examinations was revised to reflect the use of adjusted corrosion length data for the 2H TSP corrosion profile.
		Section 4, p.27	Changed reference to Ref. 9 from Ref. 8.
		Section 5, p.28	Reference 8 (new) was added to the list of references.
		Table 3, p.30	FDMS data was added to Table 3.
		Table 13, p.37	A column for adjusted length data was added to Table 13.
		Figure 59, p.94	A note was added to qualify the measurements shown in the figure.
		Figure 76, p.105	Figure 76 was replaced with a new figure showing the depth of IGSCC plotted against adjusted axial distance.

Examination of Diablo Canyon Unit 1 Steam Generator Tube No. R20C54

51-5046570-01

Final Report, August 2004

Framatome ANP, Inc. • 155 Mill Ridge Road • Lynchburg, Virginia 24502-4341
434.832.3000 • www.framatech.com

Citations

This report was prepared by

Framatome ANP, Inc.
155 Mill Ridge Road
Lynchburg, Virginia 24502-4341

Principal Investigator
P. A. Sherburne, P.E.
Advisory Engineer

Examination of Diablo Canyon Unit 1 Steam Generator Tube No. R20C54, August 2004, Framatome ANP, Inc. Document No. 51-5046570-01.

Acknowledgements

The author would like to acknowledge and thank the following people for their significant contributions to this project: Jim Begley, Jeff Fleck, Mark Harris, B.J. Hefner, AC Martin, George Owen, Greg Pillow, Mike Pop, and Steve Jensen and Woody White of BWXT.

EXECUTIVE SUMMARY

Sections of steam generator (SG) tube no. R20C54 were removed from Diablo Canyon Power Plant Unit 1 (DCPP-1) during the 1R12 outage in April 2004. This tube was removed from SG 11 to meet the three-cycle frequency requirement of EPRI Report No. 1006255. Tube no. R20C54 had 3 eddy current (EC) indications representative of axially oriented OD stress corrosion cracks (ODSCC) at the 1st TSP (1H) intersection.

Laboratory examination of the pulled tube was subsequently conducted in support of NRC GL 95-05 requirements for voltage-based alternate repair criteria (ARC) for axial ODSCC. The primary objectives of the examination were the following:

- To physically characterize the tube degradation for correlation with field NDE results and to verify that the degradation morphology is consistent with the assumptions made in NRC GL 95-05.
- To determine the effect of degradation on the burst strength of the tubing and the leak rate under main steam line break (MSLB) conditions.

These examinations included receipt inspection and verification of identity, eddy current testing, dimensional measurements, ambient temperature leak rate and burst testing, visual and stereovisual inspections and photography, scanning electron microscopy (SEM) including energy dispersive spectroscopy (EDS) and wavelength dispersive spectroscopy (WDS), fractography, metallography, and tensile testing.

The laboratory examinations confirmed axial intergranular stress corrosion cracking (IGSCC) in the 1H TSP region of this tube. A through wall defect was present in the 1H TSP region as confirmed by leak rate testing and later by SEM fractography. The total axial extent and through wall extent of this defect were 0.70 and 0.12 inches, respectively. In addition, two smaller IGSCC cracks were present at other circumferential locations. The burst pressure for this section was 5,819 psi. The corresponding free span region without defects burst at 11,695 psi.

The burst pressure for the 2H TSP section was 10,428 psi. Post-burst inspection revealed two patches of intergranular corrosion that had not been detected during eddy current inspection prior to tube pull. These patches exhibited grid-like patterns of axial and circumferential cracks, dubbed by the industry as "cellular corrosion" by virtue of its appearance. Cellular corrosion is generally shallow and transitions to predominantly axial cracks as the cracking progresses. This behavior was confirmed in this examination by grinding radially through the two patches of corrosion. The maximum depth of the corrosion in the 2H burst region was found to be less than 48% through wall. A review of the eddy current data records confirmed that the corrosion was not detected by either the bobbin or rotating eddy current probes during the field inspection. On review, a small, single volumetric indication (SVI) was found in the post-pull rotating coil data.

SEM/EDS/WDS analysis revealed the presence of sulfur on the 2H burst rupture surface. Sulfur is known to be detrimental to Alloy 600 and has been previously implicated in intergranular corrosion.

Table of Contents

List of Tables

List of Figures

1 Introduction

1.1 Background

Diablo Canyon Power Plant Unit 1 (DCPP-1) is one of two pressurized water reactor plants operated by the Pacific Gas and Electric Company. Unit 1 is an 1125 MWe plant that went into commercial operation in May 1985. DCPP-1 has four Westinghouse Model 51 recirculating steam generators with 3388 U-tubes each. The tubing material is 7/8 inch OD mill annealed Alloy 600, with a nominal wall thickness of 0.050 inch. The tubes were initially roll expanded into the tubesheet several inches from the primary side. Before unit startup, the tubes were expanded along the full tubesheet depth using the WEXTEX explosive process to eliminate the tube to tubesheet crevice. The tubes are supported along their length by drilled-hole carbon steel tube support plates (TSP).

During the scheduled 1R12 outage in February 2004, sections of 1 tube – R20C54 - were removed from steam generator 11 to meet the three-cycle frequency requirement of EPRI Report No. 1006255. During inspection, this tube was found to have a field bobbin coil eddy current (EC) indication at the 1st TSP (1H) intersection. This indication was confirmed by rotating coil EC to be axially oriented OD stress corrosion cracking (ODSCC).

1.2 Examinations Performed

Laboratory examinations of the pulled tubes were conducted by Framatome ANP, Inc. (FANP) and by BWX Technologies, Inc. (BWXT) under contract to FANP, in support of NRC GL 95-05 requirements for voltage-based alternate repair criteria (ARC) for axial ODSCC. The primary objectives of the examinations were the following:

- To characterize tube degradation (i.e., morphology, size, and extent) for correlation with field NDE results and to verify that the degradation morphology is consistent with the assumptions made in NRC GL 95-05.
- To determine the effect of degradation on the burst strength of the tubing and the leak rate under main steam line break (MSLB) conditions.

These examinations included receipt inspection and verification of identity, eddy current testing, dimensional measurements, leak rate and burst testing, visual and stereovisual inspections and photography, scanning electron microscopy (SEM) including energy dispersive spectroscopy (EDS), fractography, metallography, and tensile testing. Data from these examinations[1] are summarized and discussed in this report.

[1]Destructive examination data included in this report is from the following document: *Examinations of Diablo Canyon Unit 1 Steam Generator Tube Sections from R20C54,* BWX Report No. 1140-031-04-12, August 2004.

1.3 Quality Assurance

All examinations were performed as Safety Related work in accordance with Framatome ANP QA Program and Quality Management Manual 56-5015885-02. This program meets the requirements of 10CFR50, Appendix B. A QA Data Package for this work will be maintained by FANP in accordance with applicable procedures.

2 Tube Failure Analysis

2.1 Receipt Visual Inspection

Sections of tube number R20C54 from Diablo Canyon SG 11 were received at the Framatome ANP (FANP) SERF-4 facility on Wednesday, May 5, 2004. The tube sections removed and their relative elevation in the steam generator are illustrated in Figure 1. Section (piece) numbers 3, 4, and 5, containing the 1H and 2H TSP locations and the free span tubing between these locations were unpacked, inspected, and prepared for testing. Results of the receipt inspection are documented in Reference 1 and are summarized in Table 1.

Figure 2 illustrates the typical as-received appearance of tube number R20C54 at the 1H TSP intersection. As can be seen in the photograph, the location at which the support plate contacted the tube is clearly visible from the remaining accumulation of deposits.

Note the almost complete absence of scale on the OD. With the exception of the TSP locations, the OD of all sections of R20C54 inspected was free of the scale normally found on pulled tubes. This is attributable to steam generator chemical cleaning operations conducted prior to tube removal. A small amount of deposit remains at the TSP locations; at the 2H TSP, the remaining deposit had the appearance of having been "packed", or compressed, in the tube to TSP crevice region.

In general, the OD of the tube was gun-metal grey in color, with axial patches and spots of copper colored oxide (Figure 2) present on all of the sections.

During the receipt inspection, an axial notch ~50% TW was placed on the OD at the bottom end of each tube section using a Dremel® tool and small cut-off wheel. In subsequent examinations, all field and laboratory axial positions are referenced from the bottom end of the tube sections and all angular orientations are referenced to the notch, with angles increasing in the clockwise (CW) direction looking at the bottom end of the tube.

2.2 Eddy Current Inspection

Following receipt inspection and prior to leak rate testing, tube sections R20C54-3 and R20C54-5 were inspected with bobbin coil and 3-coil rotating pancake coil (RPC). These inspections used a Zetec 0.720 inch diameter M/ULC bobbin coil and a Zetec 0.720-inch diameter Delta head 3-coil RPC containing a 0.115-inch diameter pancake coil, a +Point coil, and a 0.080-inch diameter high frequency pancake coil. Zetec ZAC/EddyNet 11i Patch 1.11 software was used for data acquisition and 11i Patch 1.9 software was used for data analysis. The Examination Technique Specification Sheets (ETSS's) in PG&E Procedure NDE ET-7 Rev. 4 were followed for all data acquisition and analysis. Complete details of the examinations, including graphics, can be found in Reference 2.

Results of the receipt eddy current inspection are summarized and compared with data from both the initial in-generator examination (pre tube pull) and the on-platform (post tube pull) examination in Tables 2 and 3. In Table 3, the angular orientation of the indication in degrees is included in the "Call" column as measured clockwise (CW) from the reference slit in the bottom of the tube section.

The following paragraphs discuss the results for each tube section inspected.

R20C54-3, 1H

The field bobbin coil inspection identified a 5.60 volt (V) DOS[2] indication approximately in the middle of the 1H TSP. The +Point coil identified three single axial indications (SAI) at this location, with the largest indication measured at 4.00V. Following tube pull, the bobbin voltage increased to 6.71V (on platform) and 6.83V (in lab). The rotating probe voltage increased to 4.61V (on platform) and 4.48V (in lab). These increases in voltage may have occurred as a result of ligament tearing between micro cracks and/or a change in the width of the crack following removal of the tube from the steam generator; i.e., the primary crack may have opened up slightly when no longer constrained by the TSP or deposits within the TSP. The largest SAI was estimated to be 88 to 91% through wall and positioned 19° from the reference notch. The two smaller SAI's were positioned 330° and 292° from the reference notch.

R20C54-5, 2H

A dent indication (DNT) was recorded with the bobbin coil during the in-generator, on platform, and lab inspections in approximately the middle of the 2H TSP; however, no degradation was noted with either the bobbin or rotating coils. The dent voltage decreased following tube pull, which may reflect removal of the influence of the tube support plate on the dent signal.

Although no degradation was initially reported, 2 patches of intergranular corrosion approximately 180° apart were visually observed within the 2H TSP region following burst testing (see Section 2.8 for details). The tube had burst within the patch of corrosion centered at ~30° from the reference notch. As a result, the eddy current data acquired prior to and following the tube pull was reviewed once again to determine if the intergranular corrosion was detectable. A careful review of the bobbin coil data revealed no indication of degradation other than the dent indication that was reported initially.

Review of the rotating coil data revealed a small volumetric indication only detectable after the tube section had been removed from the steam generator. The location of the volumetric indication was ~45° clockwise from the reference notch. To provide an estimate of its depth, a phase curve was set using the ASME standard drill holes. Only the data acquired in the lab included a

[2] A "DOS" indication is defined as a distorted support plate signal with a possible OD indication.

calibration using the ASME standard, so no depth is given in the table for the platform data.

Results of the data review are summarized in Table 4.

2.3 Leak Rate Testing

Room temperature leak rate testing was performed per EPRI guidelines[3] on the two sections of tubing containing the TSP intersections. The test setup used the Framatome ANP insitu pressure test system and consisted of a full length tool head locked into the bottom end of each sample as a water supply probe and a full length tool head locked into the top end of each tube as a vent and stopper probe.

Test pressures included 1750 psi (normal operating pressure corrected for temperature and gauge effects), 2250 psi (intermediate pressure), and 2750 psi (MSLB pressure corrected for gage effects and for the effect of temperature on material properties). The tests were conducted with approximately 2 minute hold periods at each of these pressures. Results of the leak test are summarized in Table 5.

The test pressure and leak rate versus time (time in seconds) results for tube section R20C54-3 are shown in Figure 3. Tube section R20C54-5 (2H TSP) did not leak at any of the pressure differentials tested. Tube section R20C54-3 (1H TSP) developed a small leak at the highest pressure tested. The maximum leak rate recorded during the 5 minute hold period was ~0.002 gpm. After ~2 minutes, the leakage decreased first to ~0.001 gpm and then to less than detectable (<0.001 gpm). Although deionized water was used in the tests to minimize the potential for particles in the water, it's possible that particulates in the pulled tube test specimen may have deposited within the crack.

Complete details of the leak rate tests can be found in Reference 4.

Following leak rate testing, the tube sections were reexamined visually and Section R20C54-3 (1H TSP) was subjected to repeat eddy current inspection with the 3-coil rotating probe. The eddy current inspection results before and after leak rate testing for this section are summarized in Table 6. Line by line phase angle sizing comparisons for the field (in-generator and on-platform), the lab receipt (pre leak rate test), and the post leak rate test eddy current inspections are shown in Figures 4 through 6 for the 3 single axial indications. Note that the indicated flaw lengths increased for the primary defects following leak rate testing.

2.4 Furnace Oxidation

Because only the 1H intersection leaked and thus may have experienced ligament tearing during the leak rate test, Section R20C54-3 (1H TSP) was placed in an atmospheric furnace and held at 900°F for 1 hour to heat tint/oxidize any torn ligaments. The objective was to allow any tearing that occurred during leak rate testing to be distinguished from tearing that would occur later during burst testing. The time and minimum temperature required to oxidize the ligaments were selected based on a qualification test program carried out in advance of the leak rate testing.[5] Figure 7 is a photograph of tube no. R20C54-3 at ~19° rotation taken following the oxidation step. As expected, the magnetite scale took on a burnished color as a result of oxidation. Note that at this magnification, the suspected ODSCC defect at the ~19° orientation is visible.

2.5 Post Oxidation Inspections

Low magnification photographs were taken at 45° intervals at the TSP regions on both tubes to document their overall condition following the leak rate testing and furnace oxidation. These photographs are provided in Figures 8 - 23. The bottom end of each tube segment is always positioned to the left in these photographs.

A photo mosaic of the axial crack that was detected by eddy current testing at ~19° on 1H is presented in Figure 24. It was visible from ~0.2 inches to ~0.6 inches from the bottom of the TSP region (after burst testing, the actual length was determined to be 0.7 inches, beginning at the bottom of the TSP region). Possible cracks were also visible near ~285°, extending from ~0.3 inches to ~0.4 inches from the bottom of the TSP, as shown in Figure 25. These may correspond to the eddy current indication (SAI #3) identified at 292°. No visible cracks were found that could be attributed to the eddy current indication (SAI #2) at 330°.

No visible evidence of corrosion was found in the 2H TSP region.

2.6 Sectioning Diagrams

Detailed sectioning diagrams for all of the tube sections examined are provided in Figures 26 - 31. The secondary defect locations indicated by eddy current testing are shown in Figure 27.

In the following discussions of test results, reference will be made to specific tube sections as defined in these diagrams.

2.7 Burst Testing

Sections containing the 1H (R20C54-3B) and 2H (R20C54-5B) TSP regions were subjected to burst testing at room temperature in accordance with EPRI guidelines for leak and burst testing[6], along with a free span region from Section R20C54-4. In addition, a control sample of virgin tubing was tested for baseline purposes. The burst tests were performed simulating free span conditions with no supports enveloping the tube segments. Silicon plastic bladders were used in all the samples, and 0.006" thick brass shim was used at the 1H defect location in accordance with the EPRI guidelines. These guidelines also stipulate a pressurization rate of 20 - 500 psi/sec, as measured between ~2,000 psi and ~6,000 psi (prior to yield), or up to the point of rupture in the case of the defect specimens. During these tests, the pressurization rates ranged from 602 to 772 psi/second. The higher pressurization rate is not believed to have affected the test results, since previous guidelines[7] had stipulated a pressurization rate of 200 – 2000 psi/sec, and hence these higher pressurization rates are consistent with earlier test guidelines and results.

Burst test results are summarized in Table 7. Dimensional measurements required by the EPRI guidelines are provided in Tables 8 - 11. All fish mouth burst openings were axially oriented. Specimen R20C54-3B, which contained the 1H TSP, burst at 5,819 psi. Specimen R20C54-5B, which contained the 2H TSP, burst at 10,428 psi. Specimen R20C54-4B, which was the free span section, burst at 11,695 psi. The tube control sample, from heat #754225, burst at 10,145 psi.

2.8 Macro Photography/Stereovisual Examinations of Post-burst Regions

Following burst testing, visual inspections were performed at low magnification to characterize the burst ruptures and associated areas of interest. Low magnification photographs were taken at 45° intervals in the TSP regions, and of the burst opening on the free span section of tubing. Photographs were taken of additional selected areas during the stereovisual examinations of these tube sections as described in the following paragraphs. The bottom end of each tube segment is always to the left in these photographs.

R20C54-3B (1H TSP)

Macro photographs of this tube section in 45° intervals are provided in Figures 32 - 39, and a similar photograph centered over the fish mouth opening at 19° is provided in Figure 40. Higher magnification photographs of the counter clockwise (CCW) and clockwise (CW) burst rupture surfaces, showing the oxidized intergranular corrosion areas, are provided in Figures 41 and 42. The burst region was located at approximately 19°, with the bottommost extent of the oxidized defect region near the bottom of the TSP. SEM fractography (Section 2.9) later revealed a total axial extent of ~0.7 inches and a length of ~0.12 inches where the defect was 100% through wall.

A secondary crack was located at ~350°, parallel to the burst rupture, which extended from ~0.1 inches to ~0.2 inches from the bottom of the TSP. This can be seen in Figure 43. Additional secondary cracks were located at ~355°, also parallel to the burst rupture, and which extended from ~0.5 inches to ~0.7 inches from the bottom of the TSP. These can be seen in Figure 44.

R20C54-4B (Free Span)

The fish mouth rupture on (nondefect) free span specimen R20C54-4B occurred near 350°. A photograph of the burst rupture is provided in Figure 45. As described in Section 2.9, SEM fractography verified that the failure was completely ductile, with no IGSCC present.

R20C54-5B (2H TSP)

Macro photographs of this tube section in 45° intervals are provided in Figures 46 - 53, and a similar photograph centered over the fish mouth opening at 30° is provided in Figure 54. Higher magnification photographs of the CCW and CW burst rupture surfaces are provided in Figures 55 through 58. This sample was not oxidized in the furnace since it did not leak during leak rate testing. The burst region was at approximately 30°, and was contained within an area of intergranular corrosion which extended from ~0° to 90°, as shown in the schematic drawing in Figure 59. A separate area of intergranular corrosion, which is also shown in the schematic drawing in Figure 59, extended from ~235° to ~305°. From the macro photographs, it is apparent that the intergranular corrosion extended above the 0.75-inch long TSP intersection in the region from 0° to 90°. This was later confirmed by SEM fractography (Section 2.9), which revealed a total preburst axial extent of corrosion of ~0.795 inches along the burst rupture surface. This observation suggests that a small sludge pile or accumulation of deposits may have been present on top of the 2H TSP in this location from 0° to 90° during some period in time.

The intergranular corrosion in the 235° to 305° region appears to be contained within the 0.75-inch long TSP contact region.

2.9 SEM Fractography

Standard internal distance calibrations on the SEM are routinely performed at 1000X. To ensure that these calibrations were still valid at the 50X range used to obtain the photo mosaics, a section of metallic ruler that could be placed in the SEM was photographed adjacent to a calibrated stage micrometer used on the metallograph. Comparisons between the calibrated stage micrometer, the section of ruler, and the internal SEM calibrations, provided traceability and indicated that the measurements were accurate to ±1% (±0.0005 inches for a 0.050 inch nominal wall thickness).

R20C54-3B2 (1H TSP)

Low magnification photo mosaics of the counterclockwise (CCW) fracture surface from R20C54-3B2 are provided in Figure 60 (rotated 180° to keep axial bottom to the left in this report). The secondary electron (SE) image provides the best topographical information, whereas the backscattered electron (BSE) image provides information on material density (less dense materials, such as oxides and plastic bladder material, show up darker).

Higher magnification photographs typifying the areas at the bottom, center, and top of the fracture surface are provided in Figures 61 - 67 (rotated 180° to keep the axial bottom to the left throughout this report). The actual depth measurements of intergranular corrosion were obtained from photographs such as these. This data is tabulated in Table 12. The starting point for these measurements was at the bottom edge of the IGSCC, and axial lengths were measured at the mid-wall of the tubing. Based upon these measurements, the total axial extent of the intergranular corrosion was 0.7 inches, with 100% through wall cracking (>0.052 inches) extending over an axial extent of 0.12 inches. A plot of the depth of intergranular corrosion is provided in Figure 68a. No oxidized ductile tear regions, which would have indicated tearing during the leak test, were identified. Comparison of the measured crack depth profile vs. the post-leak rate test RPC data is shown in Figure 68b. The measured crack depths were normalized using a nominal wall thickness of 0.052 inches.

R20C54-5B3 (2H TSP)

Low magnification photo mosaics of the clockwise (CW) fracture surface from R20C54-5B3 are provided in Figure 69.

Higher magnification photographs typifying the areas at the bottom, center, and top of the fracture surface are provided in Figures 70 - 75. The actual depth measurements of intergranular corrosion along the fracture surface were obtained from similar photographs, and this data is tabulated in Table 13. The starting point for these measurements was at the bottom edge of the corrosion, and axial lengths were measured at the mid-wall of the tubing. Based upon these measurements, the total axial extent of the intergranular corrosion was 0.86 inches, and the maximum depth was 0.0239 inches (46% TW based on a 0.052-inch nominal wall thickness). Since the non-corroded portion of the tube wall experienced significant thinning and axial strain prior to burst, the axial extent of corrosion as measured along the fracture face was greater than the pre-burst length. The measured axial positions were adjusted in Reference 8 to account for this effect. The adjusted cumulative lengths are tabulated in Table 13 and the depth of the intergranular corrosion is plotted against these values in Figure 76 to illustrate the actual corrosion profile. As can be seen in the table and in Figure 76, the adjusted overall extent of intergranular corrosion is 0.795 inches, approximately 0.045 inches beyond the uppermost edge of the 2H TSP. The location of the deepest corrosion is between 0.679 and 0.735 inches from the bottom edge of the 2H TSP and therefore contained within the 2H TSP thickness.

R20C54-4B (Free span)

Secondary electron images showing the lack of corrosion in the free span burst sample are provided in Figures 77 and 78.

2.10 EDS/WDS Analyses

R20C54-5B3 (2H TSP Region)

Areas on the burst rupture surface of R20C54-5B3 (2H TSP) were examined using energy dispersive spectroscopy (EDS) to look for the presence of detrimental elements that may have contributed to the intergranular corrosion. This sample was selected since it had not been subjected to high-temperature oxidation in the furnace (the 1H TSP region was oxidized in this manner). Sulfur, silica, and potassium were detected on the fracture surface as shown in the EDS spectrum in Figure 79. The presence of sulfur was confirmed and trace levels of magnesium and lead were also indicated by wavelength dispersive spectroscopy (WDS) analysis.

Copper Colored Deposits in Free span Areas

Copper colored deposits were visible on some areas of the tubing OD in the free span areas. A typical example is shown in Figure 80. EDS analysis was performed to identify this material, and as shown in Figure 81, it was composed of aluminum, zinc, and oxygen. Neither copper metal nor copper oxides were detected.

2.11 Defect Metallography

Transverse Metallographic Cross-Sections

Transverse metallographic cross-sections were prepared through two areas of the 1H TSP, corresponding to the axial locations of the secondary eddy current indications (SAI #2 and SAI #3 in Figure 27). The first of these (SAI #3) was at the approximate axial centerline of the TSP at 292°, and the second (SAI #2) was approximately 0.1 inches above the axial centerline of the TSP at 330°. These transverse metallographic cross-sections provided information on the extent and depth of IGSCC around the circumference of the tube away from the actual burst region. Serial grinding was not performed on these samples, so the maximum depth of IGSCC observed does not necessarily reflect the actual maximum depth indicated by eddy current testing.

R20C54-3B2B1 (1H TSP centerline)

Figure 82 is a polished cross-section showing a 53% through wall secondary crack at 298° that corresponds to the approximate location of eddy current indication SAI #3 (at 292°). The intergranular nature of the cracking is apparent in the etched photomicrograph of the same area in Figure 83. A number of other axial intergranular penetrations were noted around the circumference of the tube at this location, and these are tabulated in Table 18.

R20C54-3B2B2 (1H TSP centerline + 0.1 inch)

Figure 84 is a polished cross-section showing a 40% through wall secondary crack at 330° that corresponds to the approximate location of a secondary eddy current indication at 330° (SAI #2). The intergranular nature of the cracking is apparent in the etched photomicrograph of the same area in Figure 85. A number of other axial intergranular penetrations were noted around the circumference of the tube at this location, and these are tabulated in Table 19. It should be noted that several relatively deep cracks (47% to 65% TW) were located on both sides of the primary crack (burst rupture) at 19°.

Radial Grinding

Serial grinding was performed normal to the tube surface (radially) on mounted specimens taken from the 2H TSP region to better characterize the two regions of intergranular corrosion (see Figures 31 and 59 for locations). Each metallographic sample was flattened in a vise prior to mounting so that the ground surface would be parallel to the flattened tube surface. Following each incremental grind, the specimens were polished and photographed using the backscattered electron imaging mode on the scanning electron microscope. Serial grinding continued in ~0.005 inch increments until all evidence of intergranular corrosion was no longer present. The depth of each polished face from the OD surface is provided in Table 14.

These areas of corrosion exhibited grid-like patterns of OD axial and circumferential cracks. By virtue of its appearance, the industry has dubbed this type of degradation as "cellular corrosion". Cellular corrosion is generally shallow and transitions to predominantly axial cracks as the cracking progresses inward from the OD. As can be seen in the photographs discussed below, this behavior was observed during the radial grinding.

R20C54-5B3BB1 (2H TSP)

Sample 5B3B1 consisted of the region immediately clockwise from the burst rupture, extending from approximately 30° to 45°. SEM fractography previously characterized the burst rupture surface along the edge of this sample. Intergranular corrosion was present through the fourth grind (0.022" from the OD), but none was present on the polished face after the fifth grind (0.028"). This is consistent with the maximum depth of 0.024" measured from SEM fractography on the burst rupture surface. Overall photo mosaics of each polished face, along with higher magnification photographs showing details of the intergranular corrosion, are provided in Figures 86 through 99.

R20C54-5B3B2A (2H TSP)

Sample 5B3B2A extended circumferentially from approximately 45° to 120°. A corroded area was present near the upper portion of the 2H TSP (~0.6" to ~0.9" from the bottom of the TSP), in the area from ~45° to 80°. A second corroded area was present in the bottom portion of the TSP (0.0" to ~0.5" from the bottom of the TSP), in the area from ~45° to ~90°. These two areas were photographed separately. Intergranular corrosion was present through the fifth grind (0.028" from the OD), but was absent on the sixth polished face (0.036"). Overall photo mosaics of each face, along with higher magnification photographs showing details of the intergranular corrosion, are provided in Figures 100 through 119. For orientation purposes, a notch was placed on the bottom end at ~90°.

R20C54-5B3B2C (2H TSP)

Sample 5B3B2C extended circumferentially from approximately 225° to 315°. A corroded area extended over the region from approximately 235° to 305° in the upper half of the TSP. Intergranular corrosion was present through the fourth grind (0.022" from the OD), but was absent on the fifth polished face (0.027"). Overall photo mosaics of each face, along with higher magnification photographs showing details of the intergranular corrosion, are provided in Figures 120 through 131. For orientation purposes, a notch was placed on the bottom end at ~270°.

R20C54-5B3B2E (2H TSP)

Sample 5B3B2E consisted of the region immediately counterclockwise from the burst rupture, extending circumferentially from approximately 340° to 30°. Intergranular corrosion was present through the second grind (0.018" from the OD surface), but was absent on the third polished face (0.026"). Overall photo mosaics of each face, along with higher magnification photographs showing details of the intergranular corrosion, are provided in Figures 132 through 137. For orientation purposes, a notch was placed on the bottom end at ~0°.

2.12 Material Properties

Tensile Testing

One sample from a free span region was tensile tested at 70°F, and the results are provided in Table 15. The engineering stress/strain curve is provided in Figure 138. The nominal tubing OD was 0.873 inches and the nominal wall thickness was 0.0524 inches.

Bulk Chemistry

A section of tubing was decontaminated for bulk chemical analysis. The analysis results presented in Table 16 are consistent with Alloy 600 material.

Microstructure

A longitudinal metallographic sample was prepared from the free span region. A dual etch procedure using phosphoric and nital acid solutions was used to characterize the carbide distribution and grain microstructure. The results are shown in Figures 139 and 140. The carbide distribution along the grain boundaries was very light, and intragranular matrix carbides were also present. Hilliard Circular intercept measurements indicated an ASTM grain size of 8.5 (16.4 μm average grain intercept distance).

Summary

The material properties discussed above are summarized and compared with the material test report values and with the ASME specification for SB-163 (Alloy 600) in Table 17. As can be seen in the table, the material properties for tube no. R20C54 are in agreement with both the material test report and the ASME specification.

3 Summary of Laboratory Examinations

The following summary observations were made based on the results of the laboratory examinations documented in this report:

- Laboratory eddy current inspection of the pulled tube sections confirmed the presence of 3 defect indications (SAI) at the 1H TSP location and a dent indication (DNT) in approximately the middle of the 2H TSP location.
- The section of tubing from the 1H TSP location developed a small leak when subjected to a pressure differential of 2750 psi (MSLB pressure corrected for gauge effects and for the effect of temperature on material properties). The maximum room temperature leak rate recorded was 0.002 gpm.
- Burst pressure for the section of tubing from the 1H TSP location was 5,819 psi. The location of the burst was at approximately 19°, corresponding to the location of the largest eddy current defect indication. SEM fractography revealed a total axial extent of IGSCC of 0.7 inches, ~0.12 inches of which was through wall. SEM fractography also confirmed that ductile tearing of ligaments had not occurred during the preceding leak rate test.
- Transverse metallography of the post-burst 1H TSP section revealed a 40% TW crack at 330° (~0.1 inches above the center of the TSP), in the approximate area of the second eddy current indication (SAI #2). A second transverse metallographic section near the centerline of the 1H TSP revealed a 53% TW indication at 298°, in the approximate area of the third eddy current indication (SAI #3) reported at 292°.
- No defects were identified in the 2H TSP crevice during field eddy current testing; however, the tube section containing the crevice region burst at 10,428 psi at ~30° in an area of intergranular corrosion. SEM fractography confirmed a preburst axial extent of intergranular corrosion of 0.795 inches, with a maximum depth of 0.0239 inches (46% TW). The maximum depth of corrosion was located within the TSP thickness toward the upper edge; however, the overall extent of corrosion suggests that a small sludge pile may have existed in this area (0° to 90°) during some period in time, creating the conditions for an aggressive environment to develop outside of the tube-TSP intersection.
- A second patch of intergranular corrosion was also present in the upper half of the 2H TSP crevice from ~235° to 305°. A review of the eddy current data records confirmed that neither area of degradation was detected by either the bobbin or rotating eddy current probes during the field inspection. A small, single volumetric indication was found in the post-pull rotating coil data at ~45°.
- Radial grinding demonstrated that the intergranular corrosion within the 2H TSP interface region became predominantly axially oriented as the corrosion progressed inward from the OD. The morphology of the intergranular

corrosion and its behavior as it progressed inward from the OD is typical of cellular corrosion.

- EDS/WDS analysis revealed the presence of sulfur on the 2H burst rupture surface.
- Material properties for tube no. R20C54 were in agreement with the material test report values and with the ASME SB-163 specification.

4 Conclusions

The laboratory examinations confirmed that axial OD intergranular stress corrosion cracking (IGSCC) was present in the 1H TSP region. The total axial extent and through wall portion of the primary defect were 0.70 and 0.12 inches, respectively. In addition, two smaller IGSCC cracks were present at other circumferential locations. The burst pressure for this section was 5,819 psi. The corresponding free span region without defects burst at 11,695 psi.

The burst pressure for the 2H TSP section was 10,428 psi. Post-burst inspection revealed two patches of intergranular corrosion that had not been detected during eddy current inspection prior to tube pull. The maximum depth of the corrosion in the burst region was determined to be less than 46% through wall. A detailed review of the eddy current data records confirmed that corrosion was not detected by either the bobbin or rotating eddy current probes during the in-generator inspection. A small, single volumetric indication (SVI) was found in the post-pull rotating coil data during the same review of the data records.

Radial grinding through these patches of intergranular corrosion showed that the orientation of the intergranular penetrations became predominantly axial as the corrosion progressed inward, which is typical behavior for “cellular corrosion”.

SEM/EDS/WDS analysis revealed the presence of sulfur on the 2H burst rupture surface. Sulfur is known to be detrimental to Alloy 600 and has been previously implicated in intergranular corrosion[9].

5 References

1. Quality Control Inspection Report No. 6033666, 6/30/2004.
2. FANP Document No. 51-5044913-00, "Eddy Current Tube Pull Examination for PG&E Diablo Canyon Unit 1 – April 2004," 6/14/2004.
3. *Steam Generator InSitu Pressure Test Guidelines: Revision 2*, EPRI TR-10007904, August 2003.
4. FANP Document No. 51-5044611-00, "Diablo Canyon Unit 1 Tube Pull Leak Rate Test Results," 5/11/2004.
5. FANP Document No. 51-5025213-00, "7/8" OD RSG Tube (Alloy 600) Oxidation Test Results," 3/12/2003.
6. *Steam Generator Tubing Burst Testing and Leak Rate Testing Guidelines*, EPRI Report No. 1006783, Final Report, December 2002.
7. *Guidelines for PWR Steam Generator Tubing Specification and Repair, Volume 4, Revision 1*, EPRI TR-016743-V4R1, December 1997.
8. FANP Document No. 32-5050059-00, "Diablo Canyon 1 SG Tube Sample R20C54-5B3B Burst Fractography," 8/25/2004.
9. *PWR Secondary Water Chemistry Guidelines – Revision 5*, EPRI TR-102135-R5, Final Report, May 2000.

Table 1. Diablo Canyon Unit 1 SG 11 Tube Receipt Inspection Summary

Sample Identification	As-received Length (inches)	On-site Length (inches)	Distance to landmark from bottom of tube section, inches	Landmark	Comments
R20C54-3	26	25 ⅞	15 ½	Bottom of 1H TSP	OD scale is absent due to on-site chemical cleaning; little smearable contamination present. Some deposit buildup remains at 1H TSP location. Patches of copper colored oxide observed below TSP location; small spots of copper colored oxide observed above TSP.
			24 ½	Circumferential saw cut	Field applied saw cut. Partial through wall axial cut ~0.4 inches long placed ~1 inch above tube section bottom with a Dremel tool to serve as 0° reference point for RPC inspection.
R20C54-4 (free span)	28 ⅛	28 ¼	26 ⅞	Circumferential saw cut	OD surface is free of scale, with spots of copper colored oxide randomly distributed over lower half of section. 0° reference point for RPC inspection transferred to Section 4 from Section 3
R20C54-5	36	36	11 ⅞	Bottom of 02H TSP	OD scale absent; regions of "compressed" magnetite present on OD within TSP location from 0 to 180°. No visible signs of denting. Brown deposit buildup present on OD at bottom of TSP crevice location. Axial bands of copper colored oxide observed below TSP from 90 to 120° and above TSP at 300 to 340°.
			35	Circumferential saw cut	0° reference point for RPC inspection transferred to Section 5 from Section 4.

Table 2. Bobbin Eddy Current Inspection Results Summary

Tube Section No.	Location in SG	Pre Tube Pull			Post Tube Pull			In Lab		
		Call	Volts	Phase	Call	Volts	Phase	Call	Volts	Phase
R20C54-3	1H + 0.13"	DOS	5.60	69	DOS	6.71	69	DOS	6.83	68
R20C54-5	2H + 0.11"	DNT	3.27	175	DNT	1.11	168	DNT	1.29	170

Table 3. Rotating Coil Eddy Current Inspection Summary

Tube Section No.	Data Source	Location in SG	Pre Tube Pull (In-Generator)			Post Tube Pull (On Platform)		Pre Leak Rate Test (In Lab)		
			Call	Volts	Phase	Volts	Phase	Call/%TW/ Orientation	Volts	Phase
R20C54-3	FDMS[a] Ref. 2	1H+0.03 1H+0.04	SAI SAI#1	4.00 3.99	61° 61°	4.61	53°	SAI/90%/19°	4.48	54°
	FDMS Ref. 2	1H+0.00 1H+0.04	SAI SAI#2	0.27 0.27	96° 94°	0.23	102°	SAI/73%/330°	0.20	79°
	FDMS Ref. 2	1H+0.07 1H+0.11	SAI SAI#3	0.08 0.11	123° 87°	0.10	125°	SAI/68%/292°	0.13	85°
R20C54-5	FDMS Ref. 2	2H 2H	NDD NDD	N/A N/A	N/A N/A	N/A	N/A	NDD	N/A	N/A

[a] Framatome ANP Data Management System

Table 4. Review of Rotating Coil Eddy Current Data for Section R20C54-5 Acquired prior to and following Tube Pull

Tube No.	Location	EC Call	Volts	Phase	Max Depth
Before Tube Pull	2H	NDD	N/A	N/A	N/A
After Tube Pull	R20C54-5 (2H)	SVI	0.18	112°	N/A
In Lab, before Pressure Testing	R20C54-5 (2H)	SVI	0.15	110°	32% TW

Table 5. Summary of Leak Rate Tests

Tube Sample No.	Pressure Hold Points, psi	Hold Time minutes	Maximum Leak Rate, gpm	Avg. Pressurization Rate, psi/sec
R20C54-3B (1H)	1750	2	0.0000	20
	2250	2	0.0000	6
	2750	5	0.0020	4
R20C54-5B (2H)	1750	2	0.0000	19
	2250	2	0.0000	12
	2750	2	0.0000	14

Table 6. Rotating Coil Eddy Current Inspection Pre and Post Leak Comparisons

Tube Sample No.	Location in SG	Pre Leak Test (In Lab)			Post Leak Test (In Lab)		
		Call	Volts	Phase	Call	Volts	Phase
R20C54-3B (1H)	1H + 0.04" (#1)	SAI 90% TW @19°	4.48	54°	SAI 92% TW @19°	4.93	53°
	1H + 0.04" (#2)	SAI 73% TW @330°	0.20	79°	77% TW @330°	0.33	77°
	1H + 0.11" (#3)	SAI 68% TW @292°	0.13	85°	67% TW @292°	0.21	88°

Table 7. Room Temperature Burst Tests

Tube Sample No.	Sample Length Inches	Pressurization Rate Psi/sec	Burst Pressure psi
Control tube	11.9	630	10,145
R20C54-3B (1H)	11.9	607	5,819
R20C54-4B (free span)	12.1	620	11,695
R20C54-5B (2H)	12.1	772	10,428

Table 8. Burst Test Dimensional Measurements – Control Specimen

Sample: Control Sample	
Defect Angle: NA	

INITIAL LENGTH 11 15/16"		Instrument = Ruler	Calibration Due = NA
INITIAL DIAMETERS:			
Bottom End, 0°or Defect	0.877		
Bottom end, ditto+90°	0.876	Instrument = BW 1-0000-3549	
Center, 0°or Defect	0.876		
Center, ditto+90°	0.877	Calibration Due: 9/18/04	
Top End, 0°or Defect	0.877		
Top end, ditto+90°	0.876		
INITIAL WALL THICKNESSES:			
Bottom End, 0°or Defect	0.05180		
Bottom end, ditto+90°	0.05170	Instrument = BW 1006009	
Bottom end, ditto+180°	0.05220		
Bottom end, ditto+270°	0.05220	Calibration Due: 4/13/05	
Top End, 0°or Defect	0.05165		
Top end, ditto+90°	0.05160		
Top end, ditto+180°	0.05210		
Top end, ditto+270°	0.05225		

POSTTEST DIAMETERS:		
Remote, aligned w/Rupture	1.061	
Remote, ditto+90°	1.057	Instrument = BW 1-0000-3549
Burst (C/L - 1"), at rupture	1.036	
Burst (C/L- 1"), ditto+90°	1.078	Calibration Due: 9/18/04
@ Burst, at rupture	1.280	
@ Burst, ditto+90°	1.125	
Burst (C/L+ 1"), at rupture	1.043	
Burst (C/L+ 1"), ditto+90°	1.077	
BURST DIMENSIONS		
Burst Rupture Length	1.959	
Burst Maximum Width	0.328	
Distance From Bottom of Tube to Bottom of Burst Region	3.390	
Burst Position, angle	90°	

Table 9. Burst Test Dimensional Measurements – R20C54-3B (1H)

Sample: R20C54-3B (1H TSP)	
Defect Angle: 19°	

INITIAL LENGTH 11 15/16"		Instrument = Ruler	Calibration Due = NA
INITIAL DIAMETERS:			
Bottom End, 0°or Defect	0.873		
Bottom end, ditto+90°	0.872	Instrument = BW 1-0000-3549	
Center, 0°or Defect	0.875		
Center, ditto+90°	0.875	Calibration Due: 9/18/04	
Top End, 0°or Defect	0.872		
Top end, ditto+90°	0.872		
INITIAL WALL THICKNESSES:			
Bottom End, 0°or Defect	0.05180		
Bottom end, ditto+90°	0.05280	Instrument = BW 1006009	
Bottom end, ditto+180°	0.05290		
Bottom end, ditto+270°	0.05230	Calibration Due: 4/13/05	
Top End, 0°or Defect	0.05185		
Top end, ditto+90°	0.05265		
Top end, ditto+180°	0.05310		
Top end, ditto+270°	0.05200		

POSTTEST DIAMETERS:		
Remote, aligned w/Rupture	0.873	
Remote, ditto+90°	0.873	Instrument = BW 1-0000-3549
Burst (C/L - 1"), at rupture	0.870	
Burst (C/L- 1"), ditto+90°	0.877	Calibration Due: 9/18/04
@ Burst, at rupture	1.005	
@ Burst, ditto+90°	0.889	
Burst (C/L+ 1"), at rupture	0.870	
Burst (C/L+ 1"), ditto+90°	0.876	
BURST DIMENSIONS		
Burst Rupture Length	1.045	
Burst Maximum Width	0.244	
Distance From Bottom of Tube to Bottom of Burst Region	5.531	
Burst Position, angle	19°	

Table 10. Burst Test Dimensional Measurements – R20C54-4B (Free Span)

Sample: R20C54-4B (Free span)	
Defect Angle: NA	

INITIAL LENGTH 12 1/16"		Instrument = Tape	Calibration Due = NA
INITIAL DIAMETERS:			
Bottom End, 0°or Defect	0.873		
Bottom end, ditto+90°	0.873	Instrument = BW 1-0000-3549	
Center, 0°or Defect	0.872		
Center, ditto+90°	0.872	Calibration Due: 9/18/04	
Top End, 0°or Defect	0.873		
Top end, ditto+90°	0.873		
INITIAL WALL THICKNESSES:			
Bottom End, 0°or Defect	0.05130		
Bottom end, ditto+90°	0.05330	Instrument = BW 1006009	
Bottom end, ditto+180°	0.05360		
Bottom end, ditto+270°	0.05235	Calibration Due: 4/13/05	
Top End, 0°or Defect	0.05160		
Top end, ditto+90°	0.05210		
Top end, ditto+180°	0.05355		
Top end, ditto+270°	0.05260		

POSTTEST DIAMETERS:		
Remote, aligned w/Rupture	1.017	
Remote, ditto+90°	1.015	Instrument = BW 1-0000-3549
Burst (C/L - 1"), at rupture	1.019	
Burst (C/L- 1"), ditto+90°	1.052	Calibration Due: 9/18/04
@ Burst, at rupture	1.246	
@ Burst, ditto+90°	1.095	
Burst (C/L+ 1"), at rupture	1.015	
Burst (C/L+ 1"), ditto+90°	1.057	
BURST DIMENSIONS		
Burst Rupture Length	1.941	
Burst Maximum Width	0.390	Instrument = BW 1-0000-3164
Distance From Bottom of Tube to Bottom of Burst Region	6.489	Calibration Due: 4/13/05
Burst Position, angle	350°	

Table 11. Burst Test Dimensional Measurements – R20C54-5B (2H)

Sample: R20C54-5B (2H TSP)	
Defect Angle: NA	

INITIAL LENGTH 12 1/16"		Instrument = Tape	Calibration Due = NA
INITIAL DIAMETERS:			
Bottom End, 0°or Defect	0.873		
Bottom end, ditto+90°	0.872	Instrument = BW 1-0000-3549	
Center, 0°or Defect	0.879		
Center, ditto+90°	0.880	Calibration Due: 9/18/04	
Top End, 0°or Defect	0.872		
Top end, ditto+90°	0.873		
INITIAL WALL THICKNESSES:			
Bottom End, 0°or Defect	0.05180		
Bottom end, ditto+90°	0.05305	Instrument = BW 1006009	
Bottom end, ditto+180°	0.05290		
Bottom end, ditto+270°	0.05180	Calibration Due: 4/13/05	
Top End, 0°or Defect	0.05145		
Top end, ditto+90°	0.05280		
Top end, ditto+180°	0.05360		
Top end, ditto+270°	0.05200		

POSTTEST DIAMETERS:		
Remote, aligned w/Rupture	0.926	
Remote, ditto+90°	0.925	Instrument = BW 1-0000-3549
Burst (C/L - 1"), at rupture	0.913	
Burst (C/L- 1"), ditto+90°	0.941	Calibration Due: 9/18/04
@ Burst, at rupture	1.160	
@ Burst, ditto+90°	0.964	
Burst (C/L+ 1"), at rupture	0.911	
Burst (C/L+ 1"), ditto+90°	0.940	
BURST DIMENSIONS		
Burst Rupture Length	1.475	
Burst Maximum Width	0.383	
Distance From Bottom of Tube to Bottom of Burst Region	5.402	
Burst Position, angle	30°	

Table 12. Defect Burst Specimen Fractography Measurements R20C54-3B2 (1H TSP)

Point	Incremental Length Segment (")	Cumulative Length (")	Depth IGSCC (")
0	0.0000	0.0000	0.0000
1	0.0231	0.0231	0.0130
2	0.0418	0.0649	0.0116
3	0.0198	0.0847	0.0217
4	0.0205	0.1052	0.0213
5	0.0215	0.1267	0.0274
6	0.0182	0.1449	0.0235
7	0.0388	0.1837	0.0290
8	0.0027	0.1865	0.0381
9	0.0314	0.2178	0.0388
10	0.0171	0.2349	0.0347
11	0.0244	0.2593	0.0440
12	0.0154	0.2746	0.0469
13	0.0133	0.2879	0.0521
14	0.0457	0.3337	0.0522
15	0.0225	0.3562	0.0522
16	0.0529	0.4091	0.0521
17	0.0390	0.4481	0.0508
18	0.0070	0.4551	0.0495
19	0.0280	0.4830	0.0363
20	0.0208	0.5039	0.0258
21	0.0150	0.5188	0.0150
22	0.0049	0.5237	0.0206
23	0.0082	0.5320	0.0131
24	0.0150	0.5470	0.0039
25	0.0038	0.5508	0.0080
26	0.0356	0.5864	0.0133
27	0.0297	0.6160	0.0085
28	0.0086	0.6247	0.0087
29	0.0242	0.6489	0.0000
30	0.0235	0.6724	0.0000
31	0.0045	0.6769	0.0039
32	0.0048	0.6818	0.0000
33	0.0066	0.6883	0.0000
34	0.0053	0.6936	0.0038
35	0.0068	0.7005	0.0000

Note: Starting reference point was at the axial bottom of the crack

Table 13. Defect Burst Specimen Fractography Measurements R20C54-5B3B (2H TSP)

Point	Incremental Length Segment, in.	Cumulative Length, in.	Adjusted Length, in.	Depth IGSCC, in.
0	0.0000	0.0000	0.0000	0.0029
1	0.0119	0.0119	0.0110	0.0100
2	0.0109	0.0228	0.0210	0.0054
3	0.0183	0.0410	0.0379	0.0185
4	0.0081	0.0492	0.0454	0.0165
5	0.0214	0.0706	0.0651	0.0173
6	0.0174	0.0879	0.0811	0.0114
7	0.0095	0.0975	0.0899	0.0056
8	0.0148	0.1122	0.1035	0.0101
9	0.0130	0.1252	0.1155	0.0048
10	0.0093	0.1346	0.1241	0.0103
11	0.0160	0.1506	0.1389	0.0174
12	0.0163	0.1669	0.1540	0.0163
13	0.0042	0.1711	0.1579	0.0102
14	0.0081	0.1792	0.1653	0.0124
15	0.0128	0.1920	0.1771	0.0064
16	0.0149	0.2069	0.1909	0.0084
17	0.0141	0.2210	0.2039	0.0154
18	0.0093	0.2303	0.2125	0.0140
19	0.0129	0.2432	0.2244	0.0046
20	0.0184	0.2616	0.2414	0.0106
21	0.0234	0.2850	0.2630	0.0047
22	0.0130	0.2981	0.2750	0.0116
23	0.0147	0.3128	0.2886	0.0159
24	0.0367	0.3495	0.3224	0.0141
25	0.0091	0.3586	0.3308	0.0166
26	0.0359	0.3944	0.3639	0.0128
27	0.0312	0.4257	0.3927	0.0147
28	0.0188	0.4445	0.4101	0.0119
29	0.0394	0.4839	0.4465	0.0142
30	0.0232	0.5071	0.4679	0.0191
31	0.0137	0.5208	0.4805	0.0153
32	0.0360	0.5567	0.5137	0.0116
33	0.0625	0.6192	0.5714	0.0189
34	0.0452	0.6645	0.6131	0.0173
35	0.0182	0.6827	0.6299	0.0136
36	0.0210	0.7037	0.6493	0.0154
37	0.0291	0.7328	0.6761	0.0101
38	0.0034	0.7362	0.6793	0.0234
39	0.0366	0.7728	0.7131	0.0226
39A	0.0060	0.7788	0.7186	0.0239
40	0.0181	0.7969	0.7353	0.0200
41	0.0132	0.8102	0.7475	0.0086
42	0.0293	0.8395	0.7746	0.0045
43	0.0221	0.8616	0.7949	0.0000

Table 14. Depth (in inches) of Radial Grinds in the 2H TSP Specimens

	Metallographic Sample			
	5B3BB1	5B3B2A	5B3B2C	5B3B2E
1st Face	0.005	0.005	0.006	0.011
2nd Face	0.011	0.011	0.011	0.018
3rd Face	0.017	0.017	0.015	0.026 (no corrosion)
4th Face	0.022	0.022	0.022	--
5th Face	0.028 (*no corrosion*)	0.028	0.027 (*no corrosion*)	--
6th Face	--	0.036 (no corrosion)	--	--

Table 15. Tensile Test Results

Property	R20C54-4C
Yield Strength (psi)	53,028
Tensile Strength (psi)	105,643
Total Elongation (%)	39.44
Reduction in Area (%)	37.8

Table 16. Bulk Chemistry Analysis

Element	Sample R20C54-4A (wt. %)	Nominal Alloy 600 (wt. %)
Ni	Balance (75)	72 min (Ni + Co)
Cr	15.5	14-17
Fe	8.29	6-10
Al	0.077	--
C	0.021	0.15 max
Co	0.047	--
Cu	0.16	0.5 max
Mn	0.19	1.0 max
P	0.009	--
Si	0.33	0.5 max
S	0.003	0.015 max
Ti	0.17	--

Table 17. Summary Material Properties for Tube No. R20C54

Property		R20C54	Mill Test Report[2]	ASME SB-163 Specification[3]
Heat Number		7777	7777	-
Yield Strength, psi		53,028	49,000	-
Ultimate Tensile Strength, psi		105,643	106,000	-
Total Elongation, %		39.44	40	-
Reduction in Area, %		37.8	Not available	-
ASTM Grain Size		8.5	-	-
Rockwell Hardness, RB		Not determined	85	-
Carbide Distribution		(Note 1)	-	-
Composition, wt%	Al	0.077	0.04	-
	C	0.021	0.04	0.15 max
	Co	0.047	0.04	Added to Ni
	Cr	15.50	15.71	14.0 – 17.0
	Cu	0.16	0.21	0.5 max
	Fe	8.29	8.22	6.0 – 10.0
	Mn	0.19	0.23	1.0 max
	Ni	75.0	75.17	72.0 min (+Co)
	P	0.009	-	-
	S	0.003	0.007	0.015 max
	Si	0.33	0.40	0.5 max
	Ti	0.17	0.33	-

Table 2-2 Notes:

(1) Carbides were primarily intragranular.

(2) Memo, David Beals to Joe Crockett dated April 17, 2004, "Tube Pull SG 11 R20C54

(3) ASME Metals handbook Vol. 1, 10th Edition, Materials Park, OH, March 1990.

Table 18. Depth of IGSCC near Axial Centerline of 1H TSP (From Transverse Metallographic Sample R20C54-3B2B1)

Angular Orientation [1] degrees	Depth	
	inches	% TW [2]
34	0.0204	39
40	0.0131	25
51	0.0079	15
52	0.0057	11
56	0.0077	15
59	0.0157	30
60	0.0062	12
62	0.0140	27
190	0.0176	34
238	0.0168	32
242	0.0194	37
298 [3]	**0.0277**	**53**
316	0.0239	46
321	0.0182	35
328	0.0271	52
332	0.0257	49
340	0.0258	50
349	0.0223	43
352	0.0154	30

Notes:
1. Angular orientations are relative and approximate.
2. % TW is based on measured 0.052-inch nominal wall thickness.
3. 298° corresponds to approximate location of SAI #3 (292°)

Table 19. Depth of IGSCC At ~0.1 inch above Axial Centerline of 1H TSP (From Transverse Metallographic Sample R20C54-3B2B2)

Angular Orientation [1] Degrees	Depth	
	inches	% TW [2]
15	0.0243	47
18	0.0306	59
20	0.0339	65
220	0.0157	30
230	0.0154	30
250	0.0137	26
258	0.0215	41
262	0.0256	49
280	0.0215	41
330 [3]	**0.0207**	**40**

Notes:
1. Angular orientations are relative and approximate.
2. % TW is based on measured 0.052-inch nominal wall thickness.
3. 330° corresponds to approximate location of SAI #2.

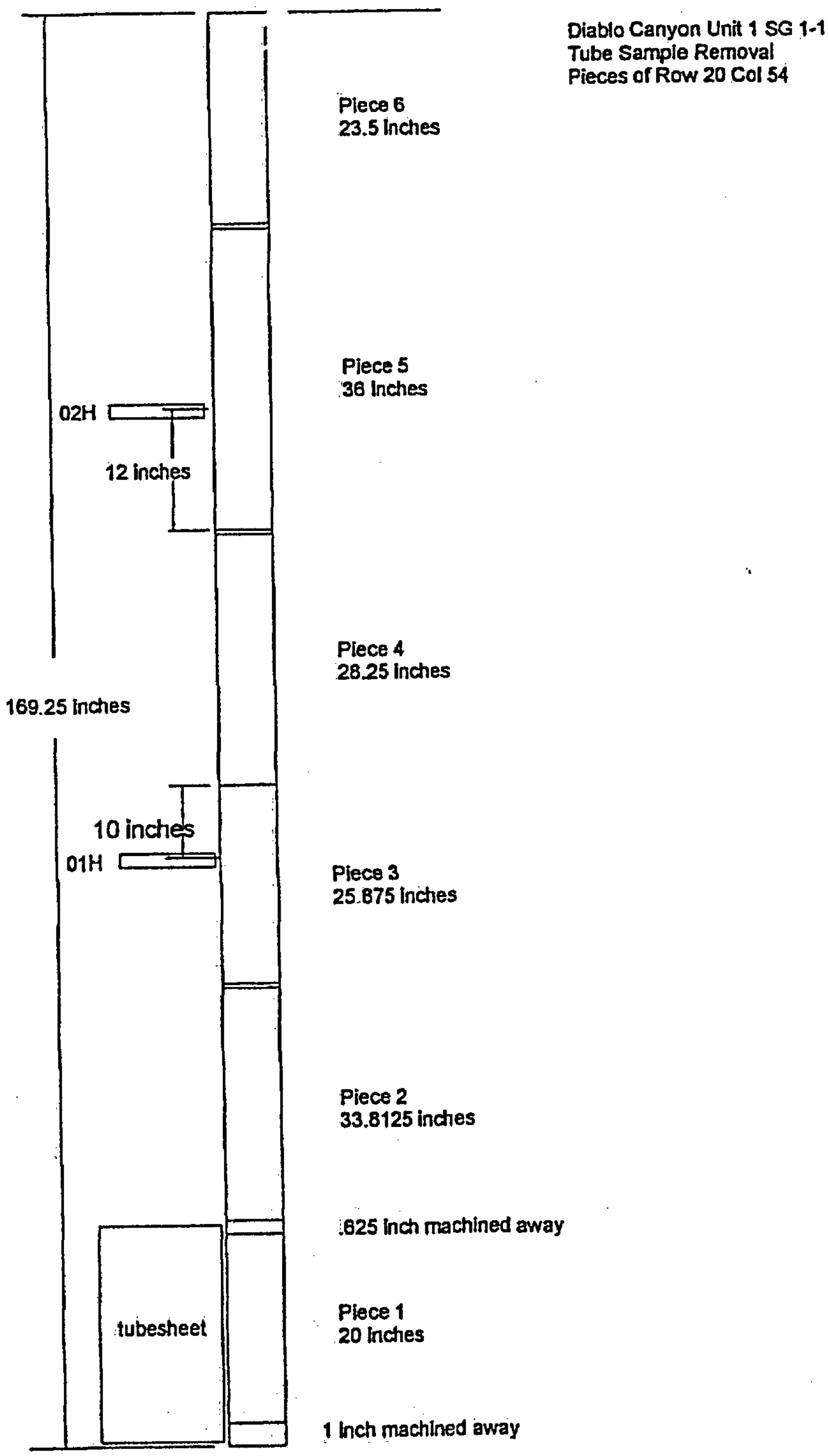

Figure 1. Pulled tube diagram – SG 11 tube no. R20C54

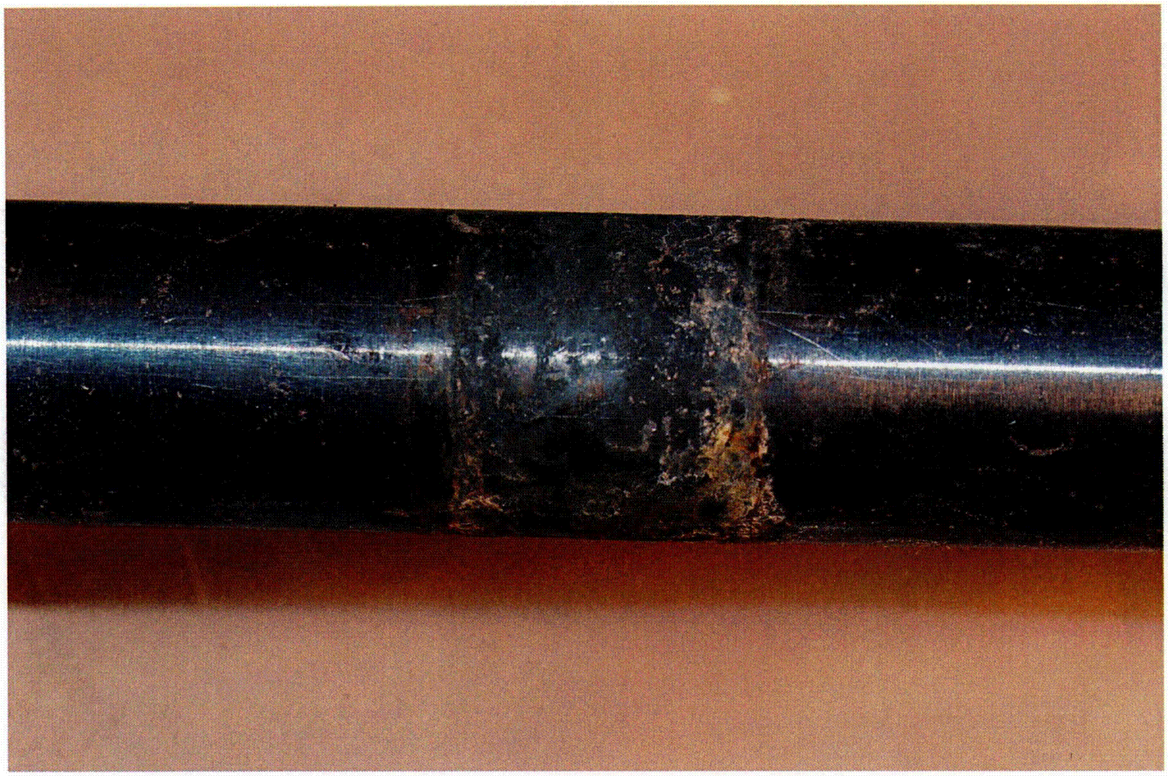

Figure 2. Receipt photograph of 1H TSP intersection (section 3) at 0 degrees. Bottom (in SG) is to the left.

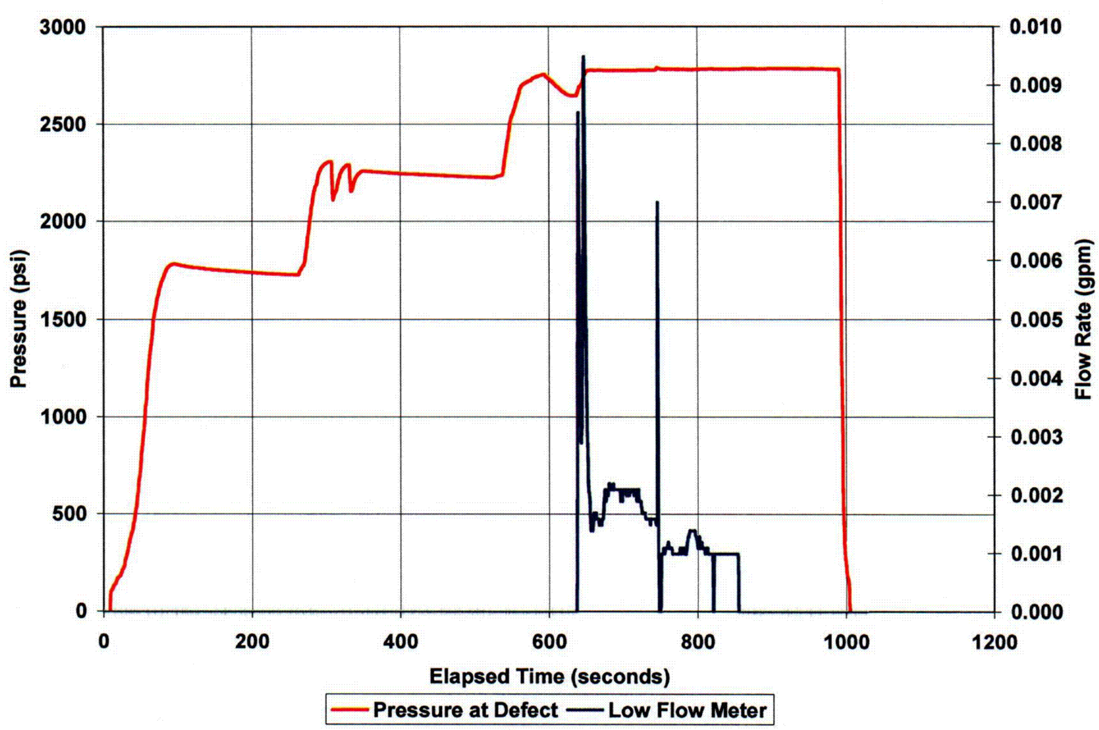

Figure 3. Room temperature leak rate for SG 11 tube no. R20C54, section 3 (1H TSP)

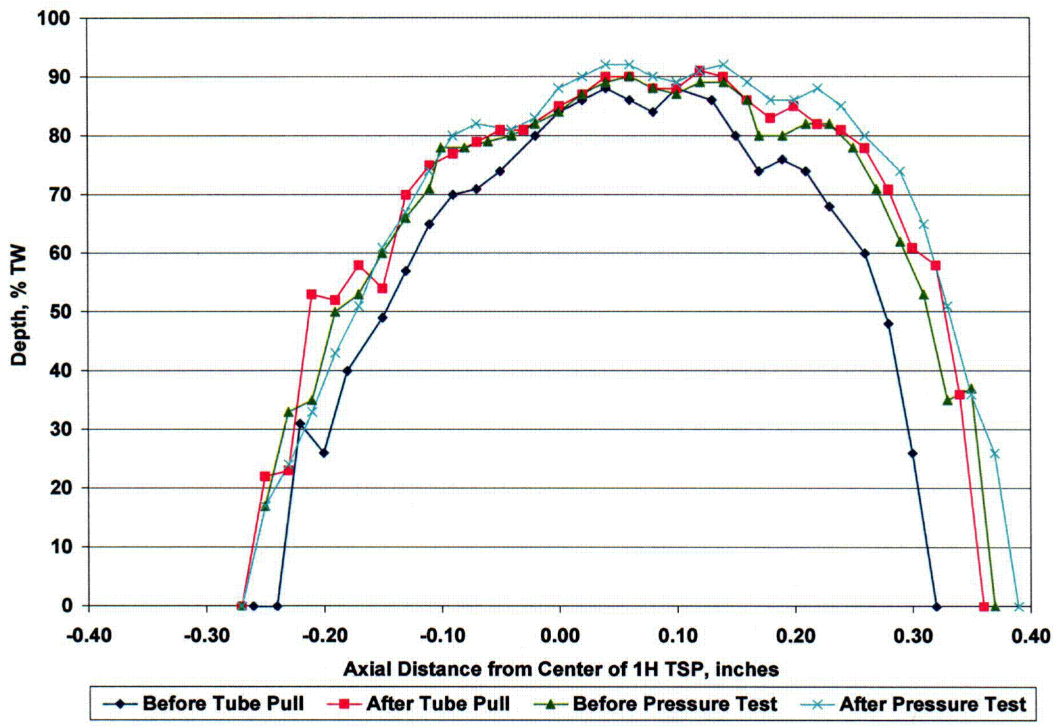

Figure 4. Axial crack NDE profile at 19° (SAI #1) at 1H TSP location for tube no. R20C54

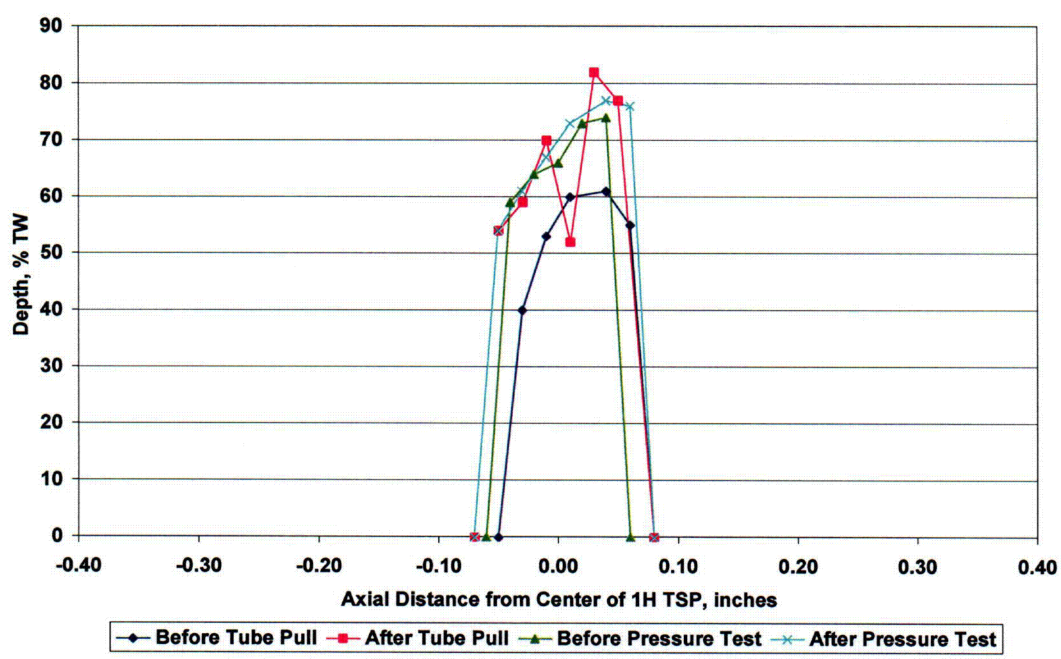

Figure 5. Axial crack NDE profile at 330° (SAI #2) at 1H TSP location for tube no. R20C54

C02

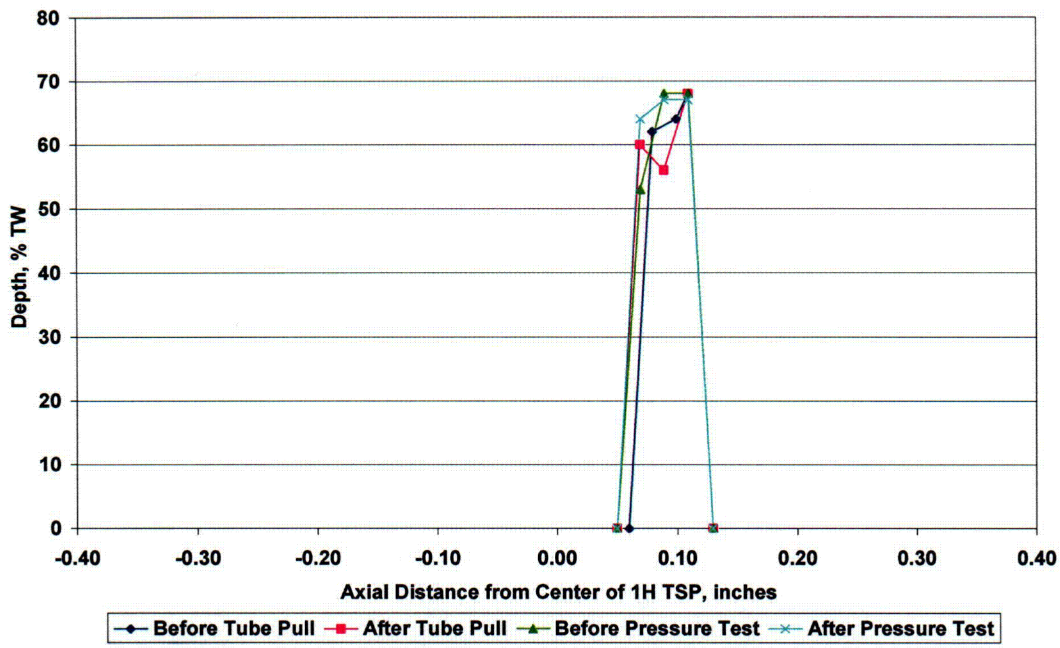

Figure 6. Axial crack NDE profile at 292° (SAI #3) at 1H TSP location for tube no. R20C54

Figure 7. Post oxidation photograph of axial crack at ~19° in 1H TSP intersection of tube section no. R20C54-3. The bottom (in SG) of the tube section is to the left. (7.6X)

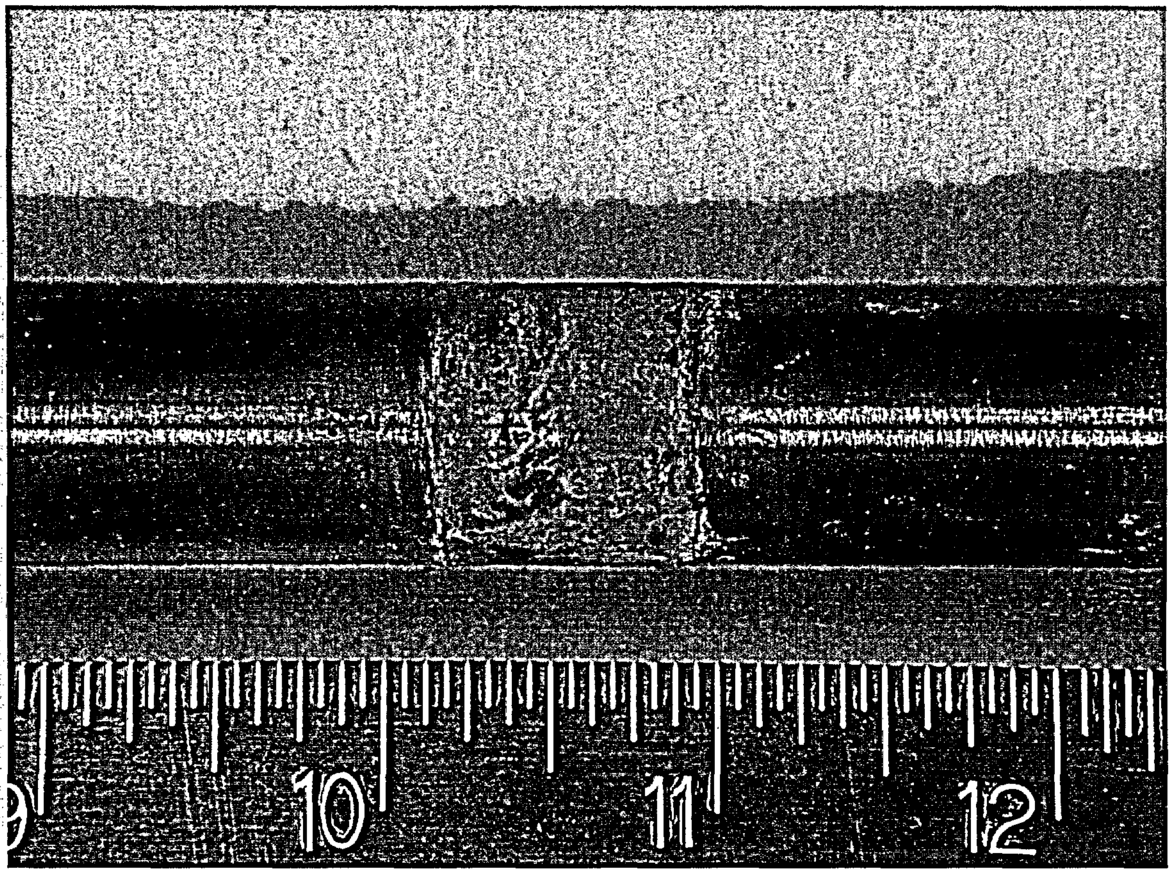

Figure 8: 1H TSP region at 0° (1.7X)

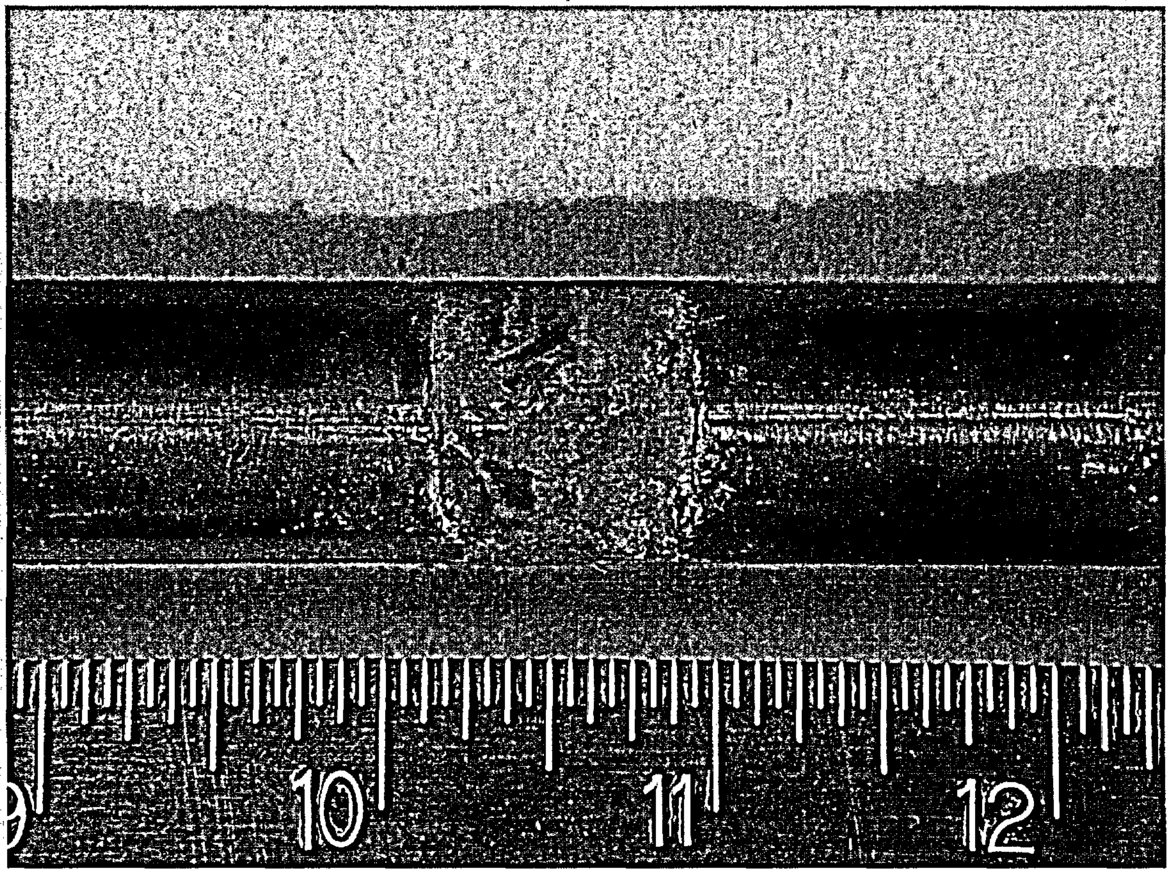

Figure 9: 1H TSP region at 45° 1.7X

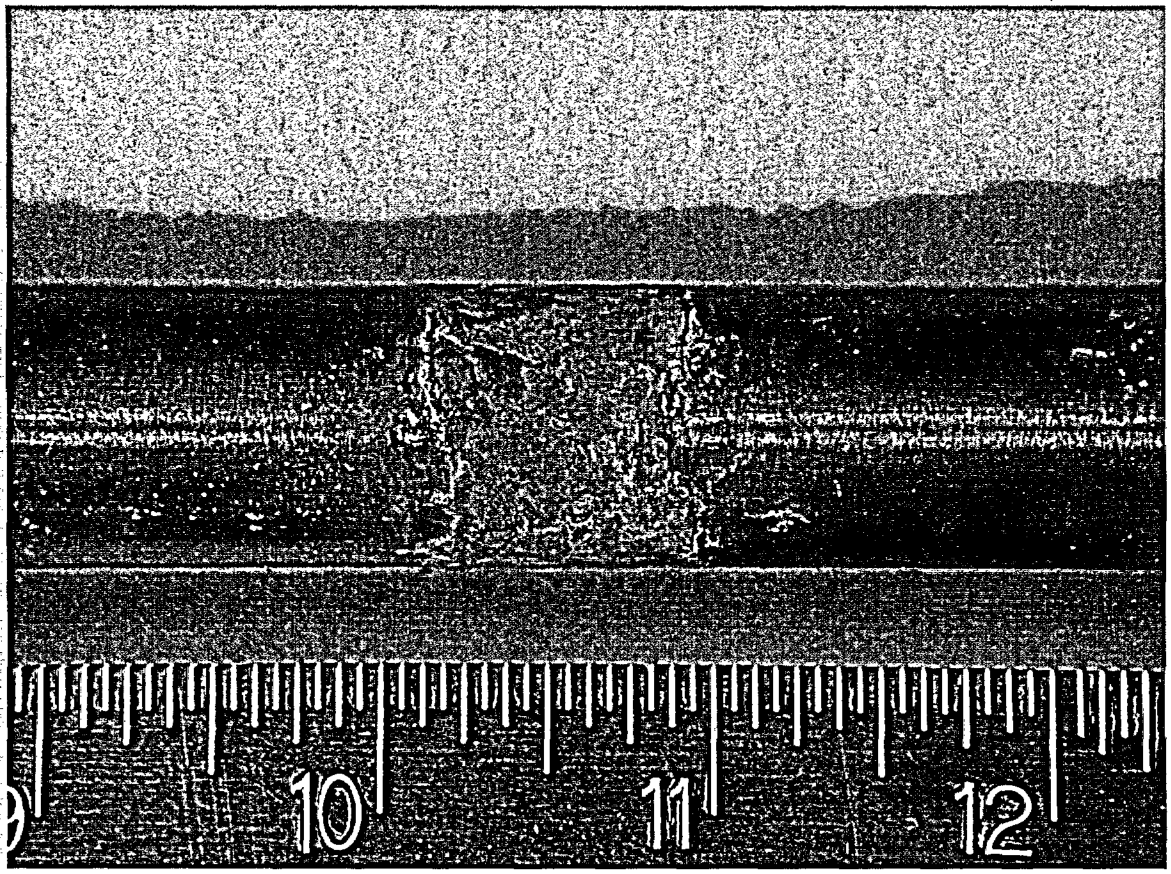

Figure 10: 1H TSP region at 90° 1.7X

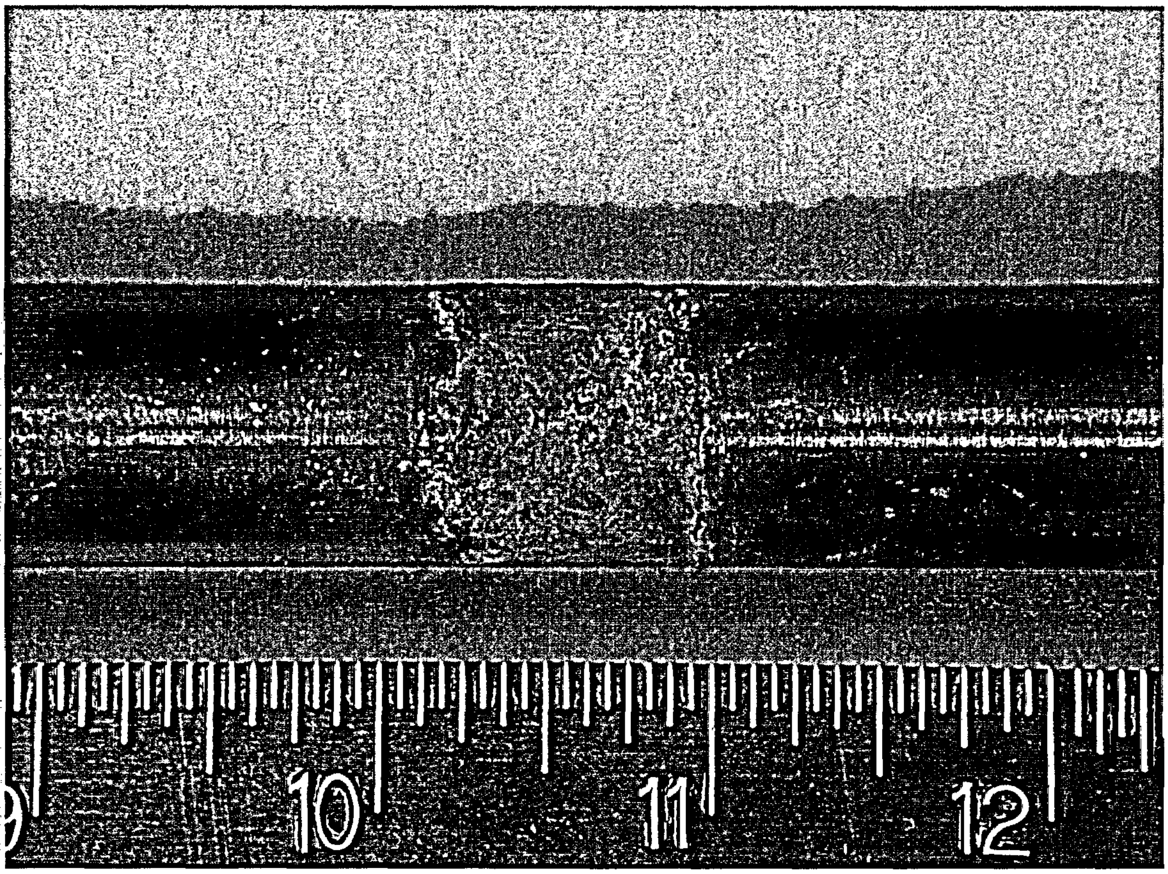

Figure 11: 1H TSP region at 135° 1.7X

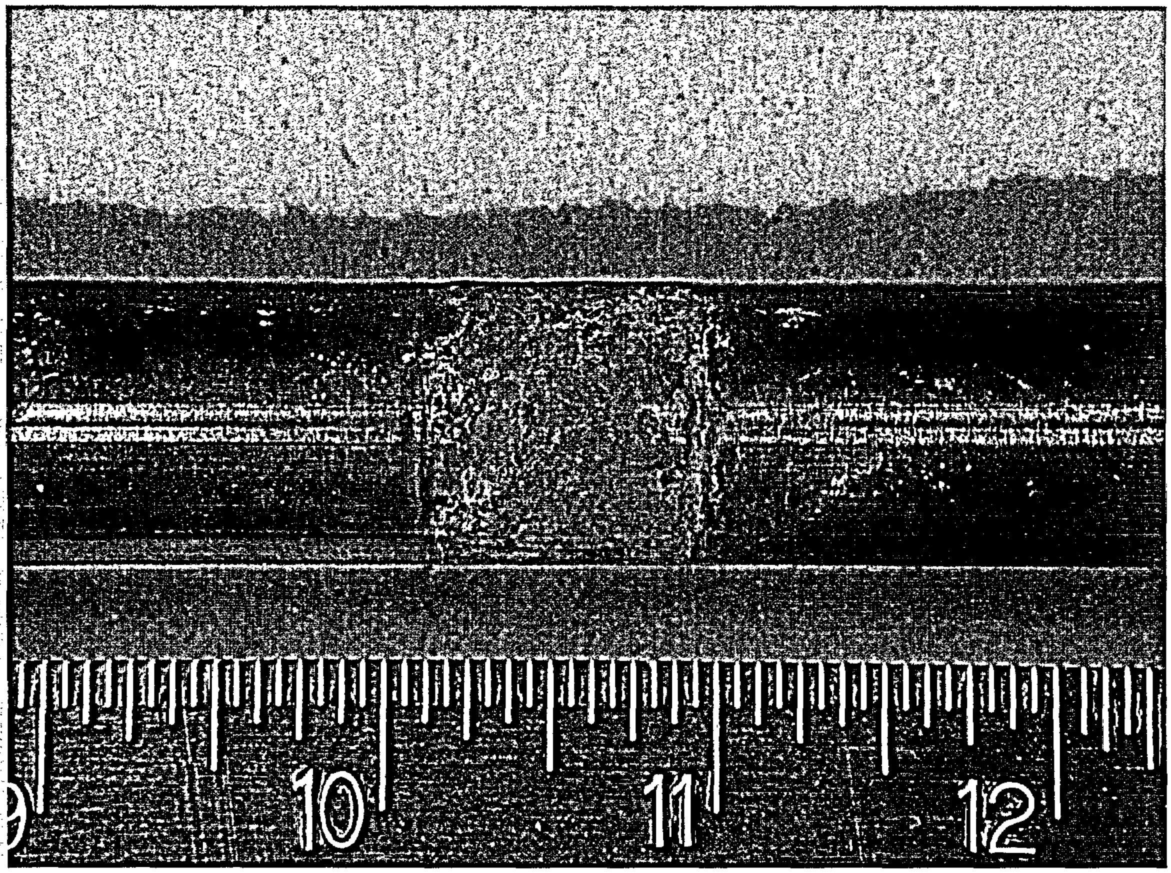

Figure 12: 1H TSP region at 180° 1.7X

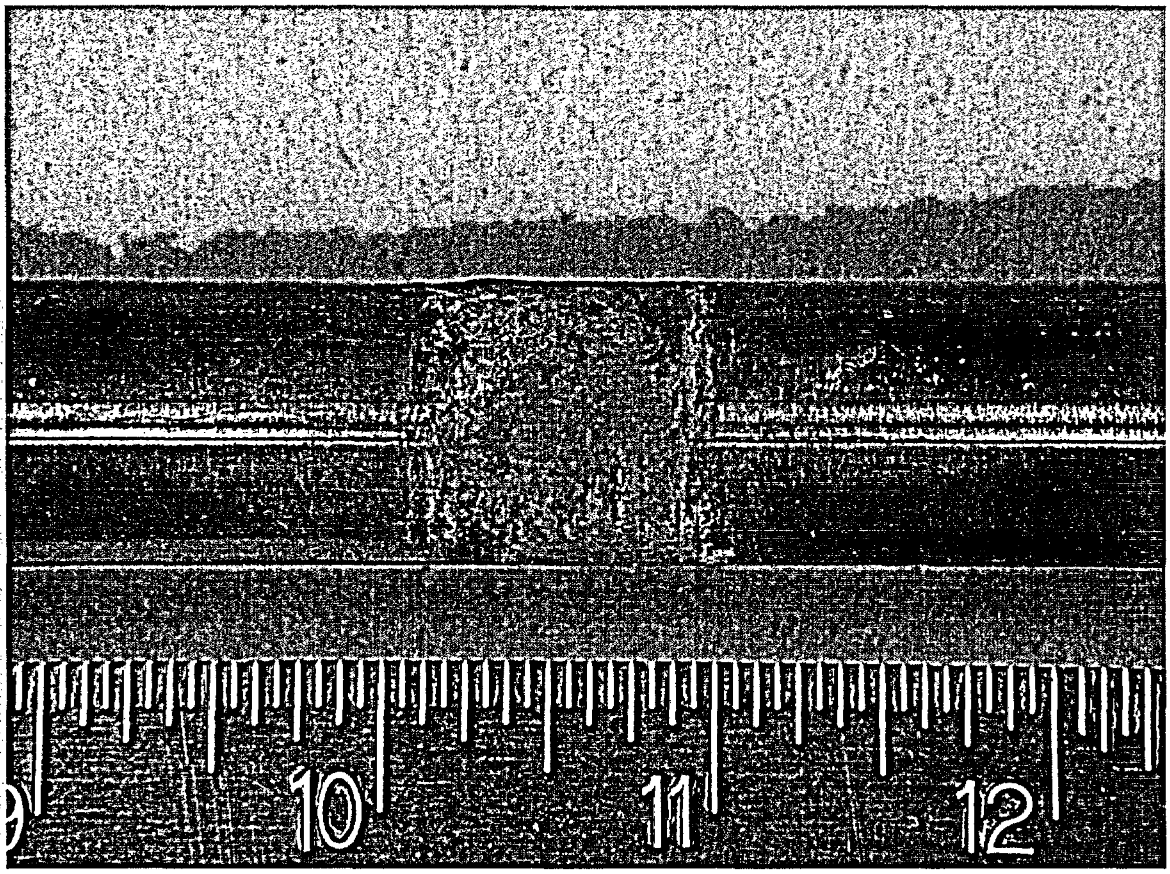

Figure 13: 1H TSP region at 225° 1.7X

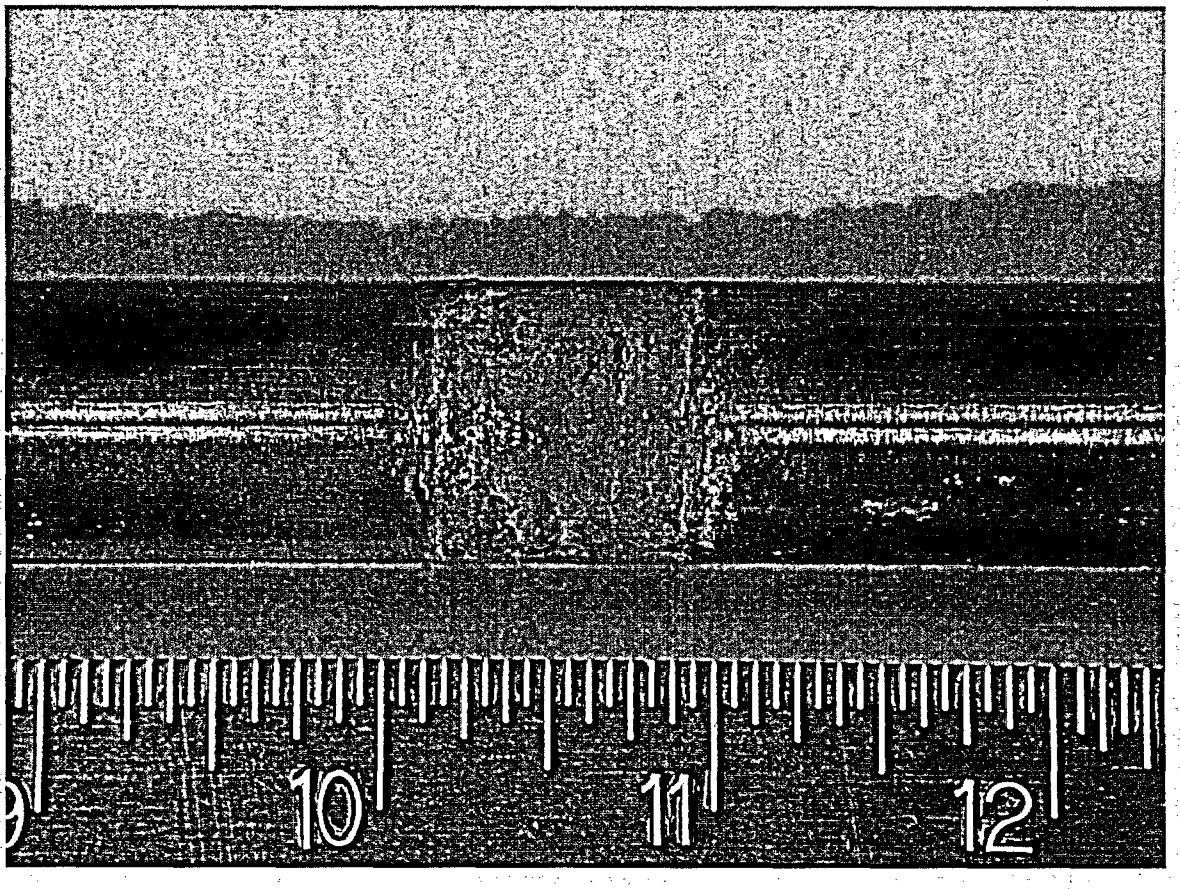

Figure 14: 1H TSP region at 270° 1.7X

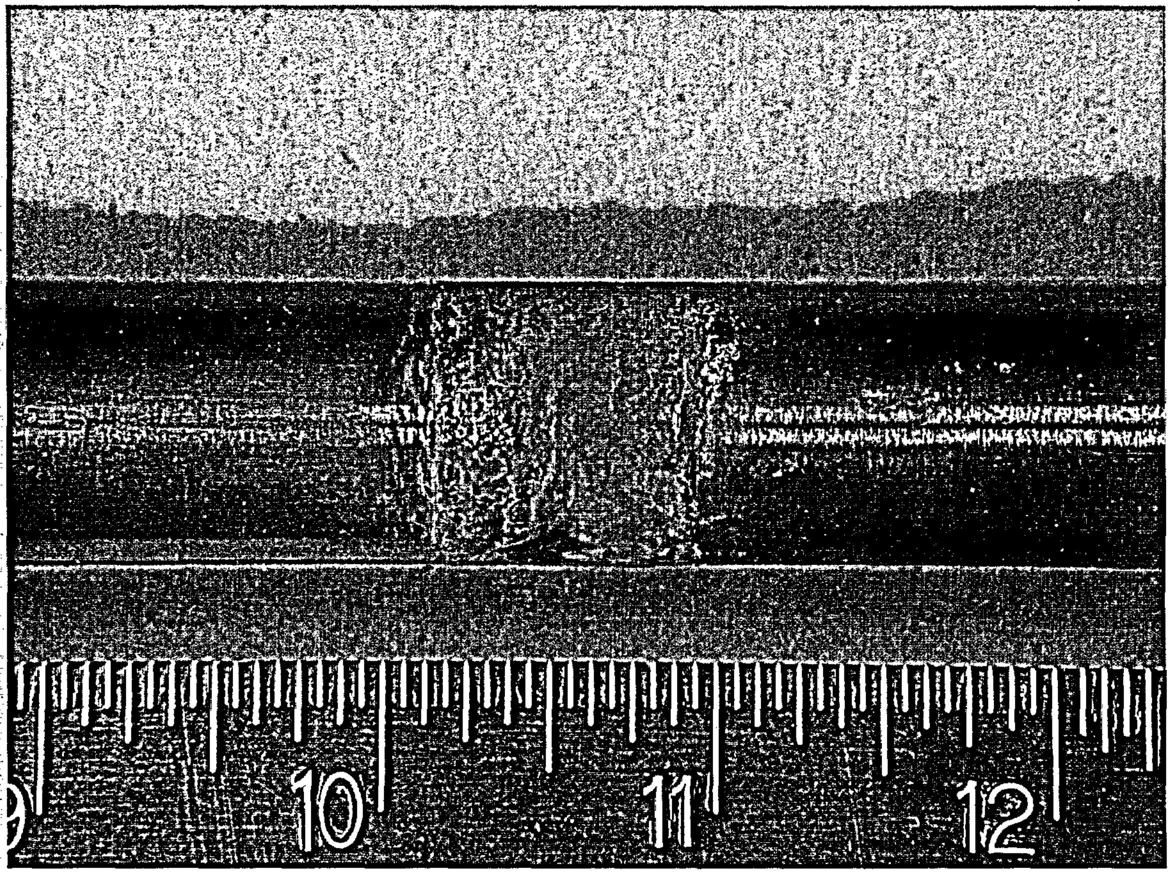

Figure 15: 1H TSP region at 315° 1.7X

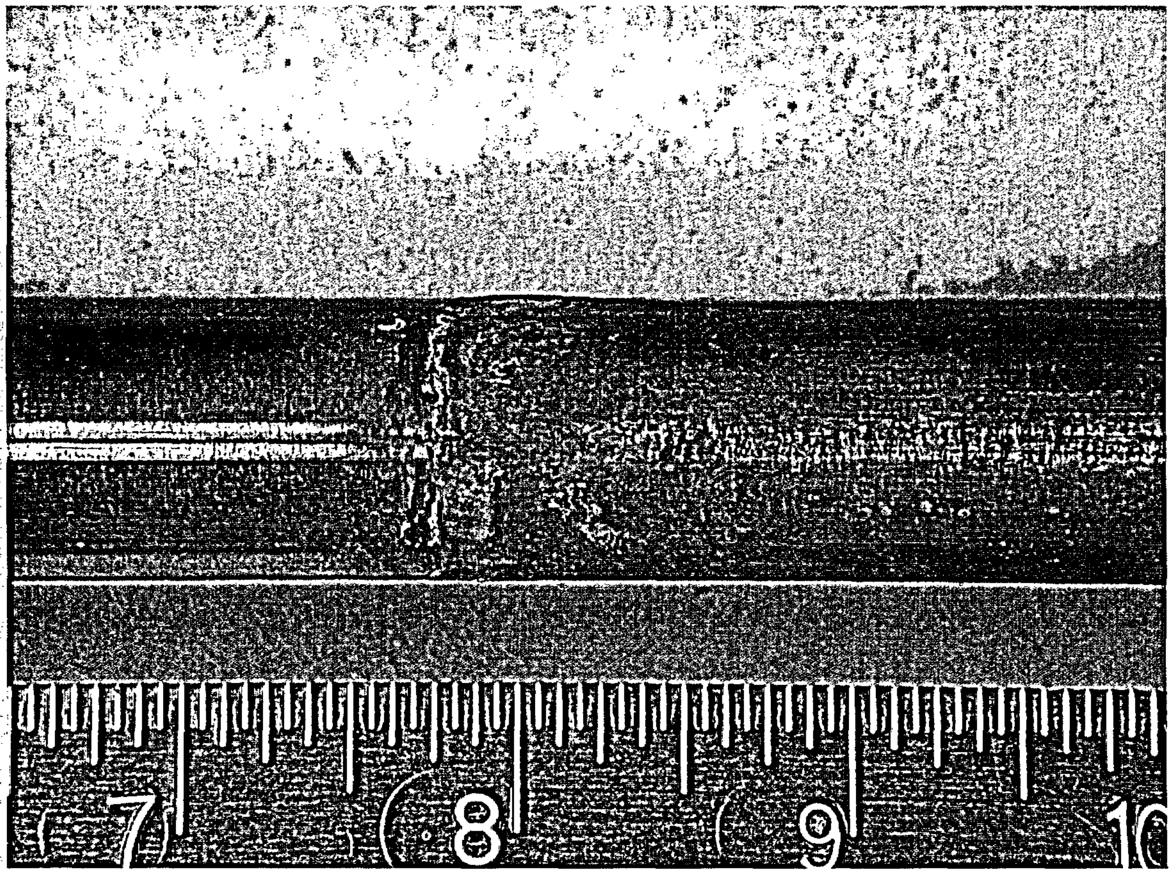

Figure 16: 2H TSP region at 0° 1.7X

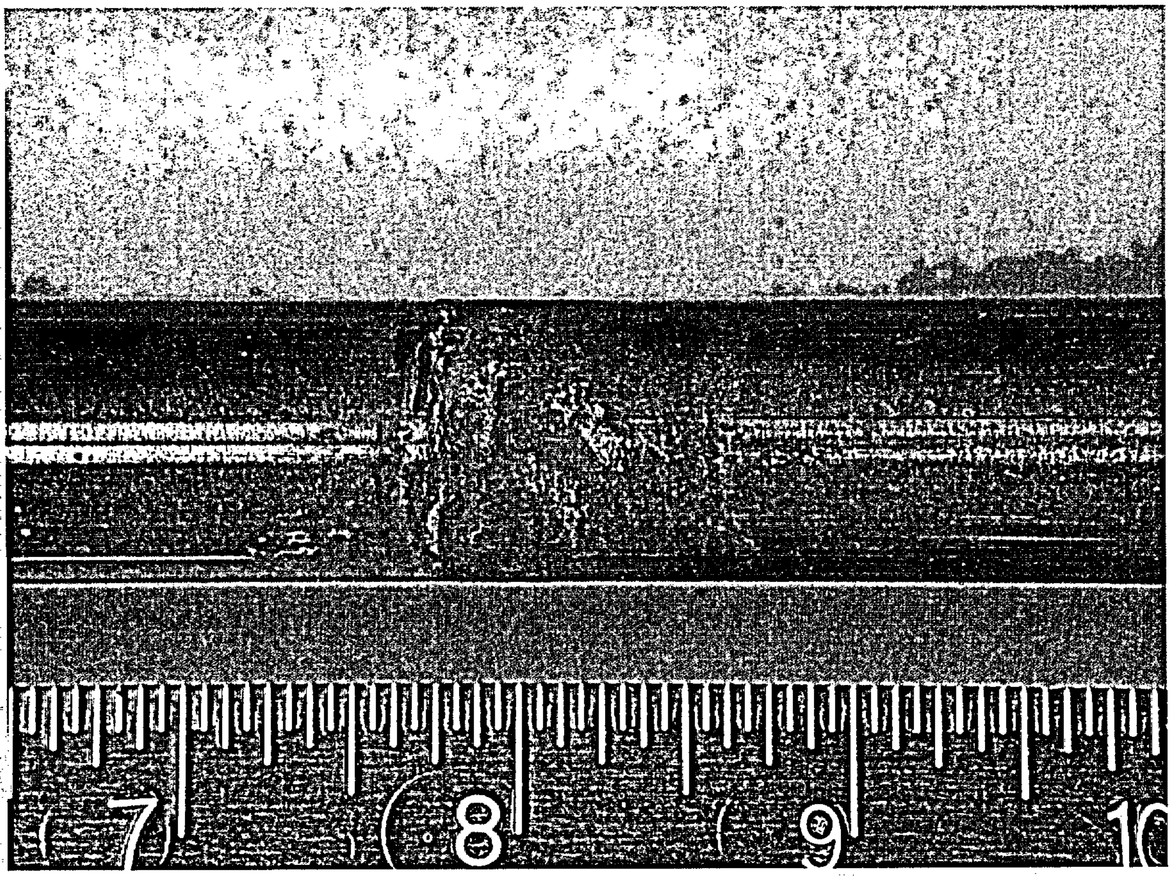

Figure 17: 2H TSP region at 45° 1.7X

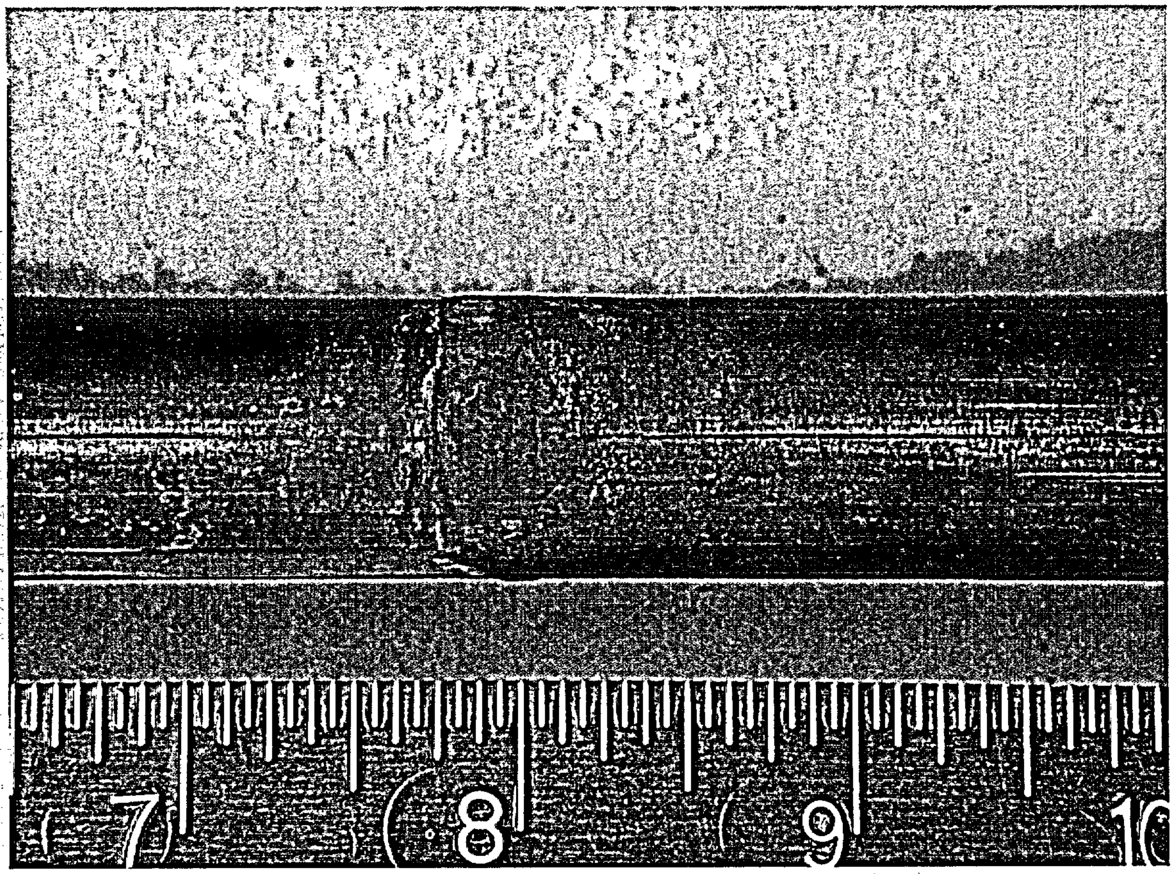

Figure 18: 2H TSP region at 90° 1.7X

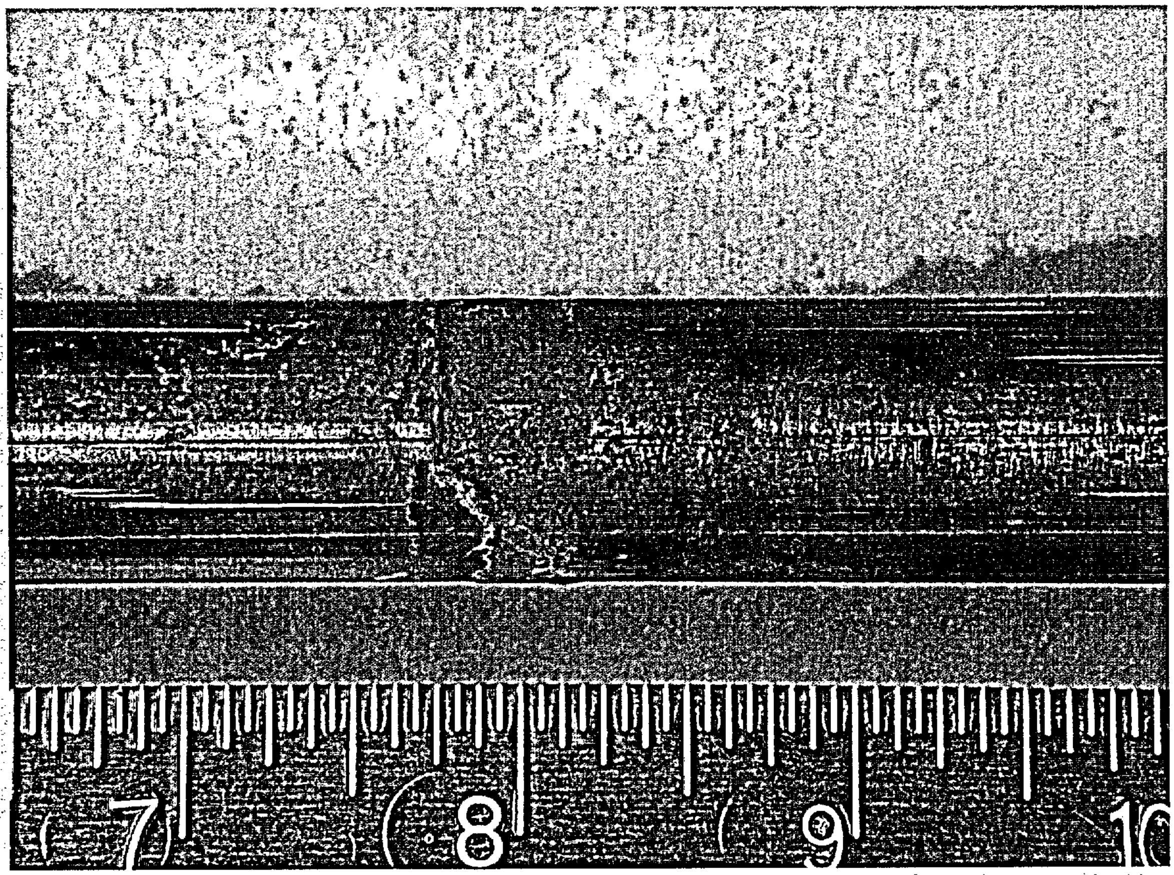

Figure 19: 2H TSP region at 135° 1.7X

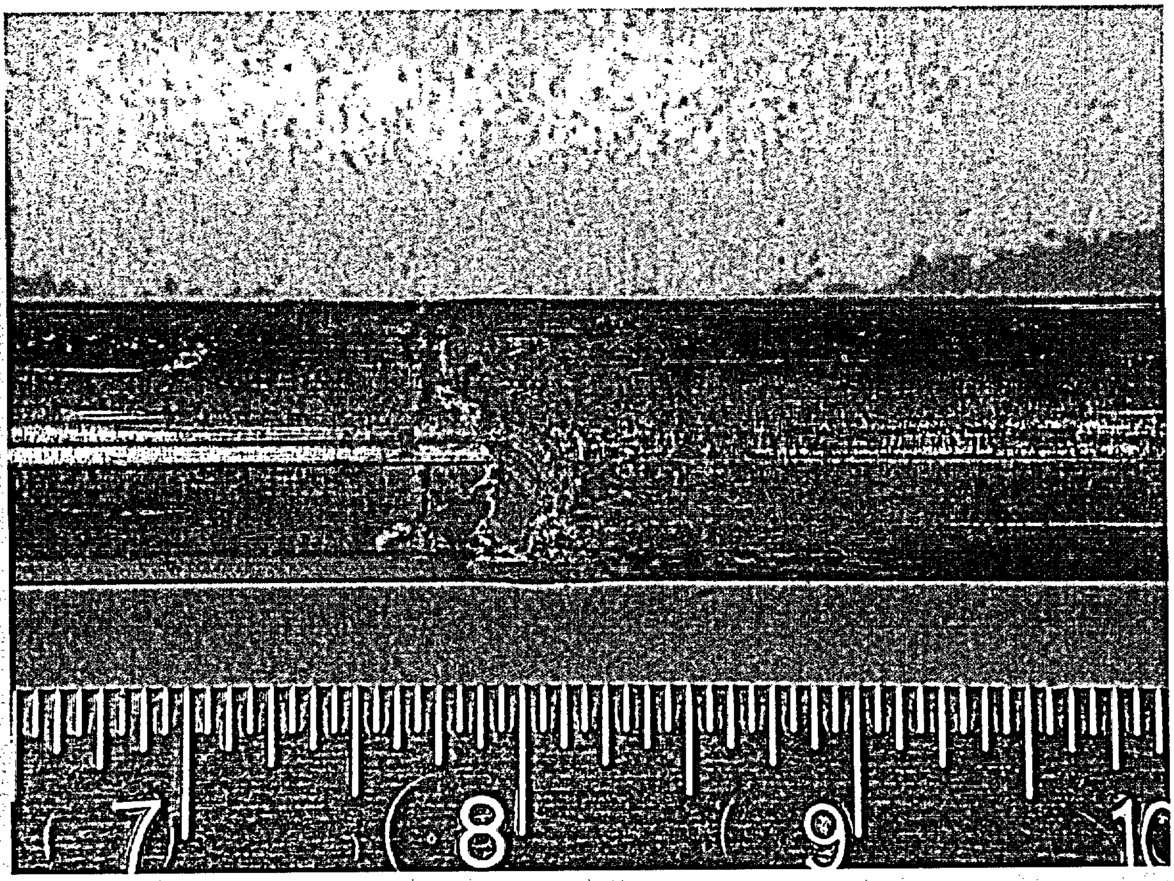

Figure 20: 2H TSP region at 180° 1.7X

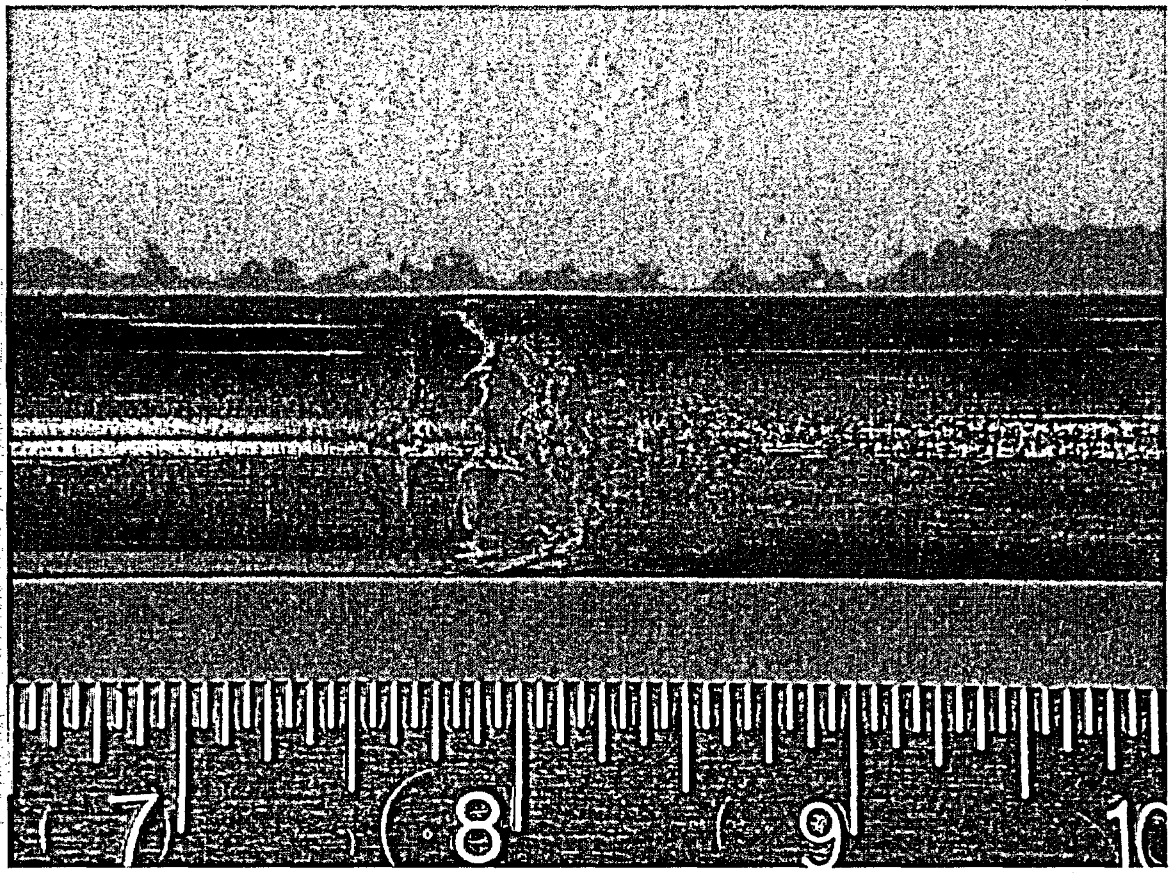

Figure 21: 2H TSP region at 225° 1.7X

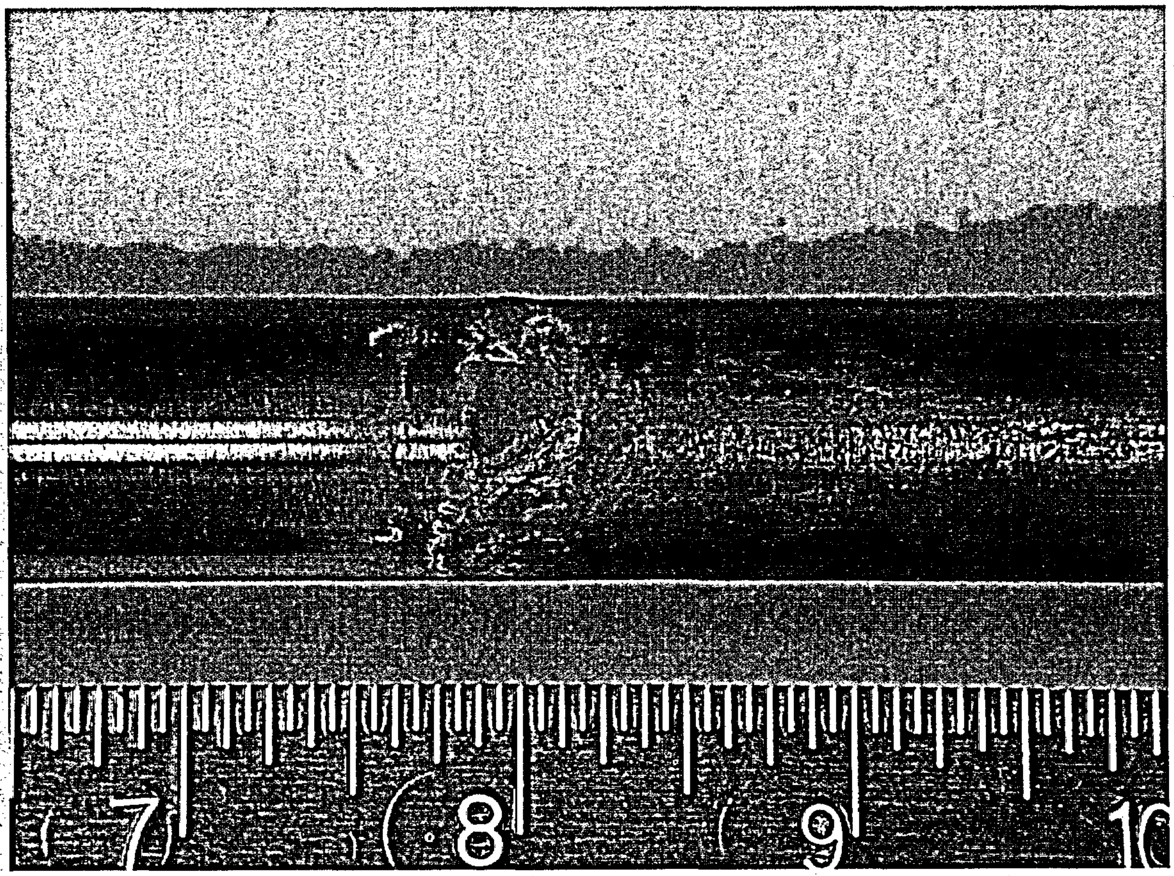

Figure 22: 2H TSP region at 270° 1.7X

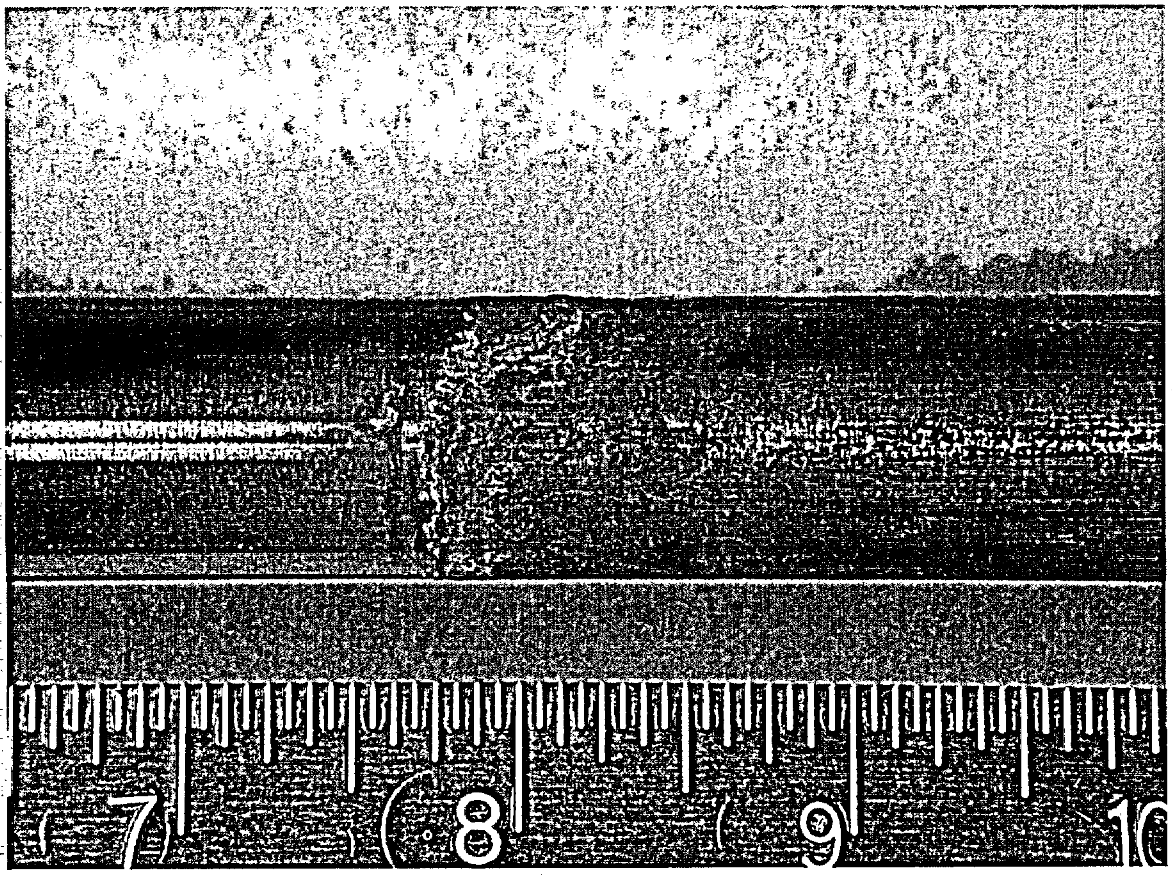

Figure 23: 2H TSP region at 315° 1.7X

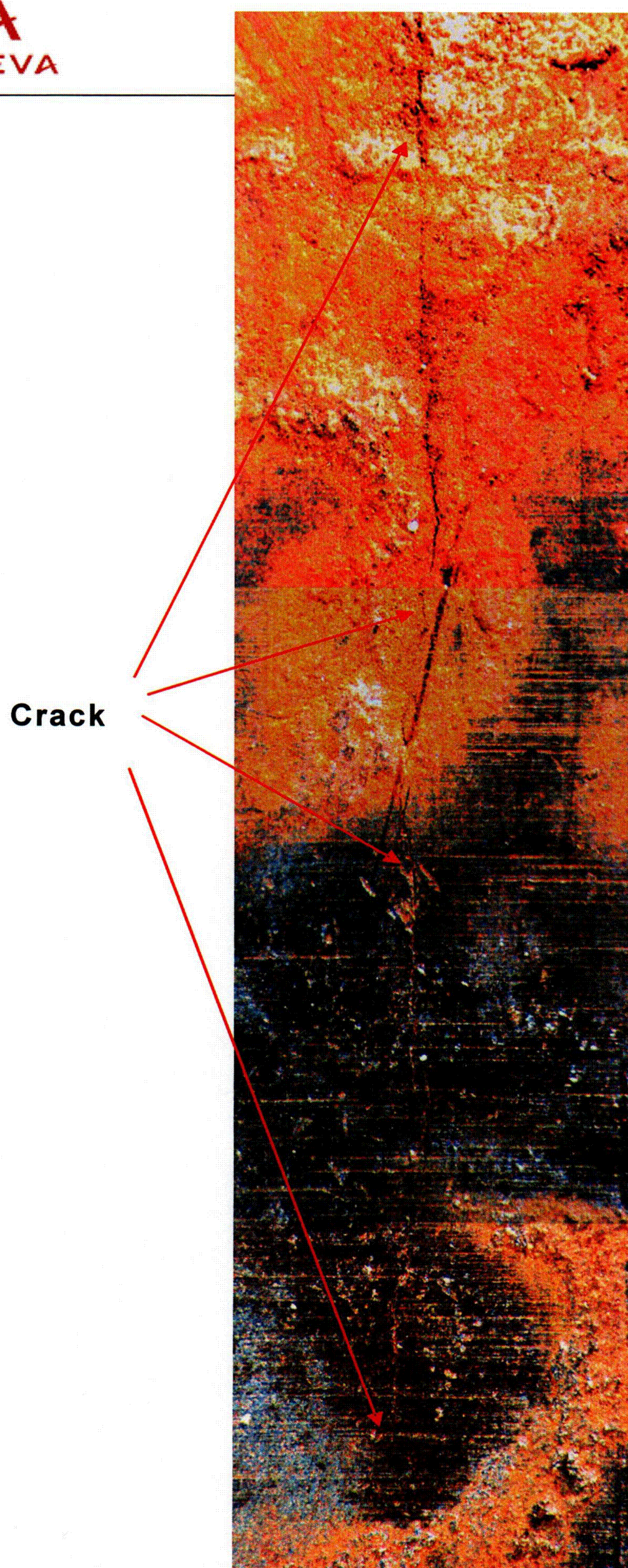

Figure 24: Axial crack at ~19° in the 1H TSP 25.7X

C04

Figure 25: Small axial cracks near 285° in 1H. 83X

C05

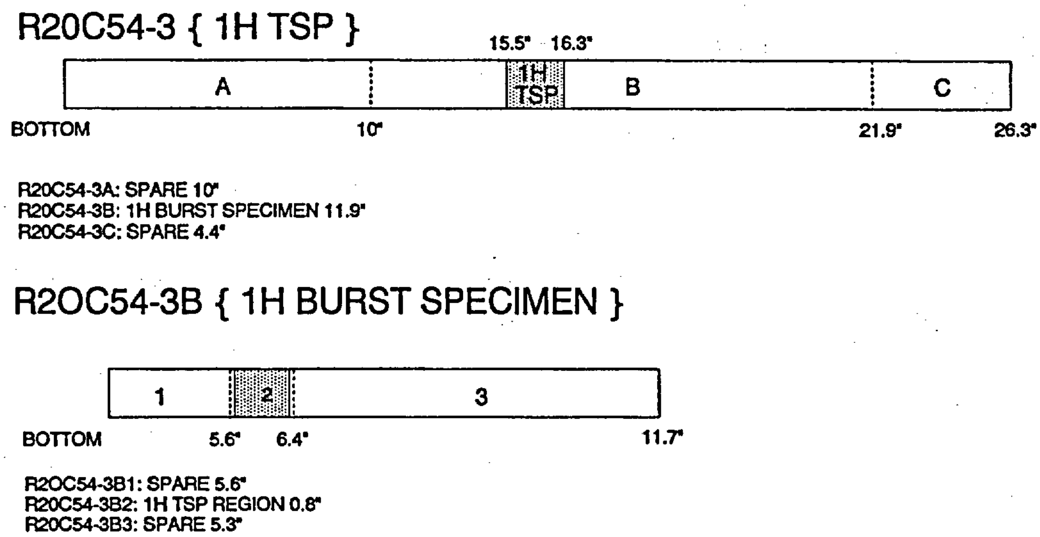

Figure 26: Overall sectioning diagram for R20C54-3B (1H TSP)

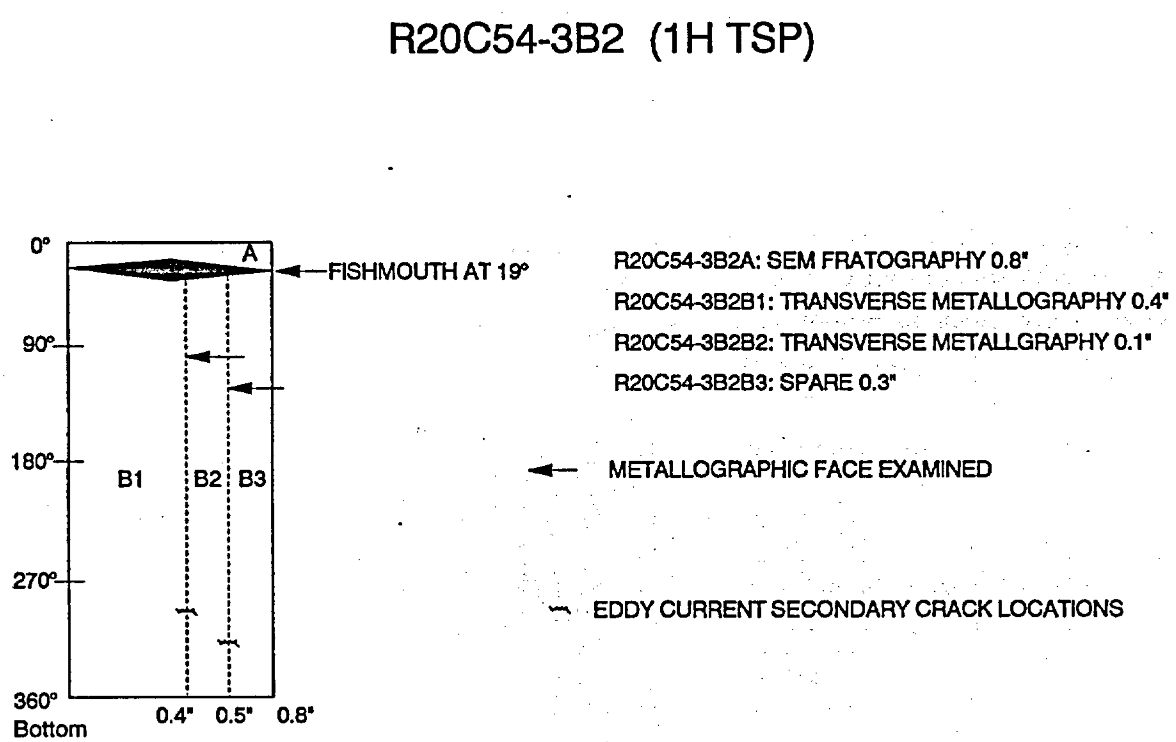

Figure 27: Sectioning of R20C54-3B2 for fractography and metallography

R20C54-4 (FREESPAN)

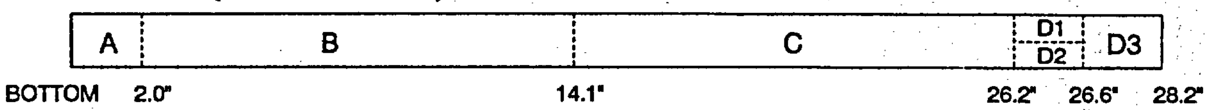

R20C54-4A: BULK CHEMISTRY 2.0"
R20C54-4B: FREESPAN BURST SPECIMEN 12.1"
R20C54-4C: TENSILE TEST 12.1"
R20C54-4D1: LONGITUDINAL METALLOGRAPHY 0.4"
R20C54-4D2: SPARE 0.4"
R20C54-4D3: SPARE 1.6"

R20C54-4B

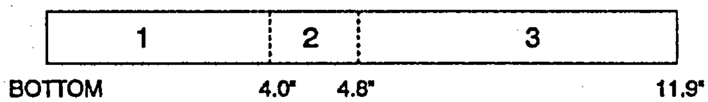

R20C54-4B1: SPARE 4.0"
R20C54-4B2: FISHMOUTH BURST REGION 0.8"
R20C54-4B3: SPARE 7.1"

Figure 28: Overall sectioning diagram for R20C54-4 (free span)

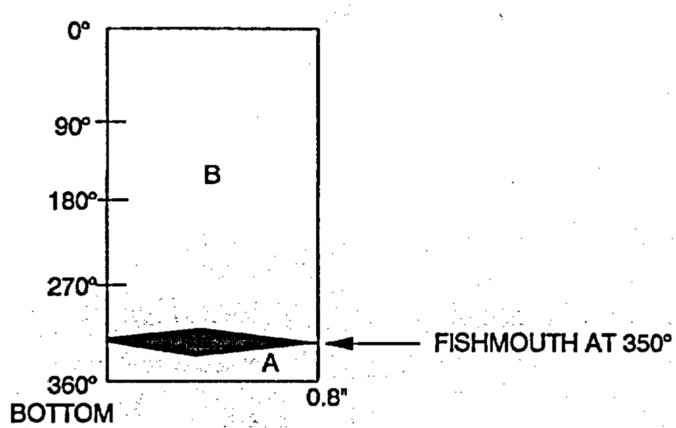

R20C54-4B2A: SEM 0.8"
R20C54-4B2B: SPARE 0.8"

Figure 29: Sectioning of R20C54-4B2 burst region for fractography

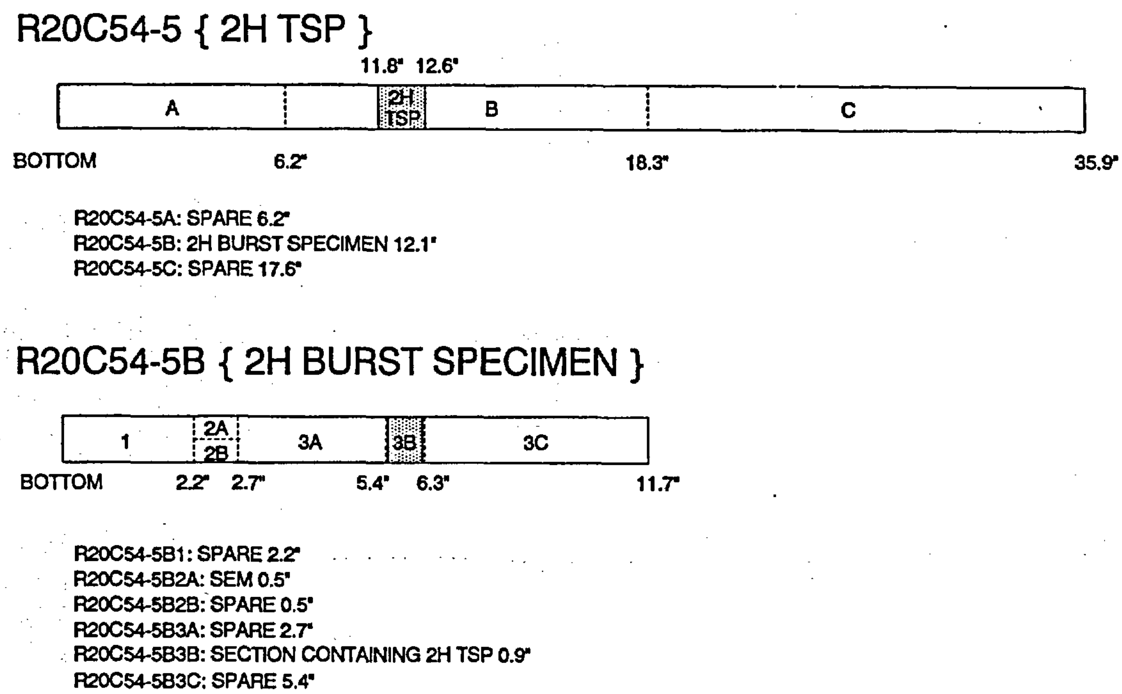

Figure 30: Overall sectioning diagram for R20C54-5 (2H TSP)

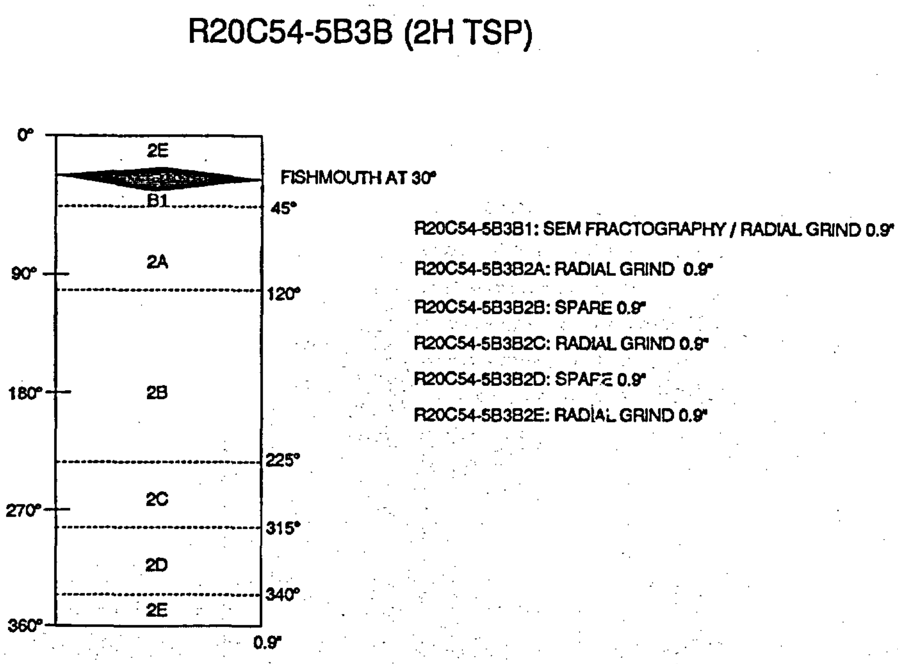

Figure 31: Sectioning of R20C54-5B3B for fractography and metallography

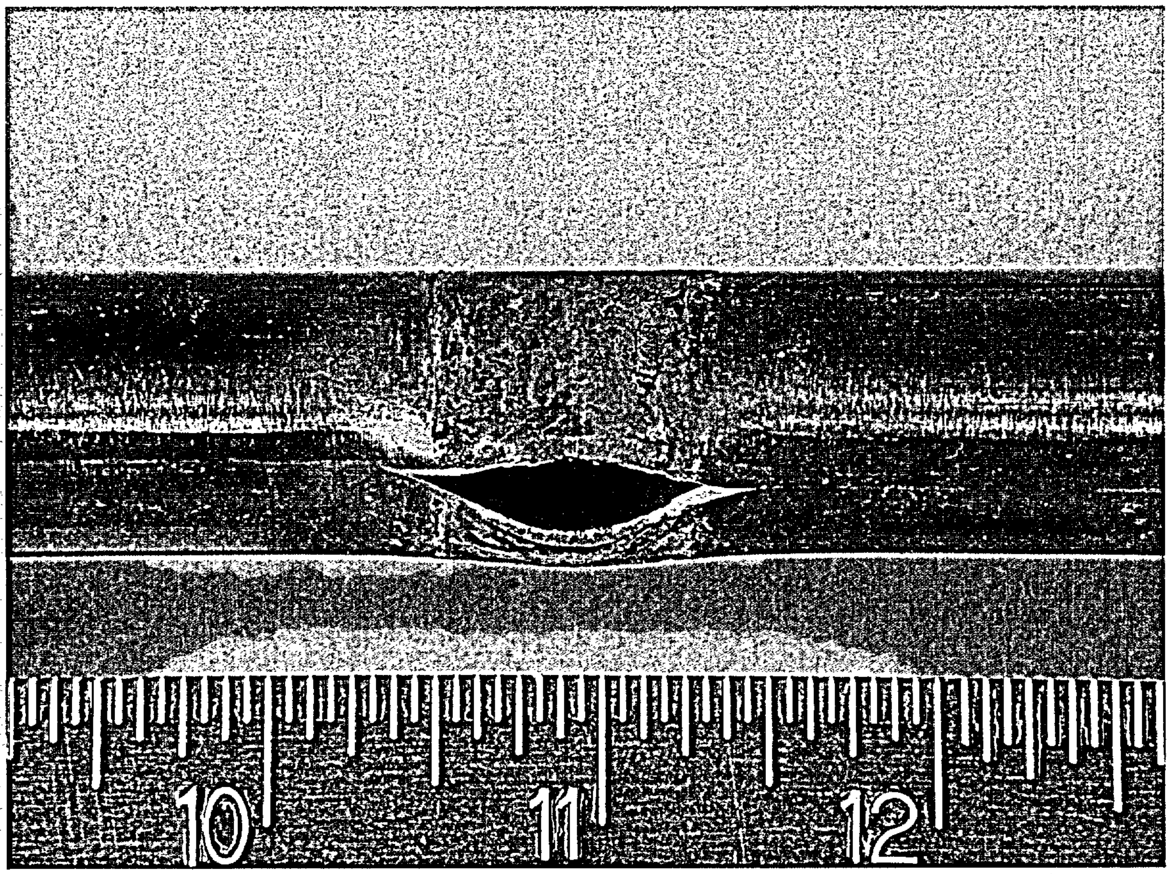

Figure 32: 1H TSP region at 0° after burst testing. 1.7X

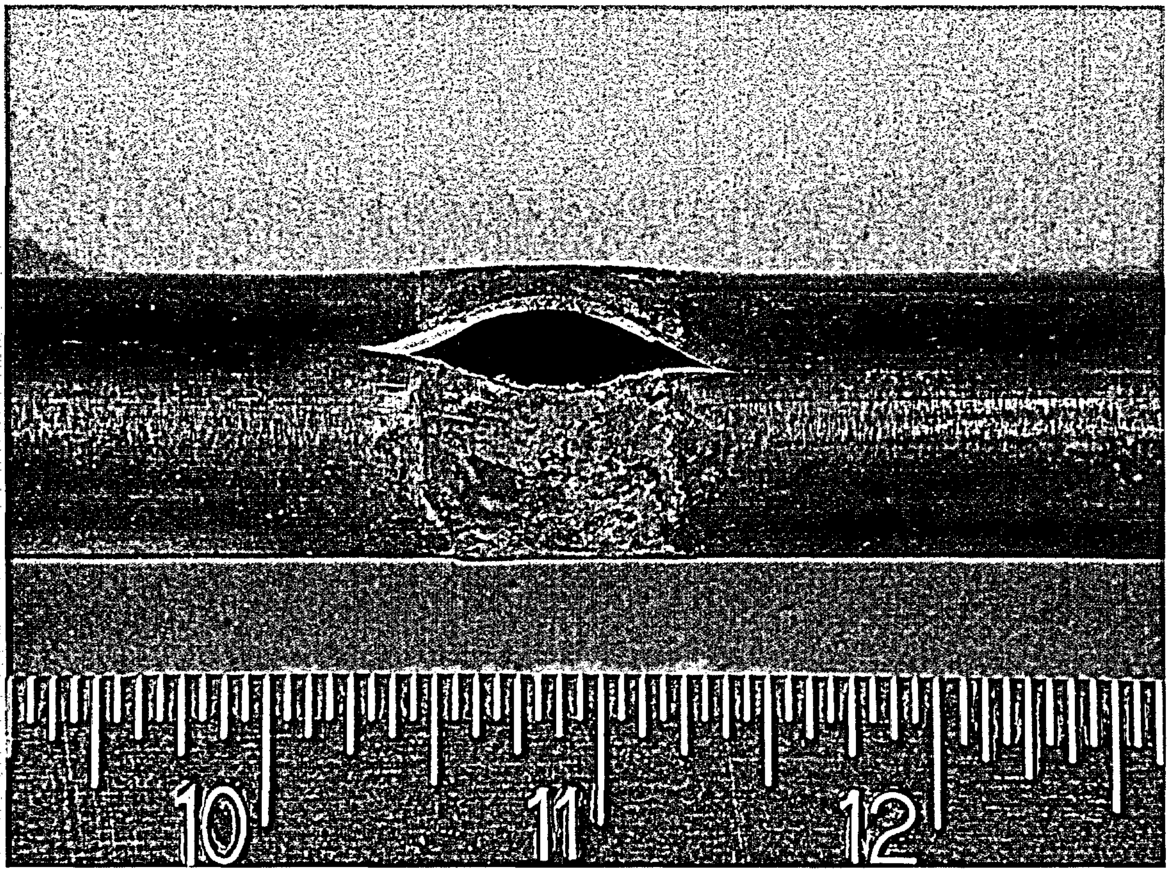

Figure 33: 1H TSP region at 45° after burst testing. 1.7X

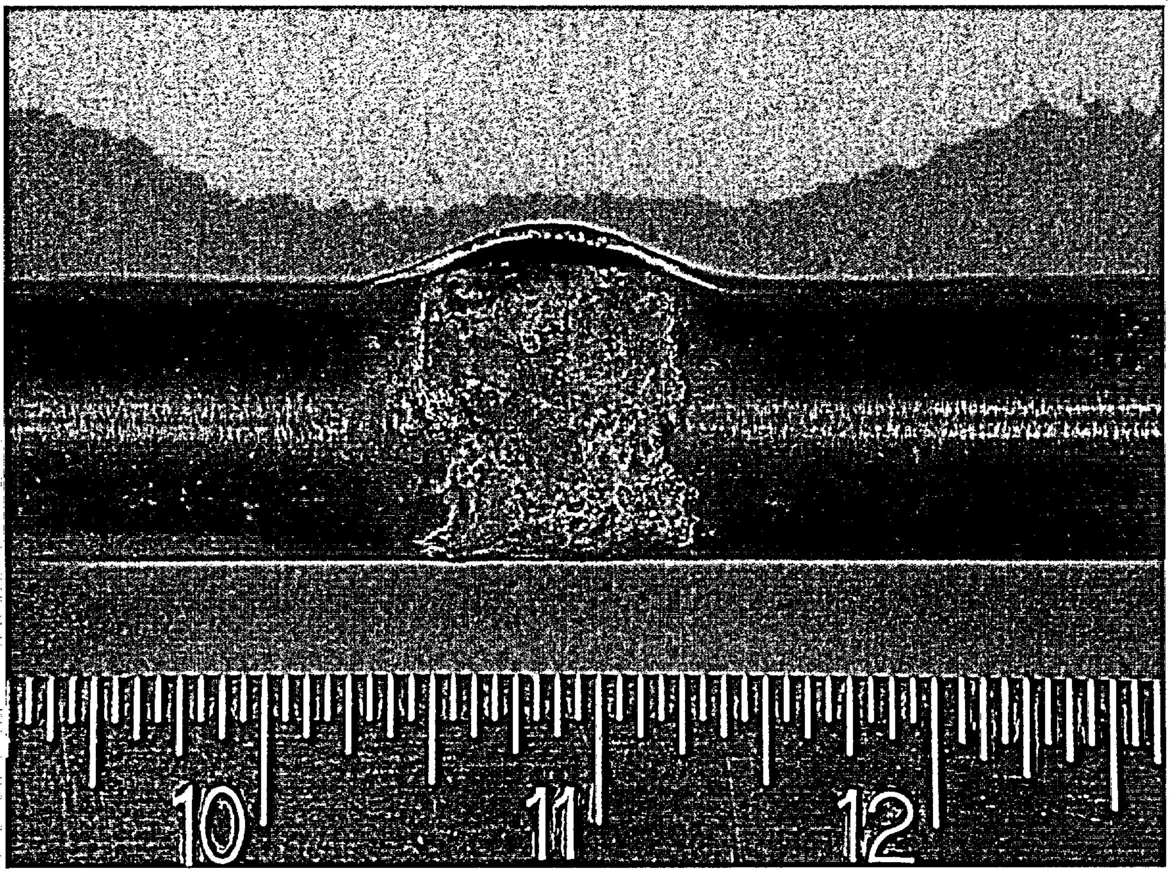

Figure 34: 1H TSP region at 90° after burst testing. 1.7X

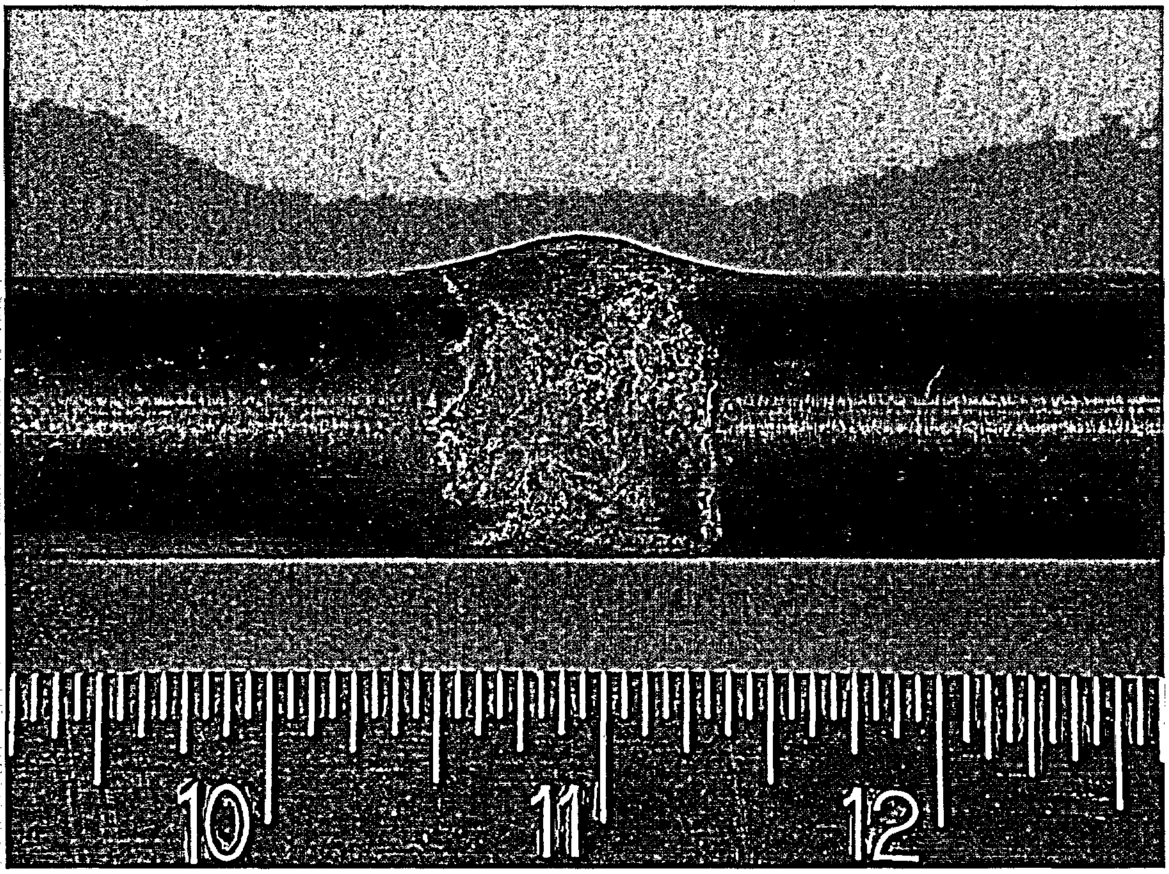

Figure 35: 1H TSP region at 135° after burst testing. 1.7X

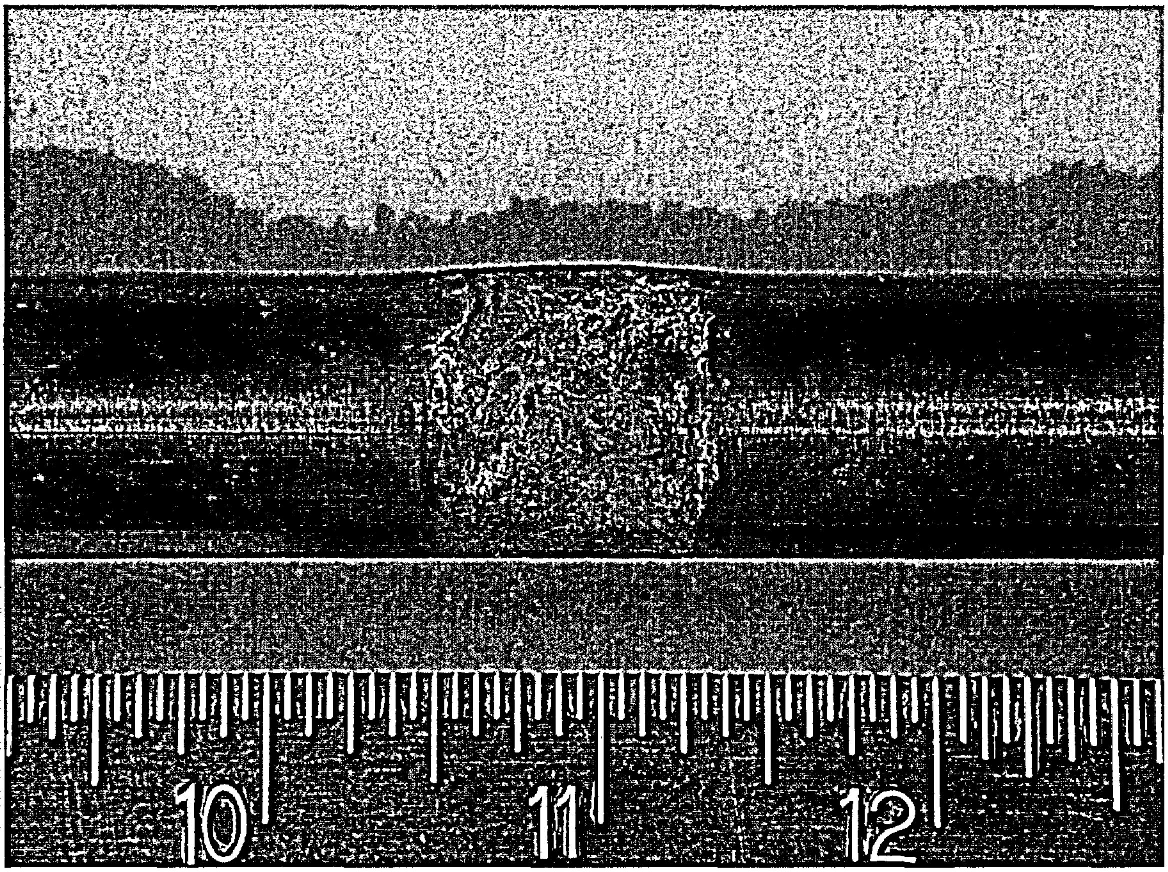

Figure 36: 1H TSP region at 180° after burst testing. 1.7X

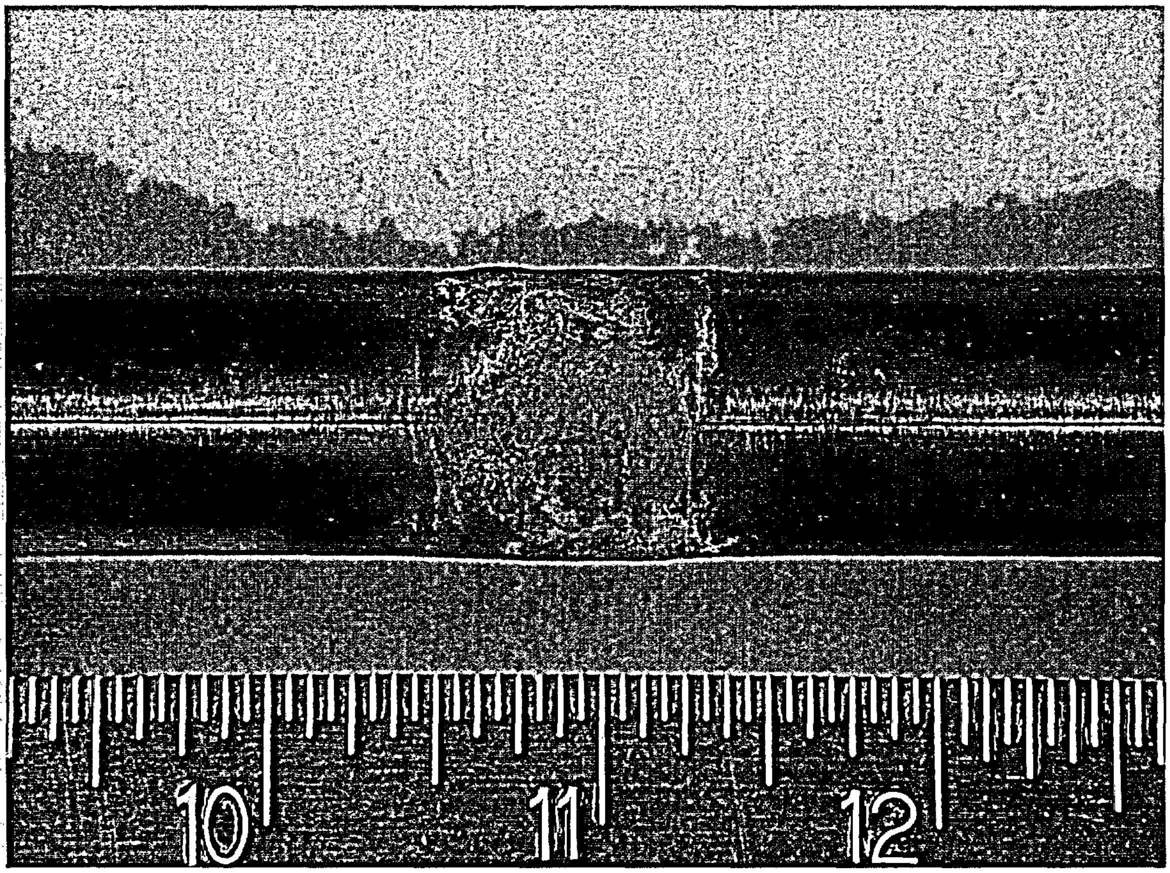

Figure 37: 1H TSP region at 225° after burst testing. 1.7X

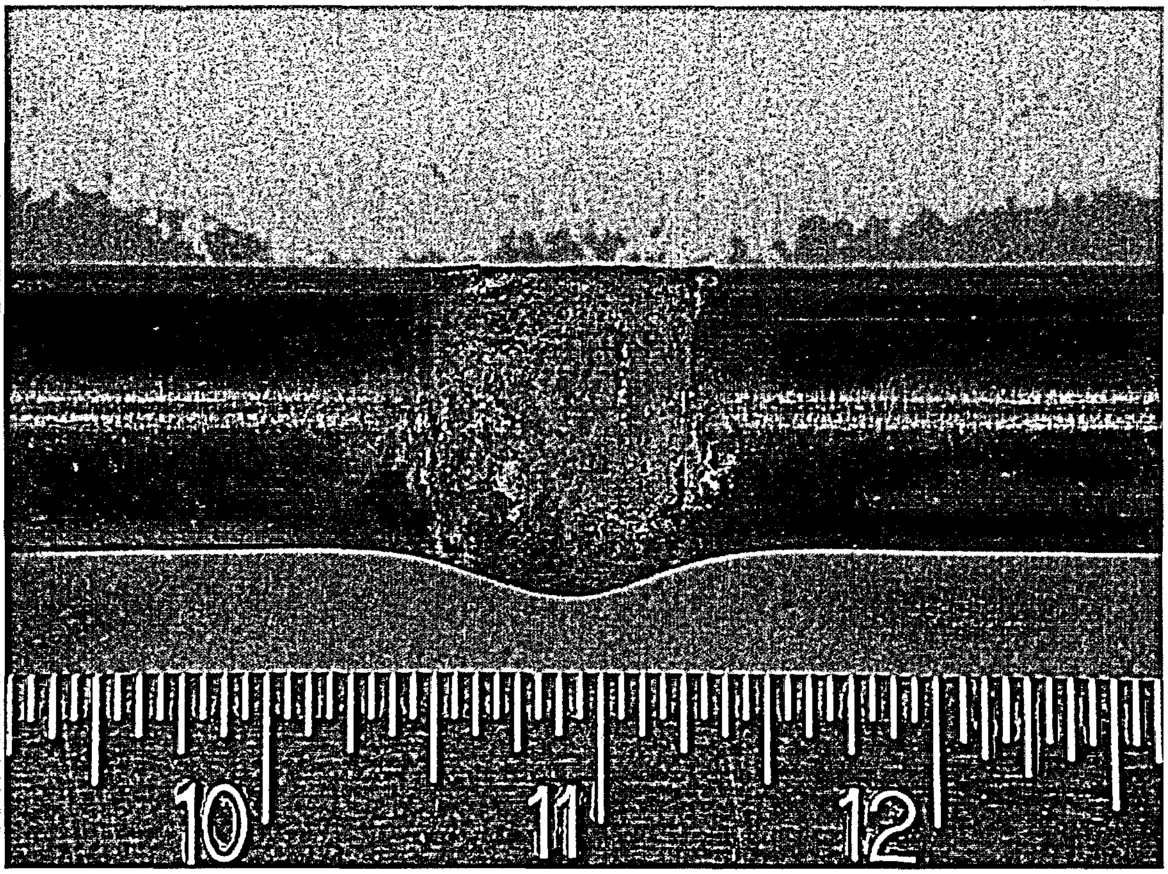

Figure 38: 1H TSP region at 270° after burst testing. 1.7X

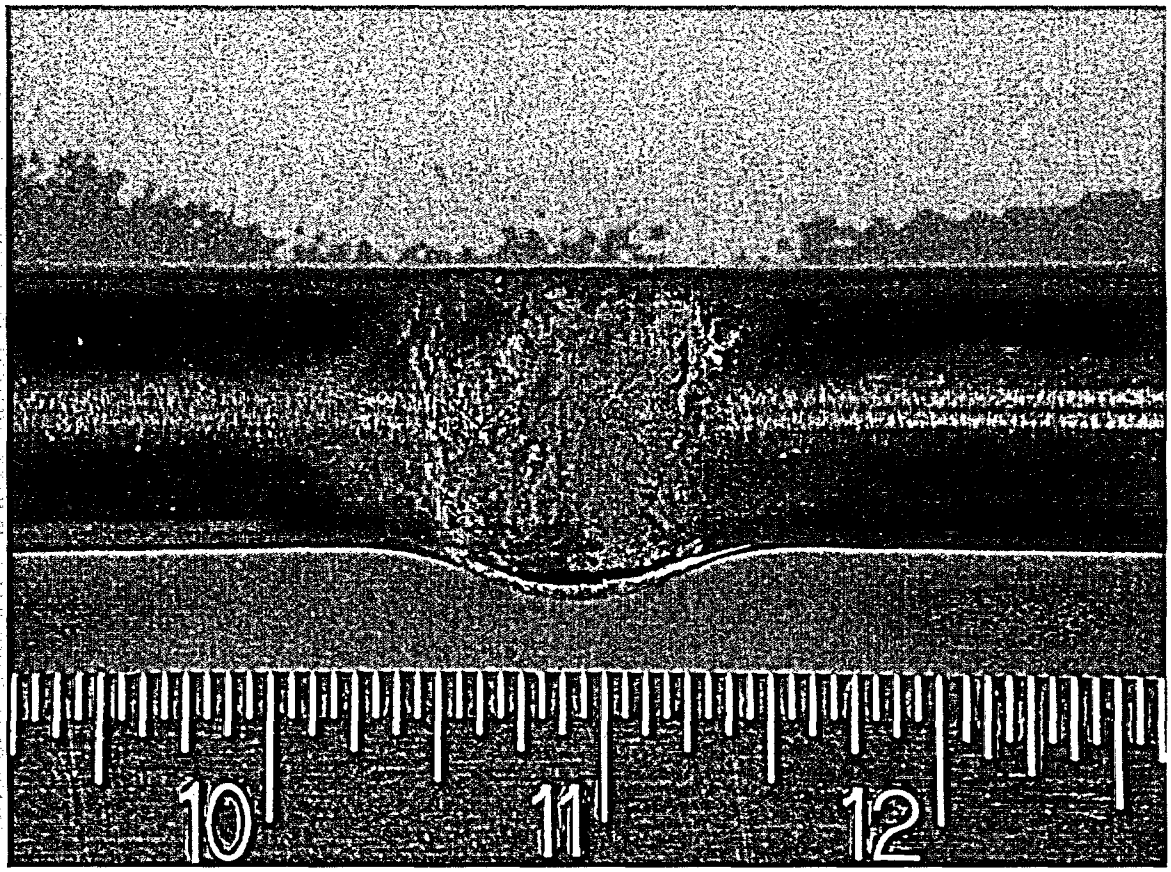

Figure 39: 1H TSP region at 315° after burst testing. 1.7X

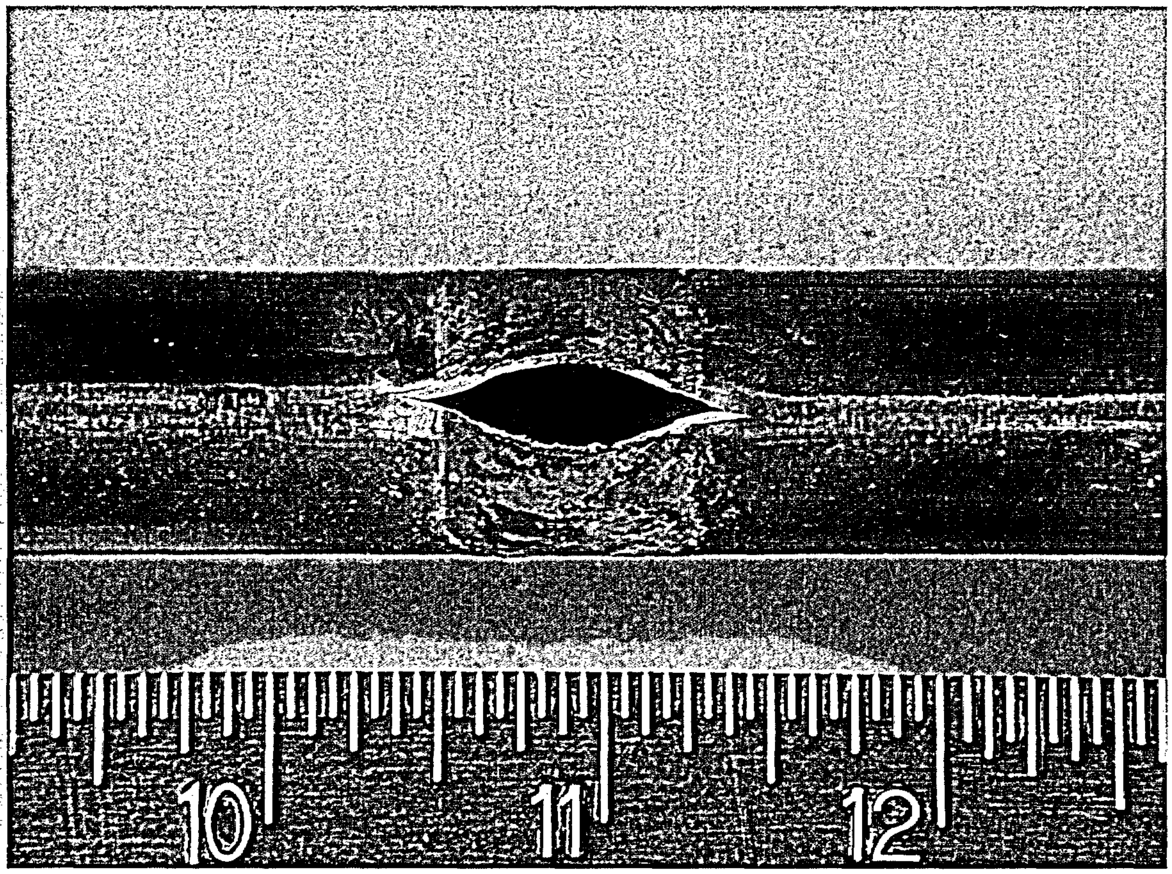

Figure 40: Burst centered at 19° in 1H TSP region. 1.7X

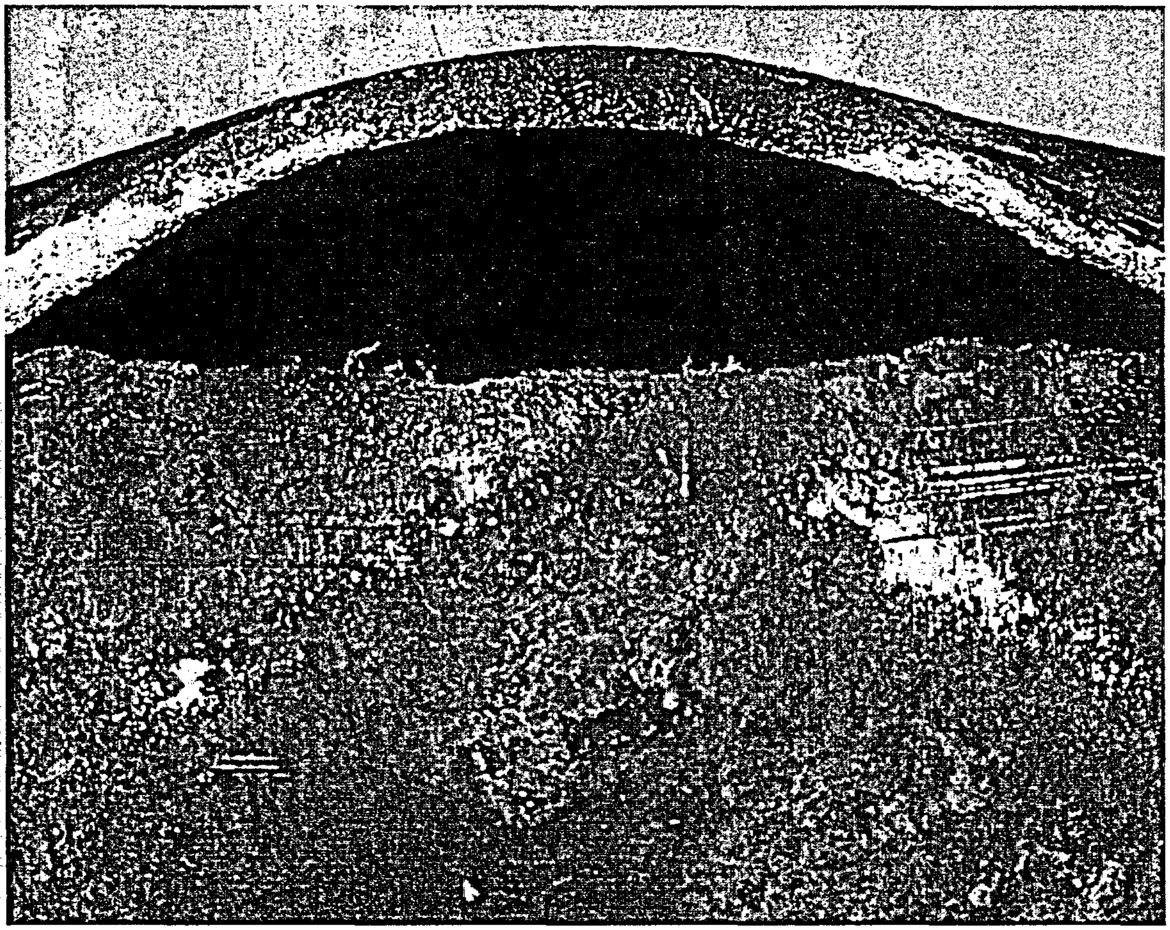

Figure 41: Oxidized corrosion area on counterclockwise burst rupture surface of 1H TSP.

8X

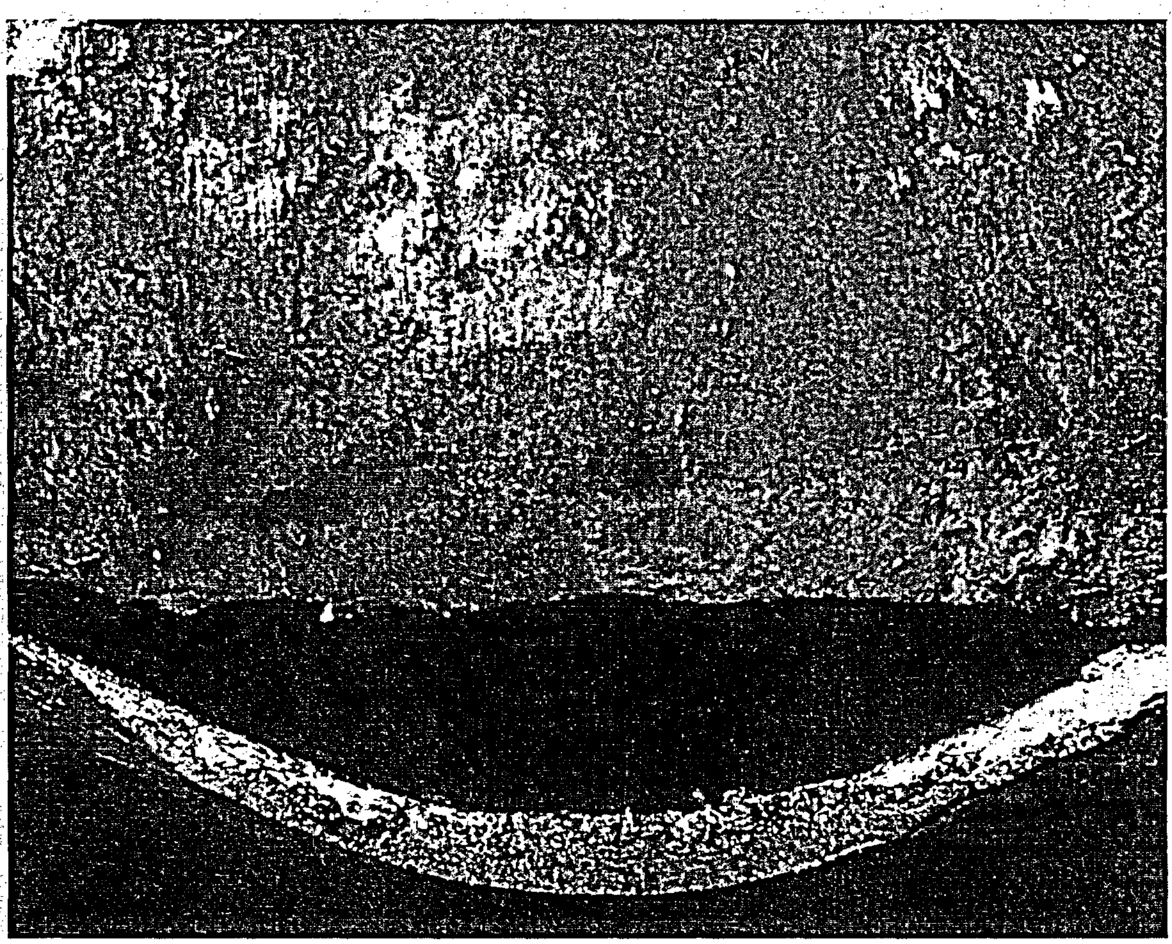

Figure 42: Oxidized corrosion area on clockwise burst rupture surface of 1H TSP. 8X

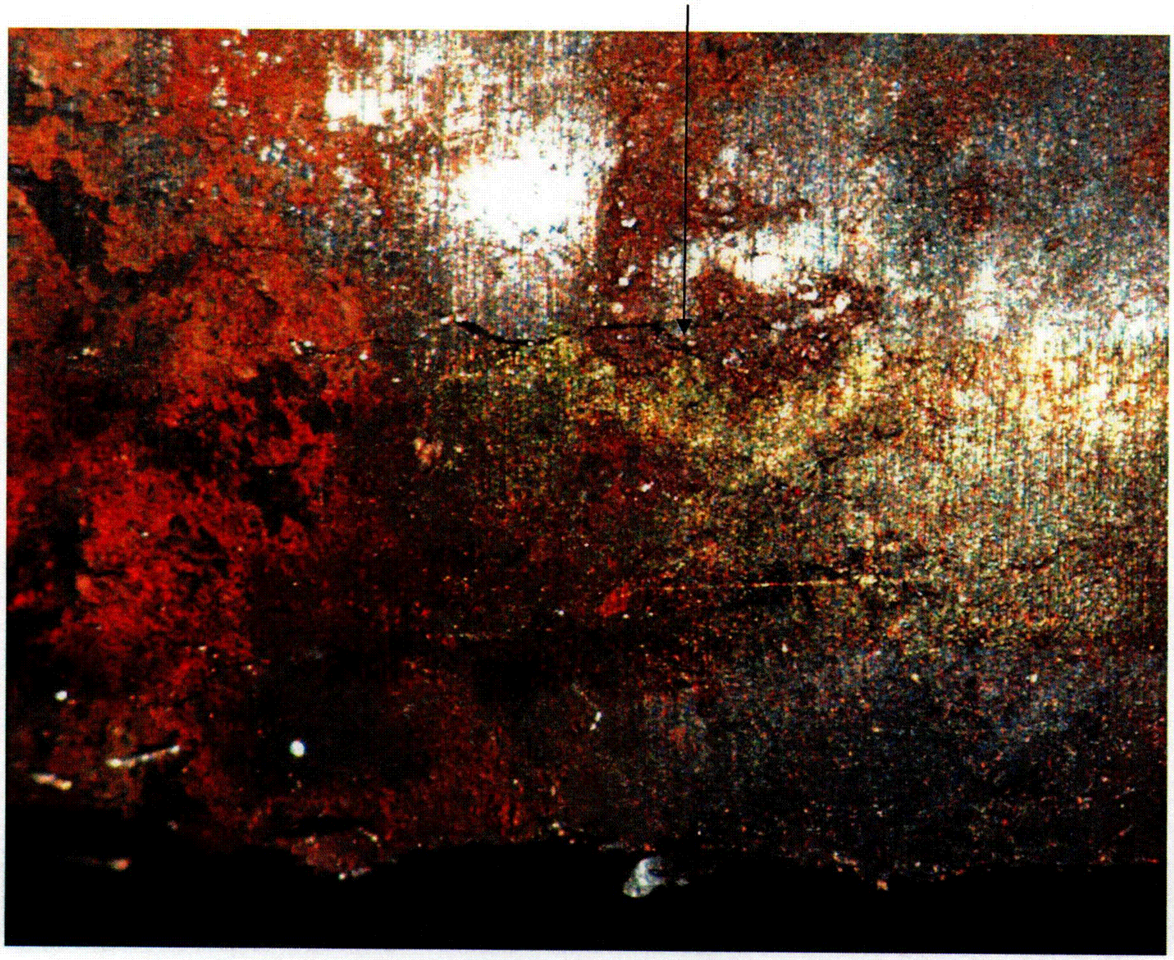

Figure 43: Secondary crack near 350° in 1H TSP, extending from ~0.1 inches to ~0.2 inches from the bottom of the TSP region. 16.6X

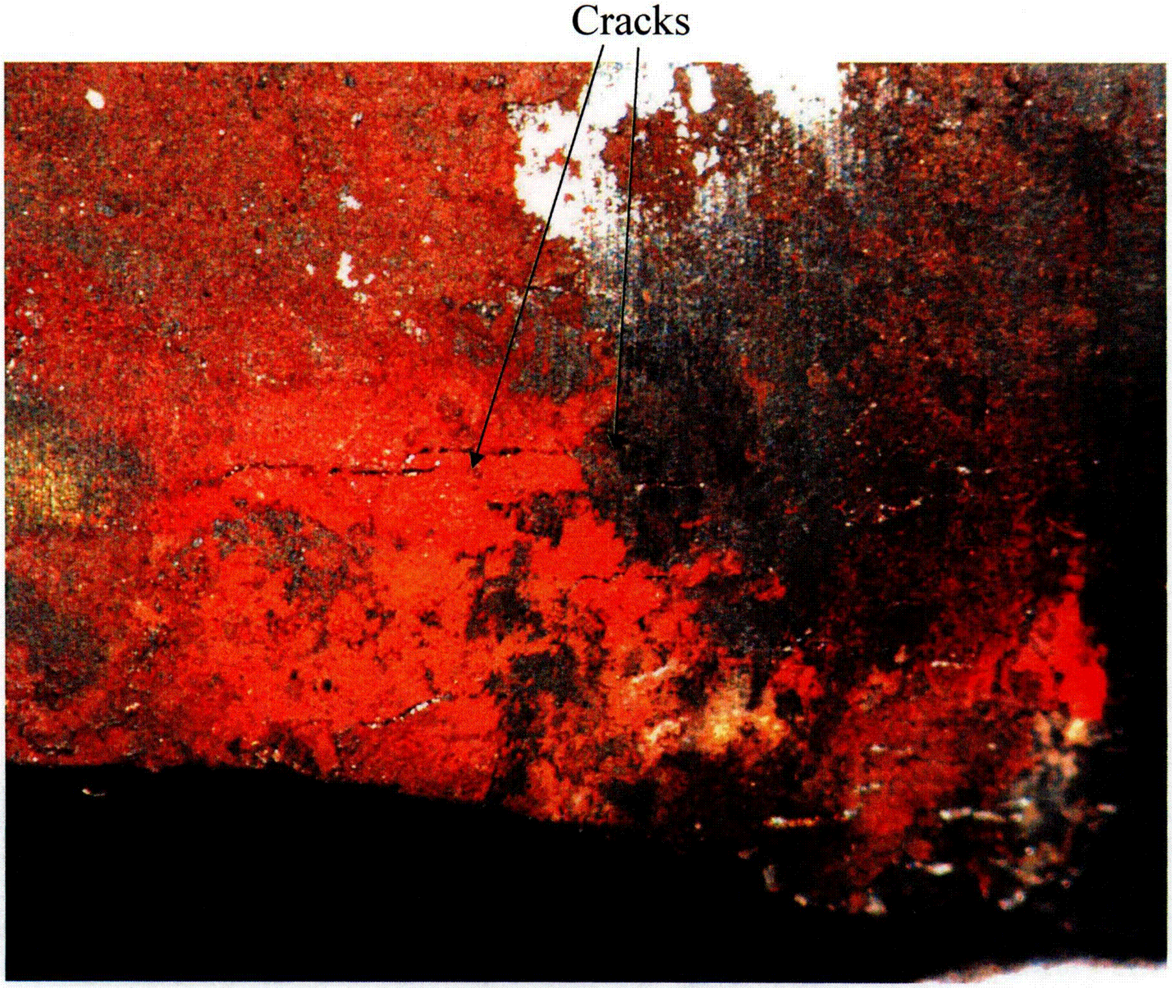

Figure 44: Secondary cracks near 355° in 1H TSP, extending from ~0.5 inches to ~0.7 inches From the bottom of the TSP region. 16.6X

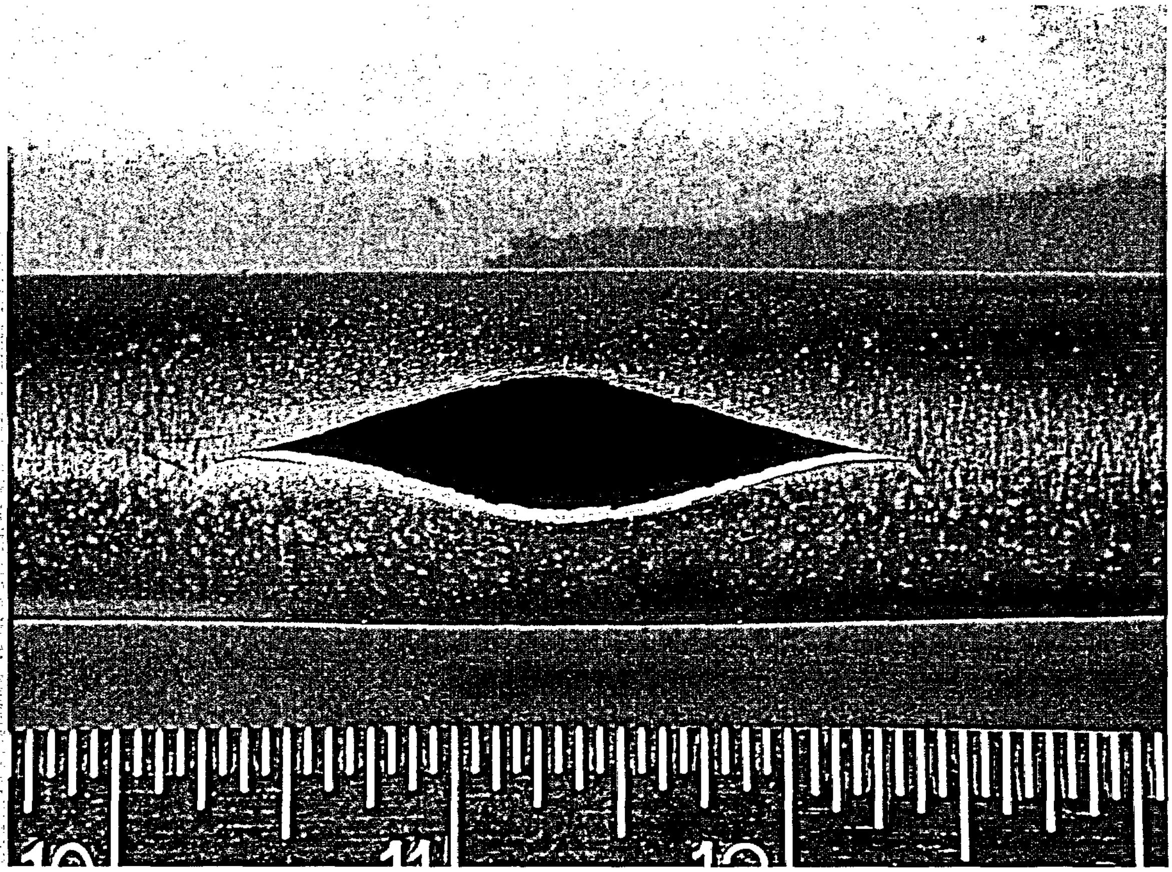

Figure 45: Fish mouth burst rupture at 350° in free span section. 1.7X

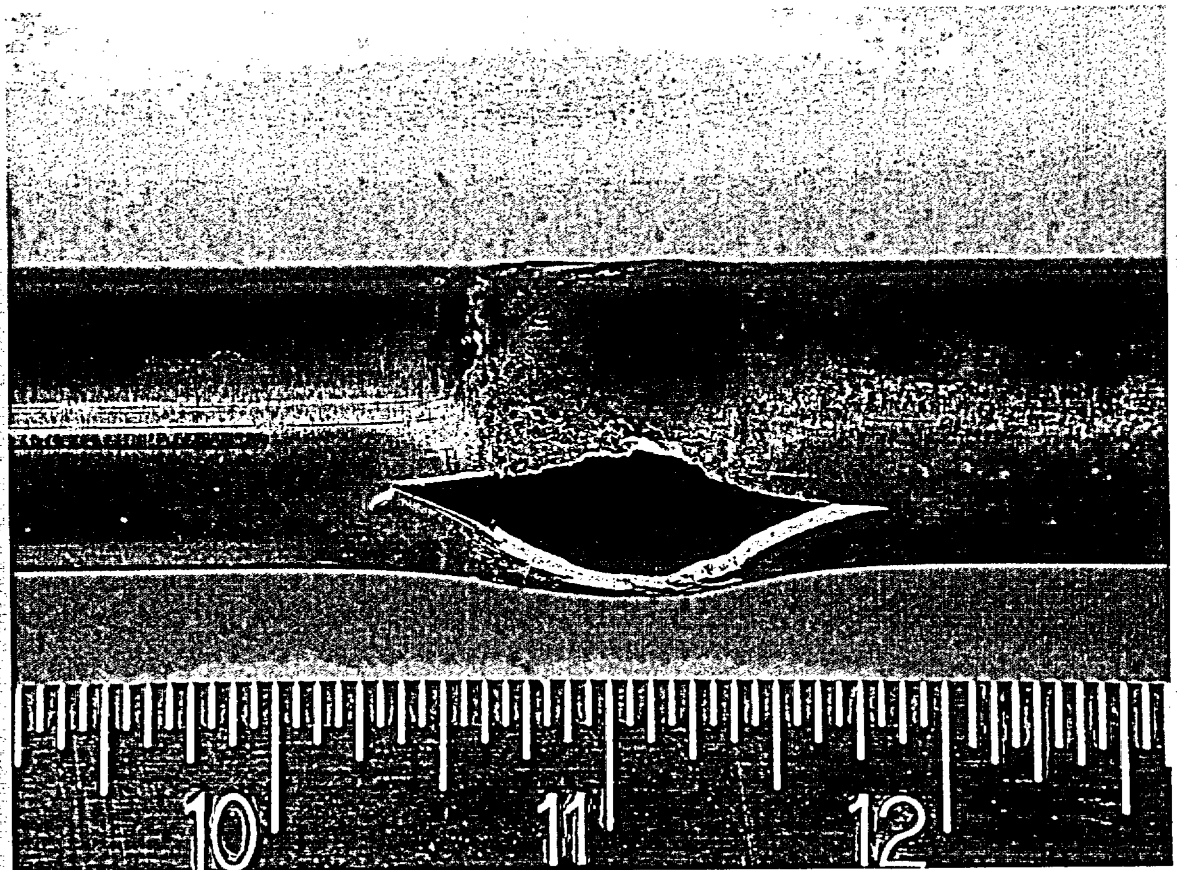

Figure 46: 2H TSP region at 0° after burst testing. 1.7X

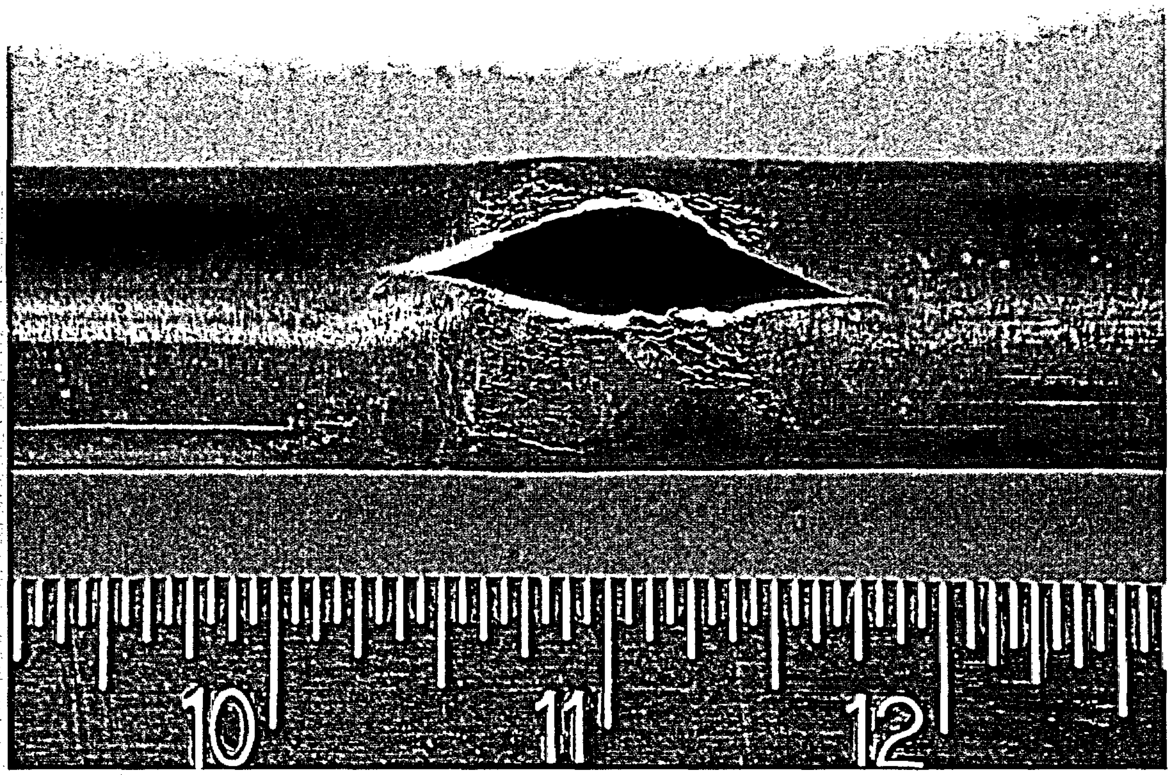

Figure 47: 2H TSP region at 45° after burst testing. 1.7X

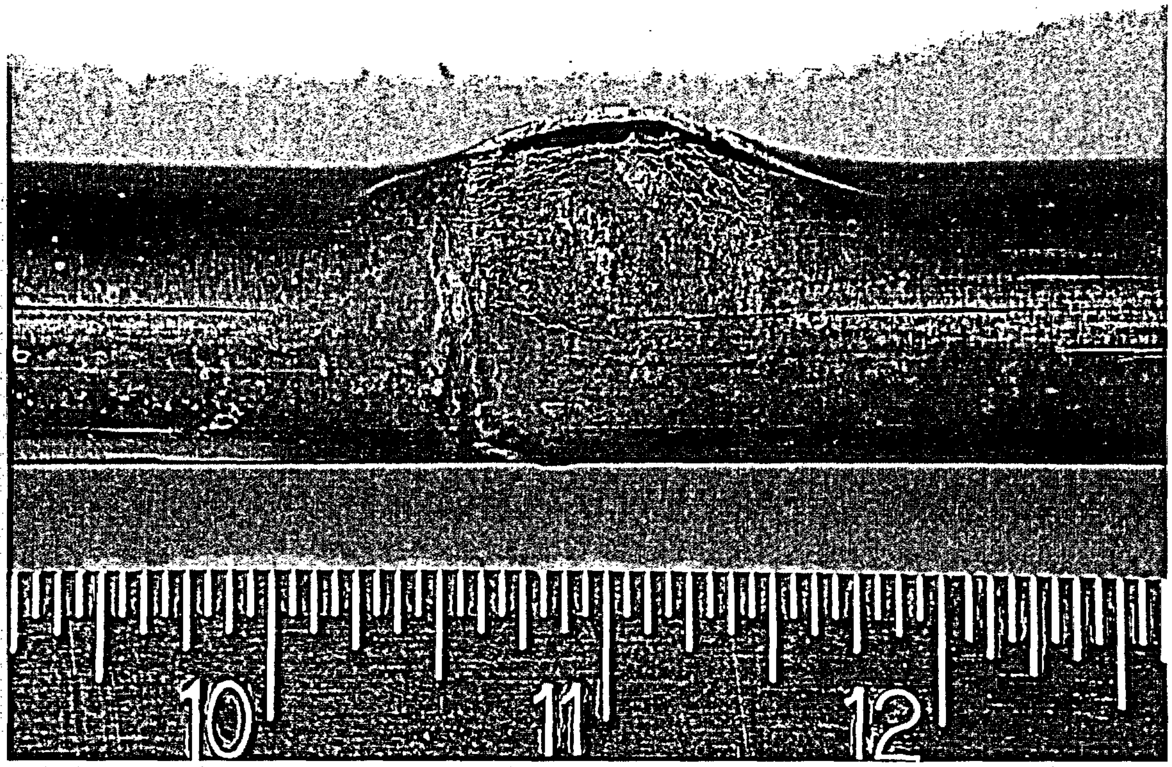

Figure 48: 2H TSP region at 90° after burst testing. 1.7X

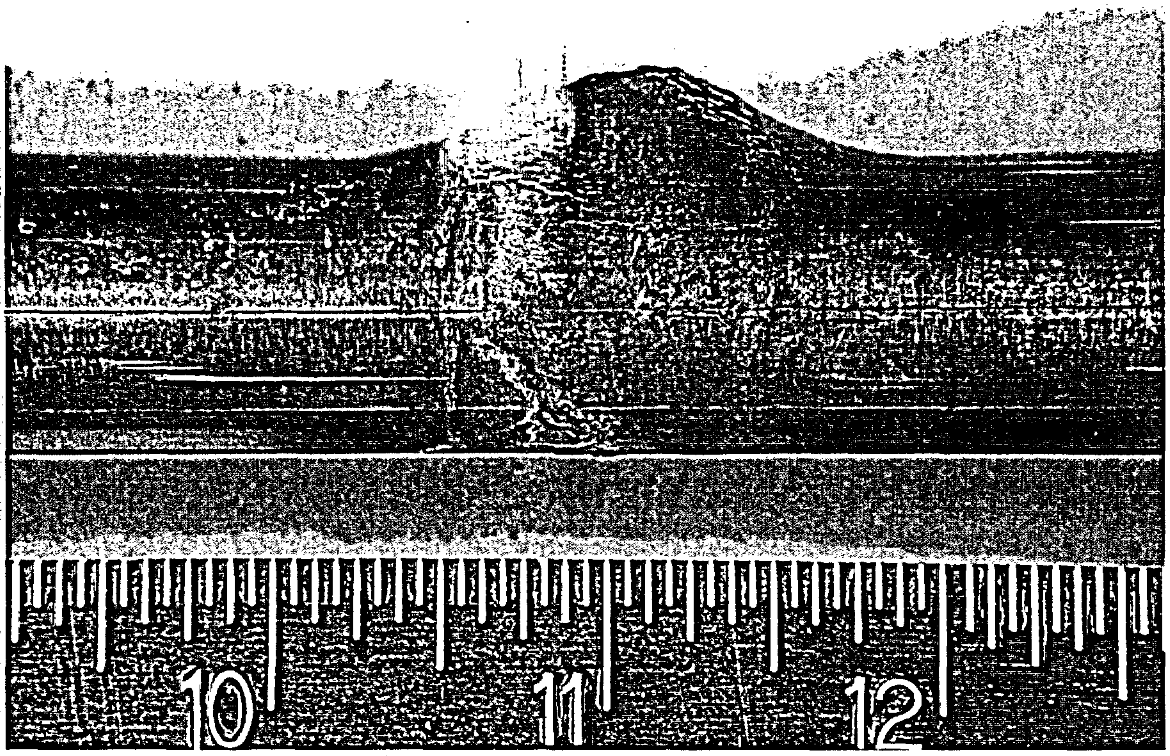

Figure 49: 2H TSP region at 135° after burst testing. 1.7X

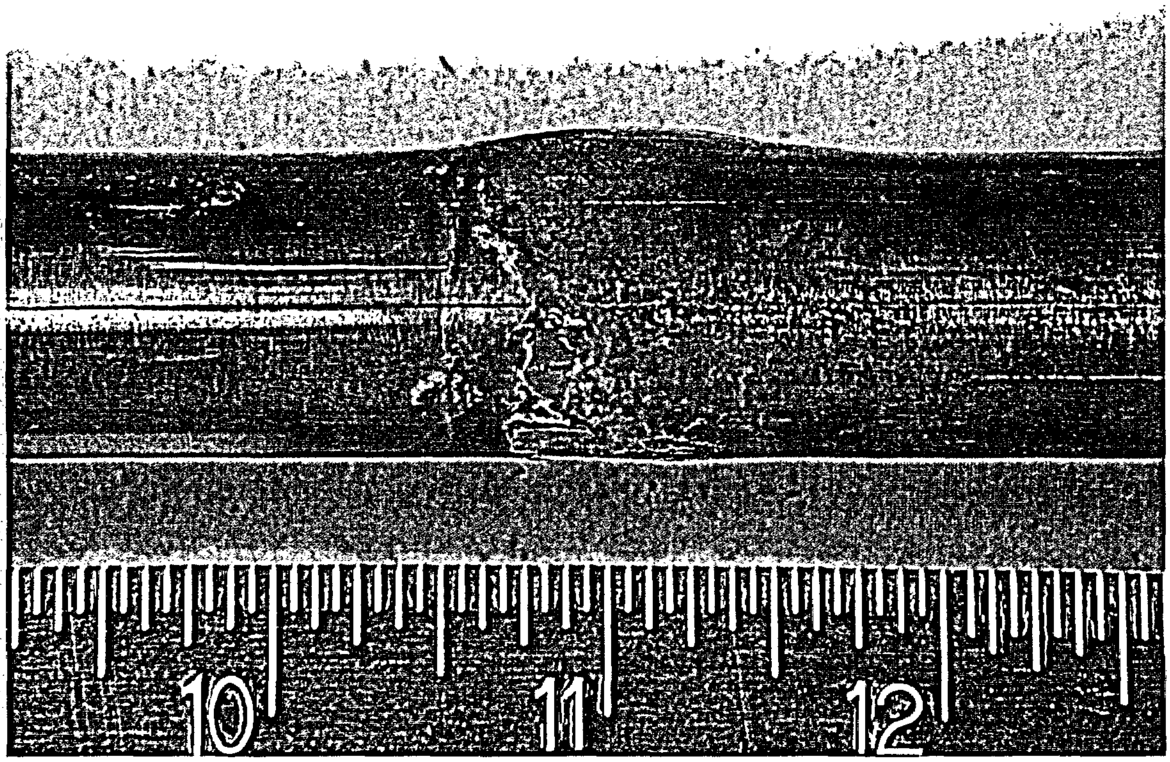

Figure 50: 2H TSP region at 180° after burst testing. 1.7X

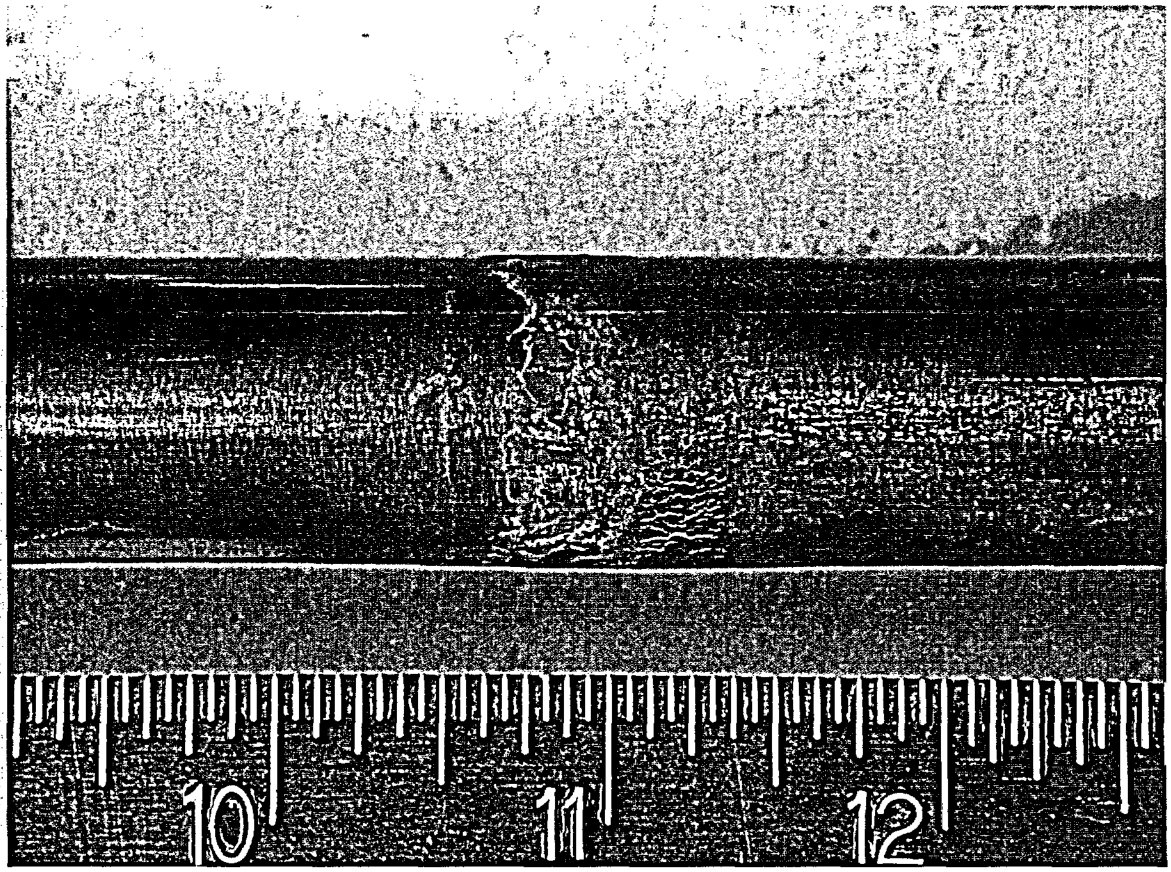

Figure 51: 2H TSP region at 225° after burst testing. 1.7X

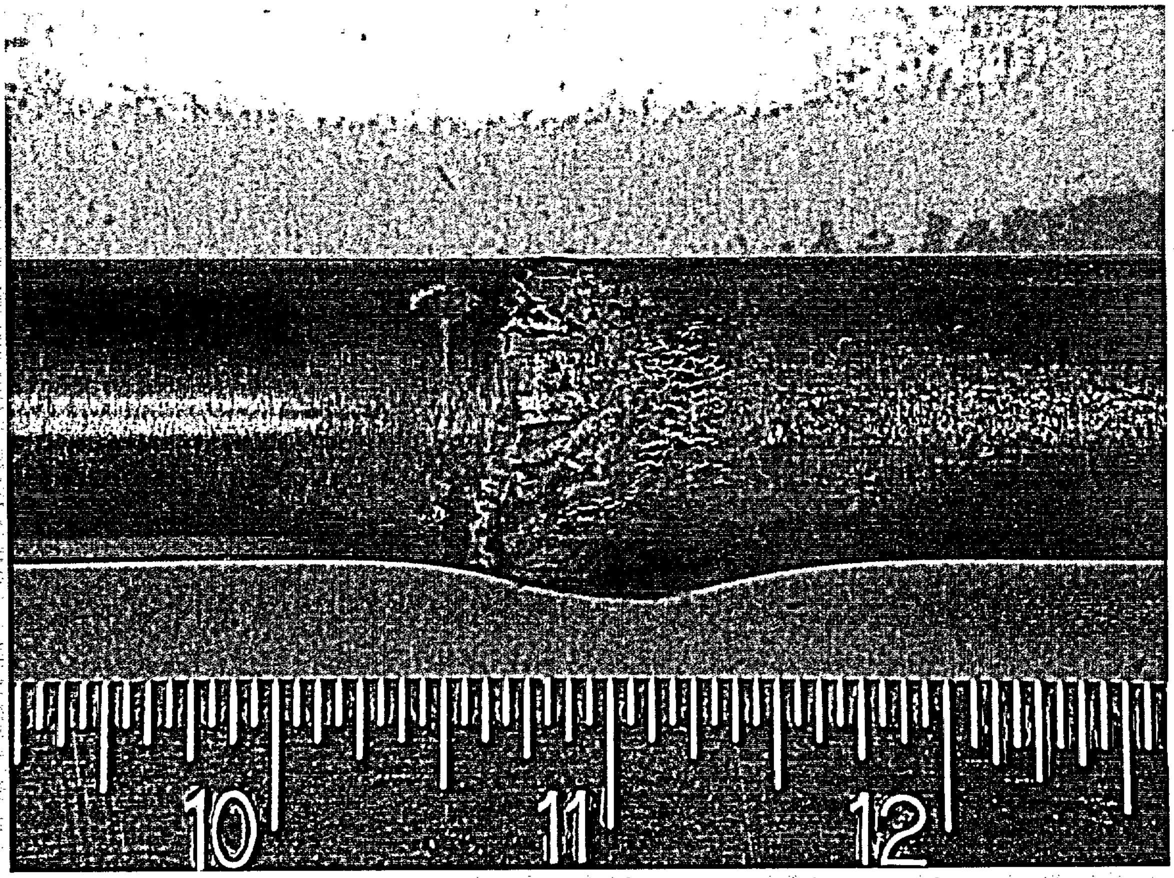

Figure 52: 2H TSP region at 270° after burst testing. 1.7X

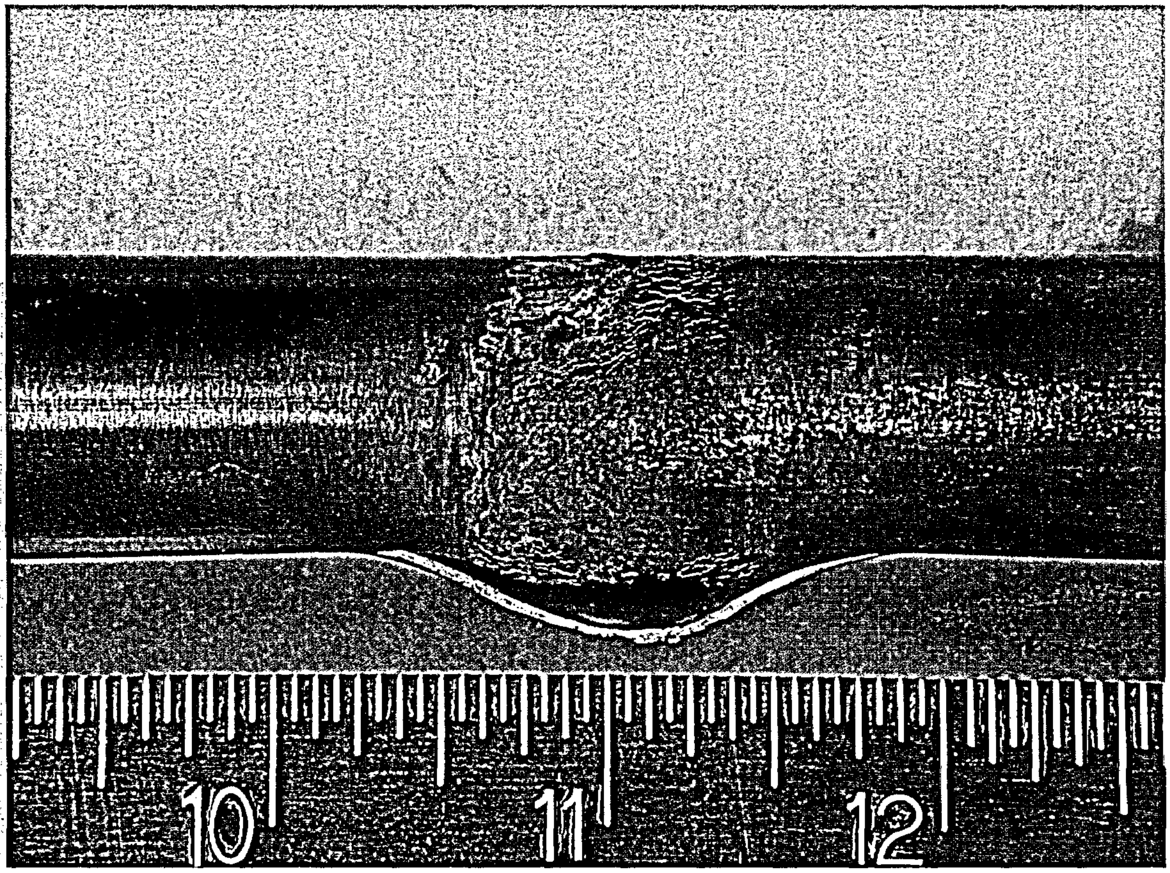

Figure 53: 2H TSP region at 315° after burst testing. 1.7X

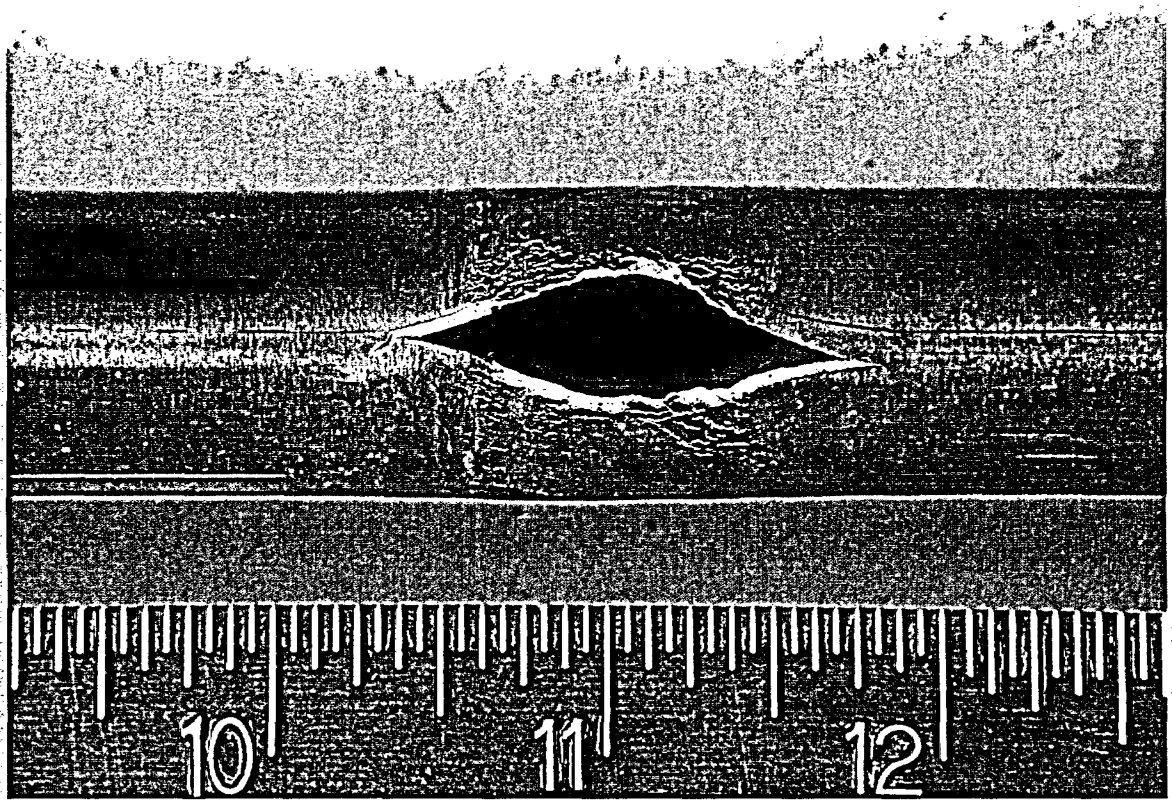

Figure 54: Burst centered at 30° in 2H TSP region. 1.7X

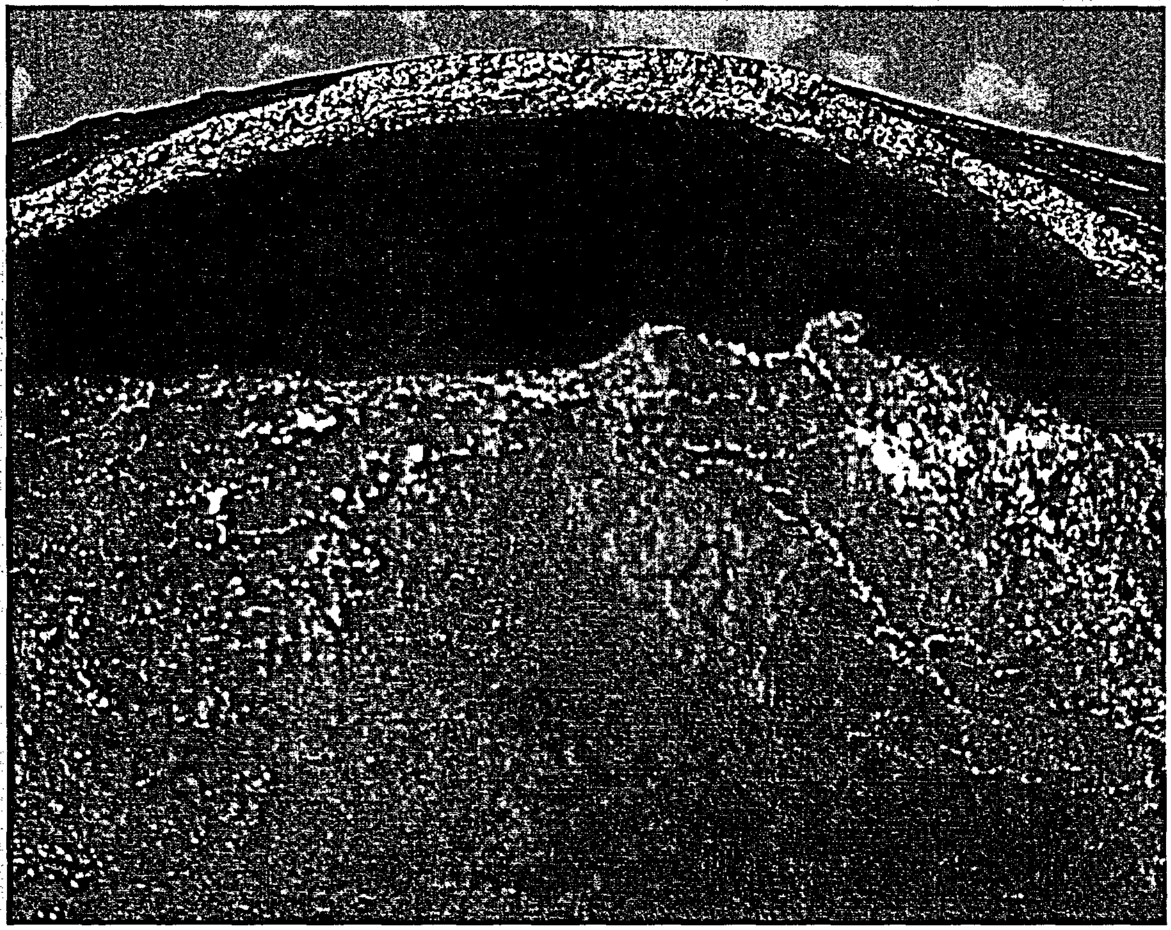

Figure 55: Counterclockwise burst rupture surface in 2H TSP. 8X

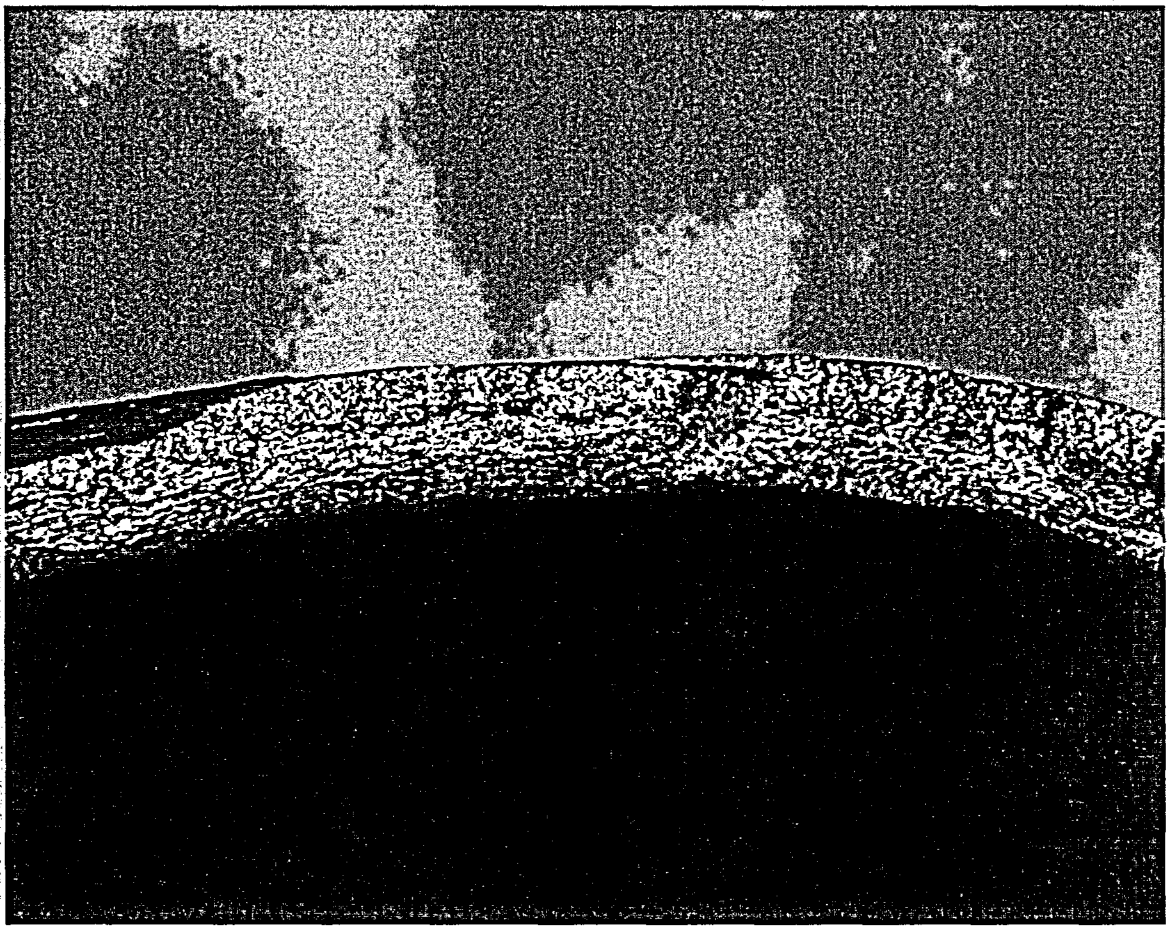

Figure 56: Apex of counterclockwise burst rupture surface in 2H TSP. 16.6X

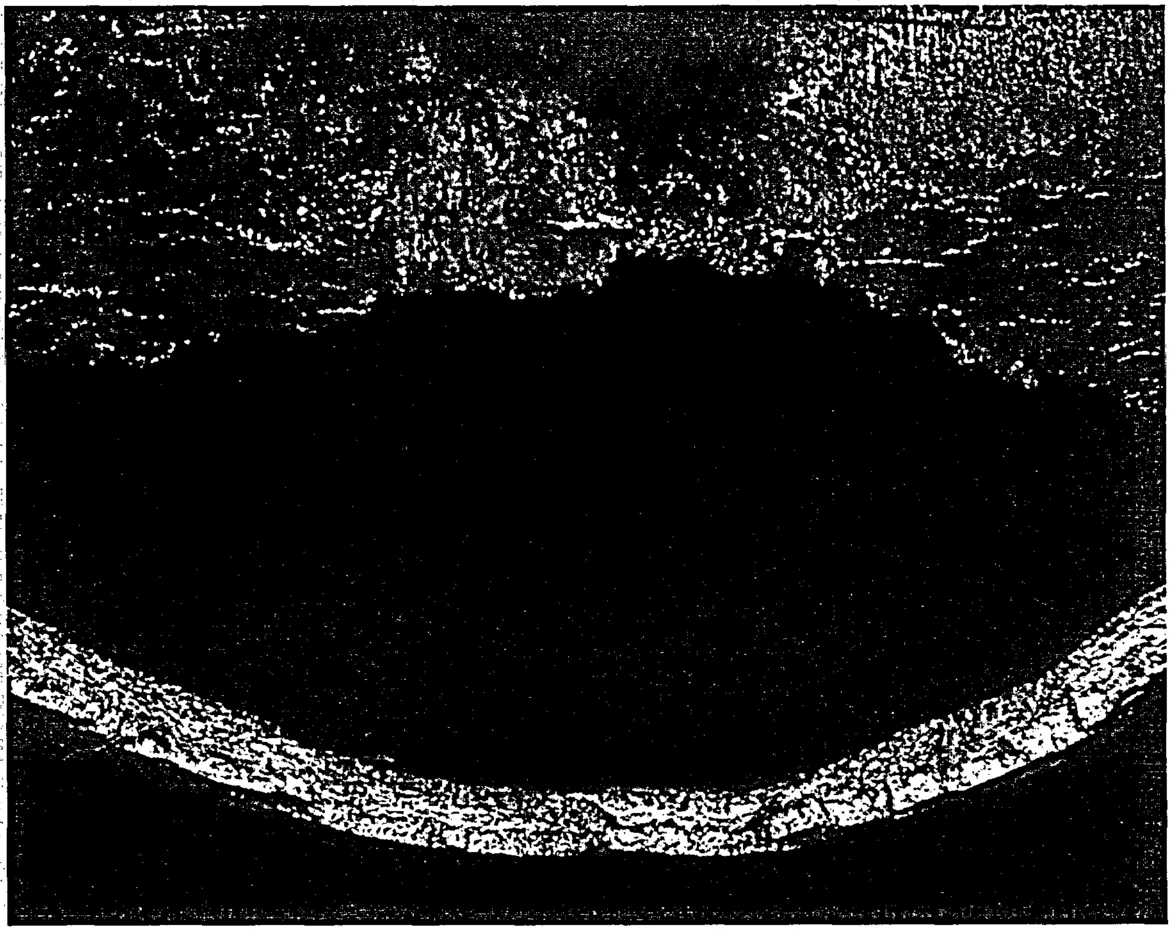

Figure 57: Clockwise burst rupture surface in 2H TSP. 8X

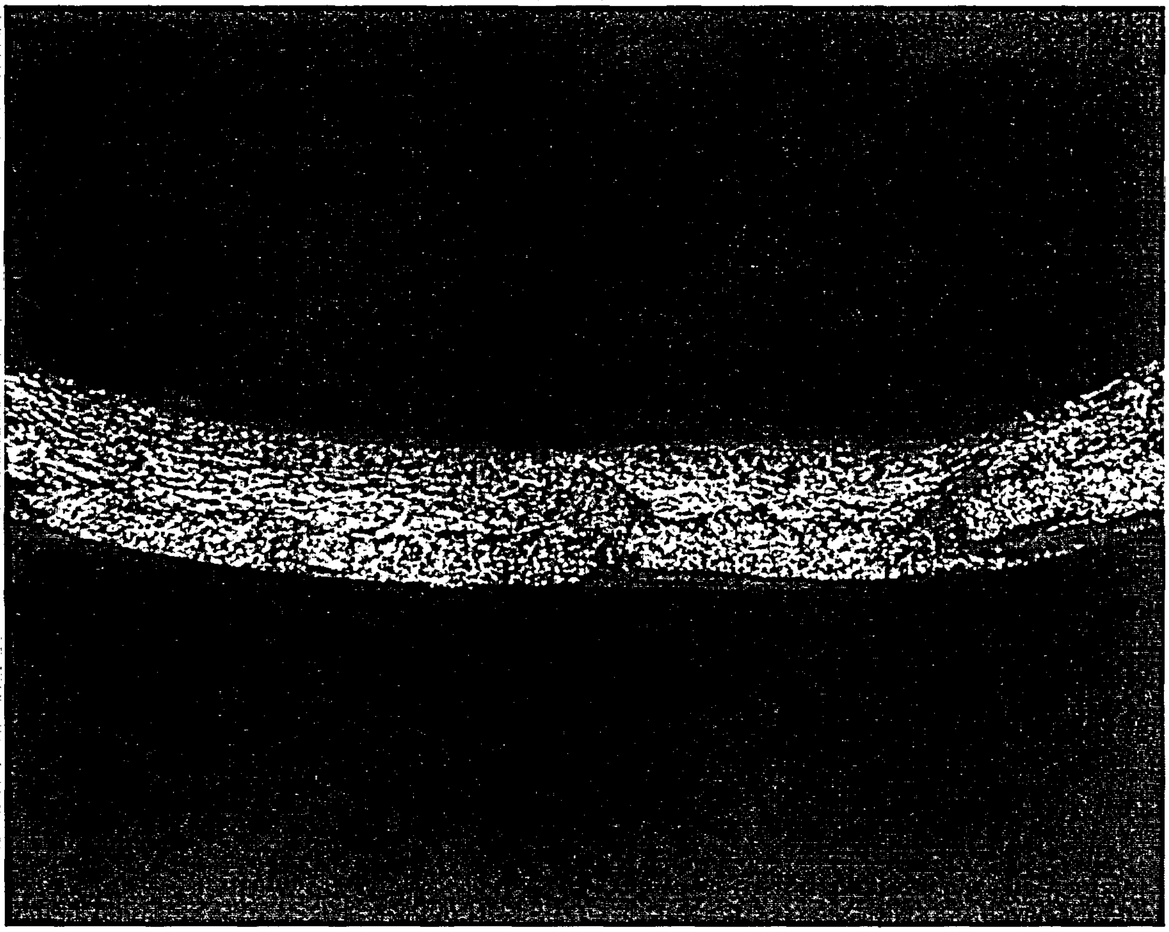

Figure 58: Apex of clockwise burst rupture surface in 2H TSP. 16.6X

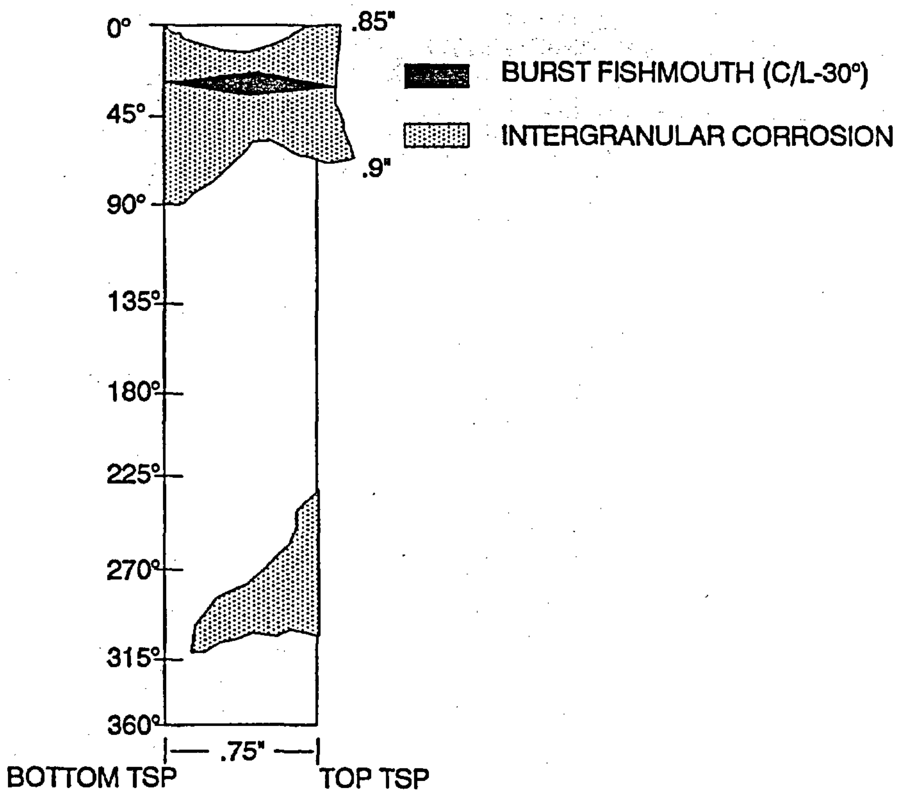

Figure 59: Areas of intergranular (cellular) corrosion in 2H TSP

Note: The above measurements are based on visual observation of the burst tube section and are not intended to be exact representations of the preburst areas of corrosion.

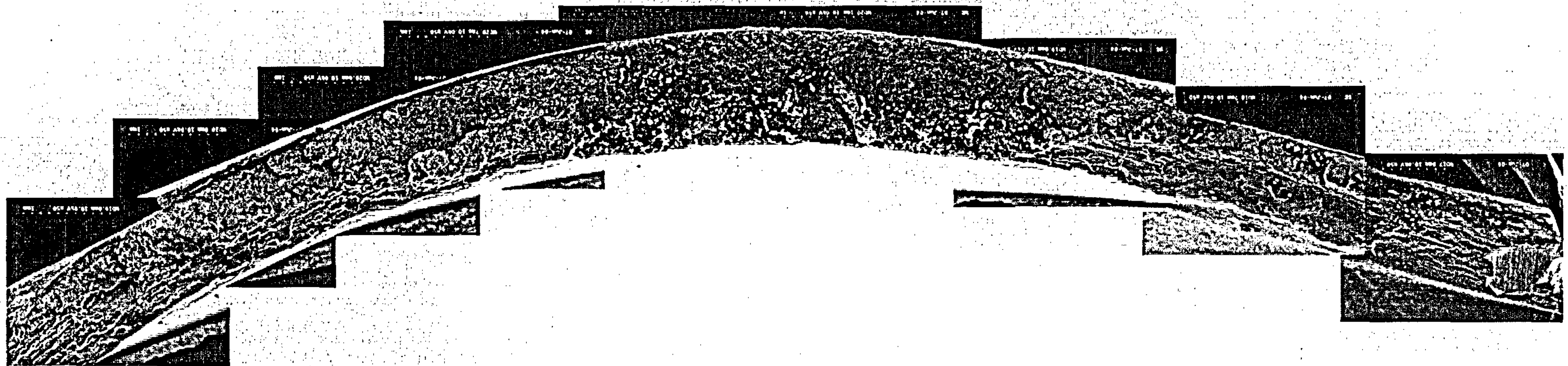

Figure 60A: Secondary electron image of 1H burst rupture surface. 14.4X

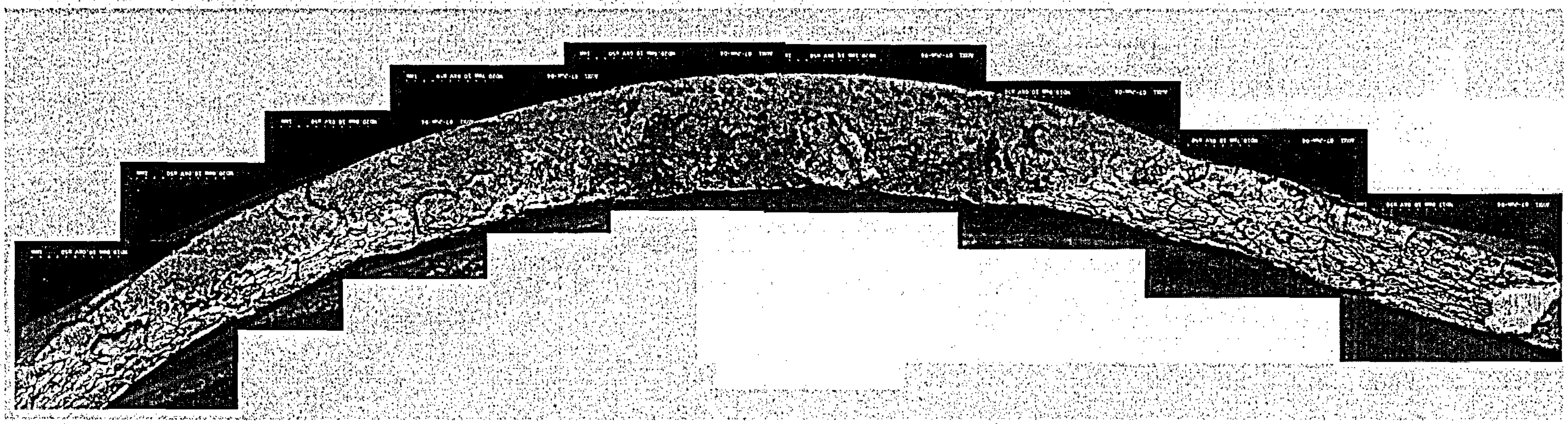

Figure 60B: Backscattered electron image of 1H burst rupture surface. 14.4X

Figure 60: SEM mosaics of 1H burst rupture surface (bottom to left)

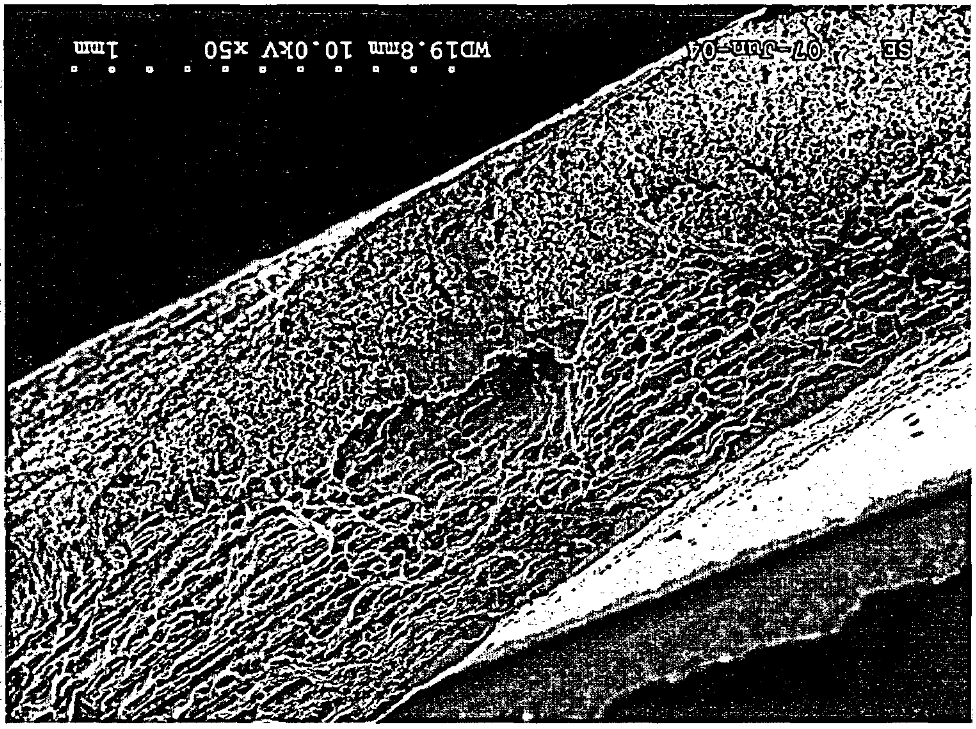

Figure 61: SE image of bottom edge of IGSCC on burst rupture surface of 1H TSP. 50X

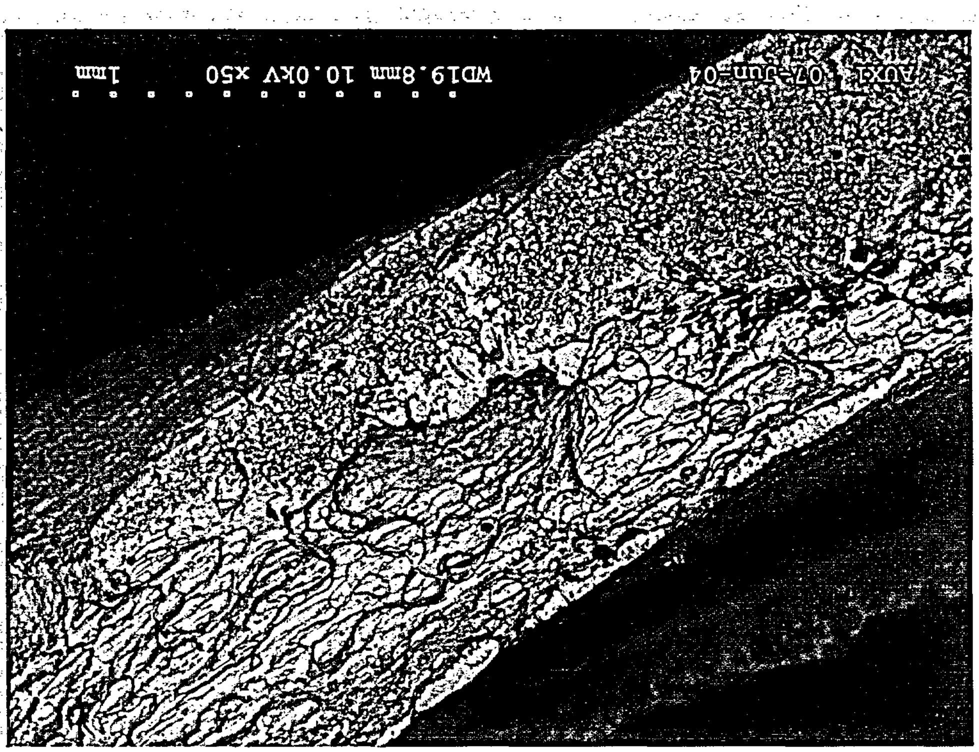

Figure 62: BSE image of bottom edge of IGSCC on burst rupture surface of 1H TSP. 50X

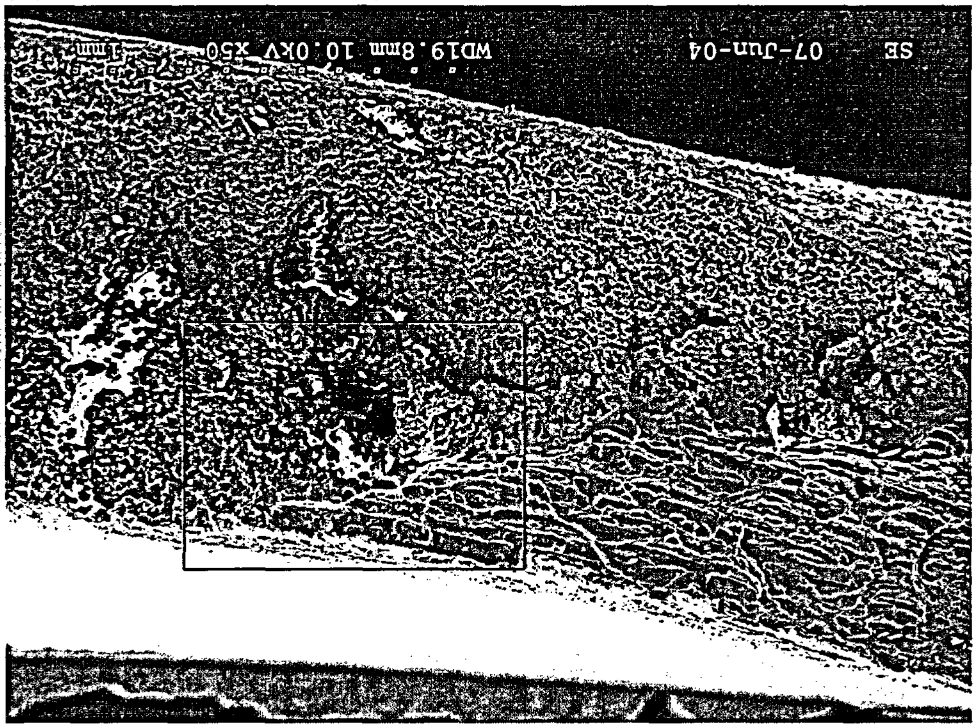

Figure 63: SE image showing transition to 100% TW IGSCC on burst rupture surface of 1H TSP. 50X

Figure 64: Detail of transition area shown in box in Figure 56. 150X

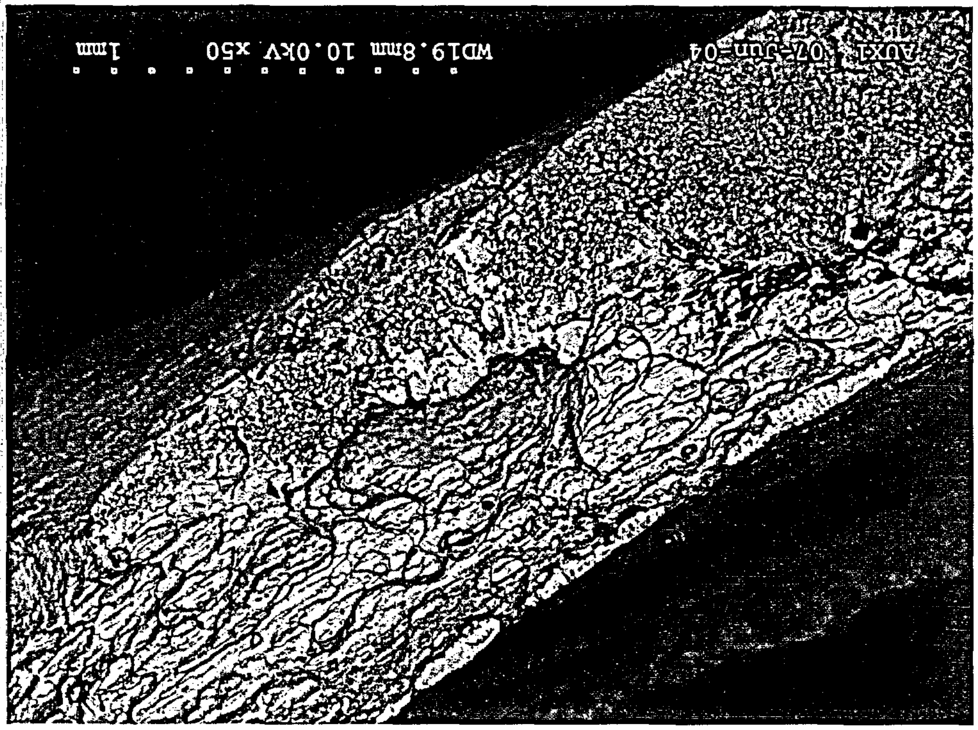

Figure 65: BSE image of transition area to 100% IGSCC on burst rupture surface of 1H TSP. 50X

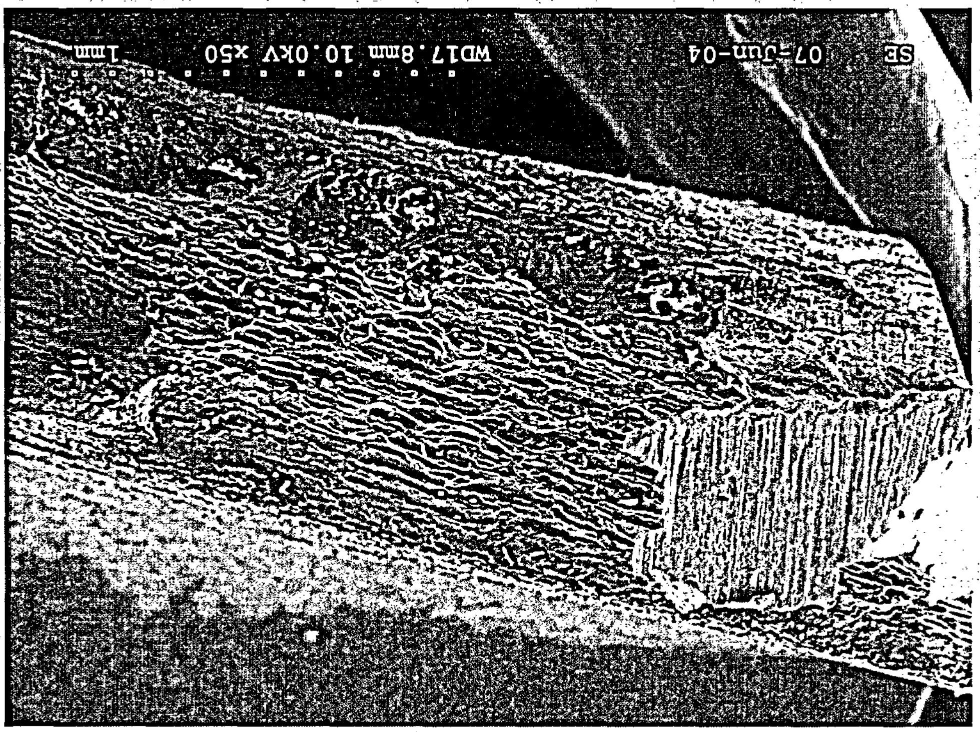

Figure 66: SE image of top edge of IGSCC on burst rupture surface of 1H TSP. 50X

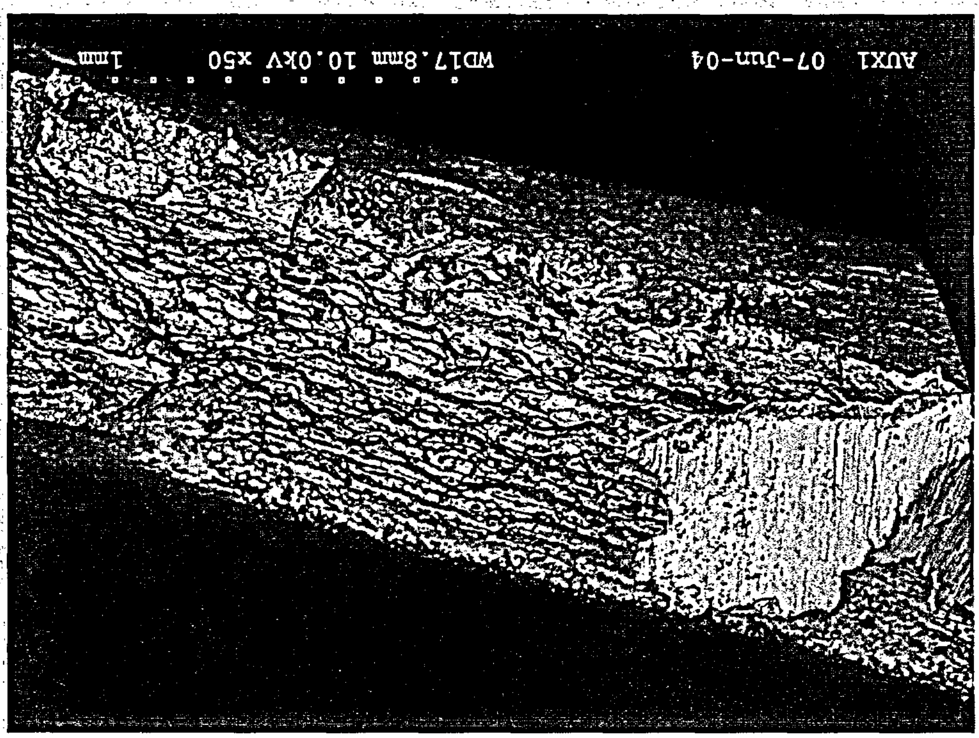

Figure 67: BSE image of top edge of IGSCC on burst rupture surface of 1H TSP. 50X

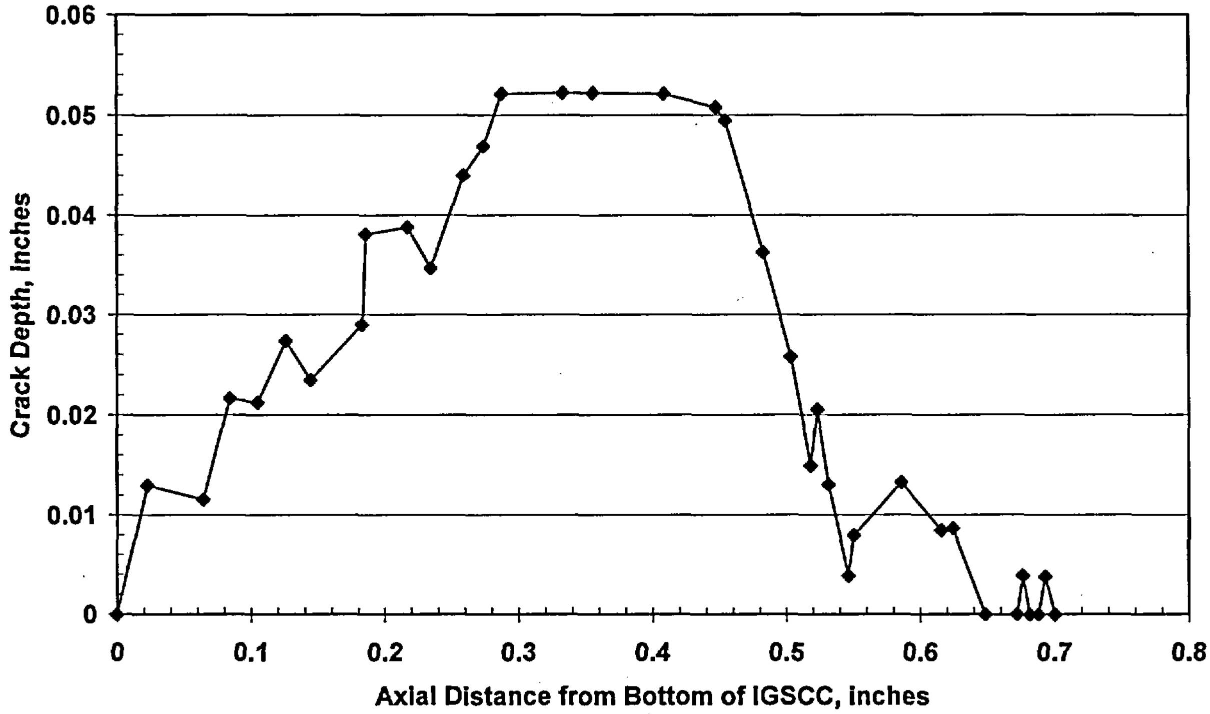

Figure 68a: Measured crack depth on burst rupture surface in 1H TSP

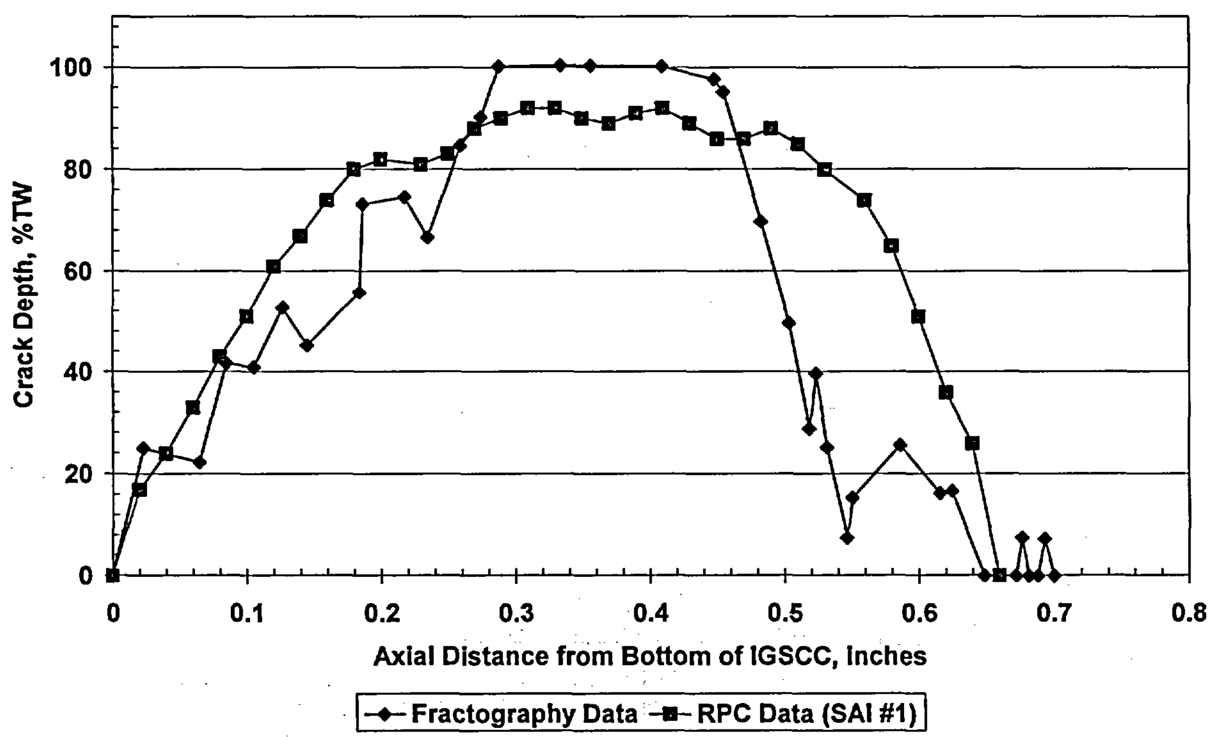

Figure 68b: Comparison of measured crack depth vs. post leak rate RPC data

Figure 68: Measured depth of IGSCC (SAI #1) in 1H TSP

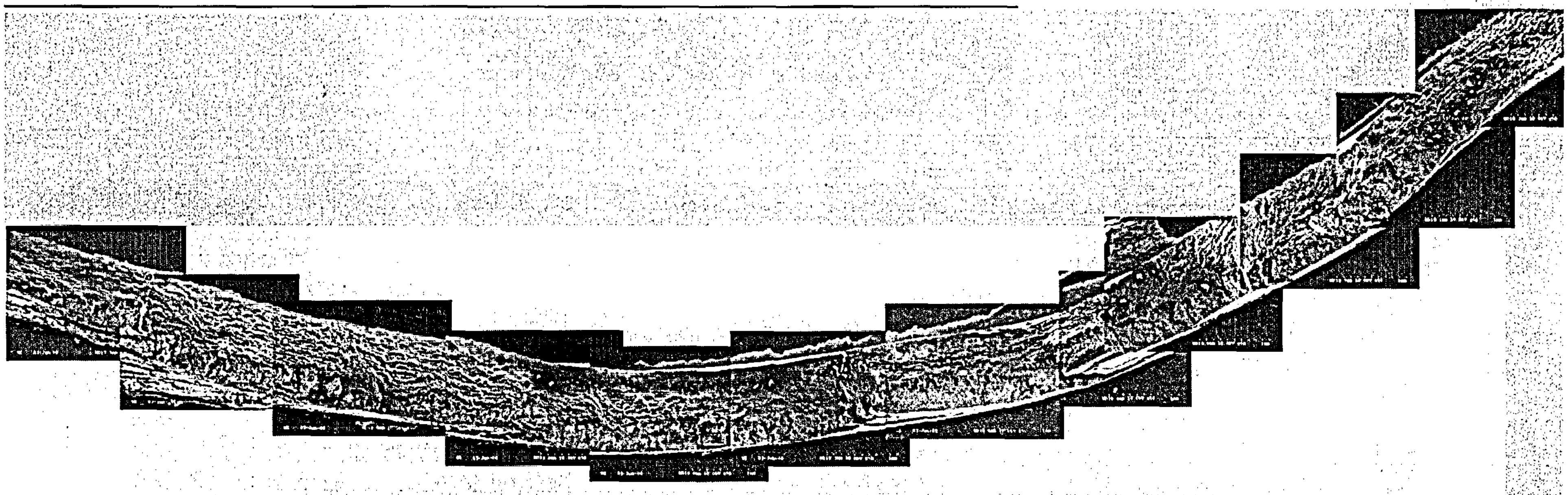

Figure 69A: Secondary electron image of 2H burst rupture surface. 11.4X

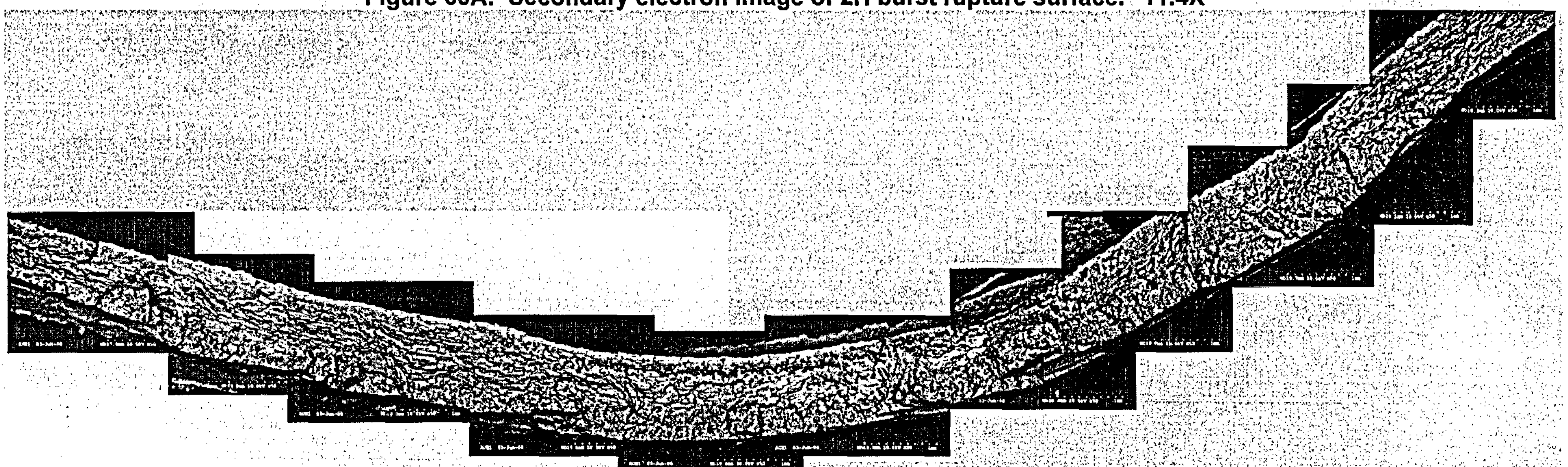

Figure 69B: Backscattered electron image of 2H burst rupture surface. 11.4X

Figure 69: SEM mosaics of 2H burst rupture surface (bottom to left)

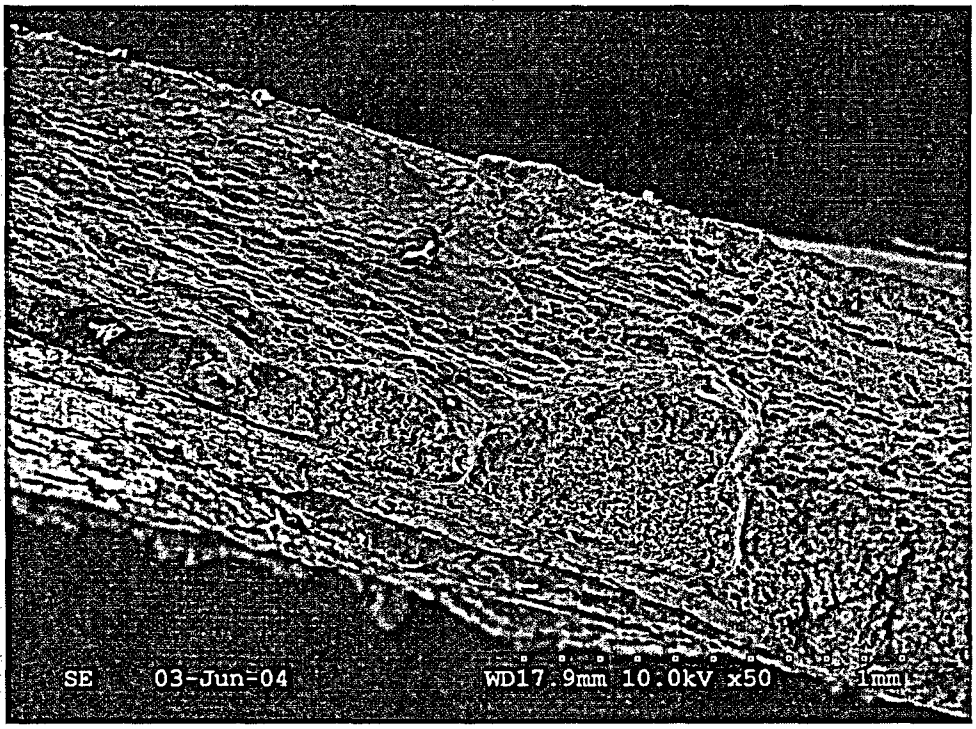

Figure 70: SE image of bottom edge of IGSCC on burst rupture surface of 2H TSP. 50X

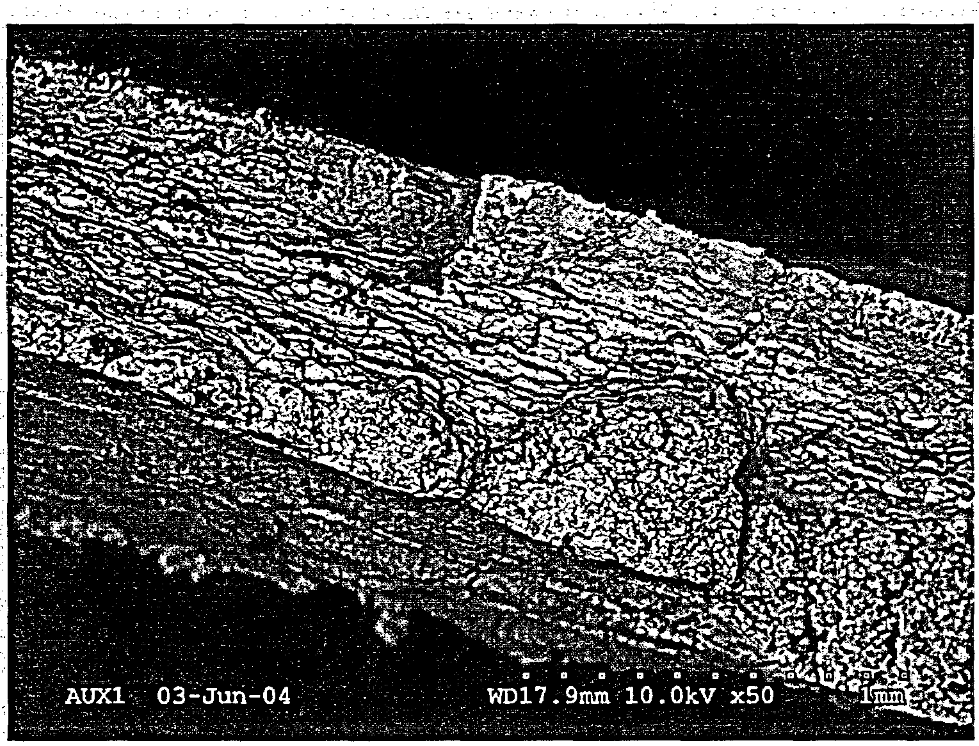

Figure 71: BSE image of bottom edge of IGSCC on burst rupture surface of 2H TSP. 50X

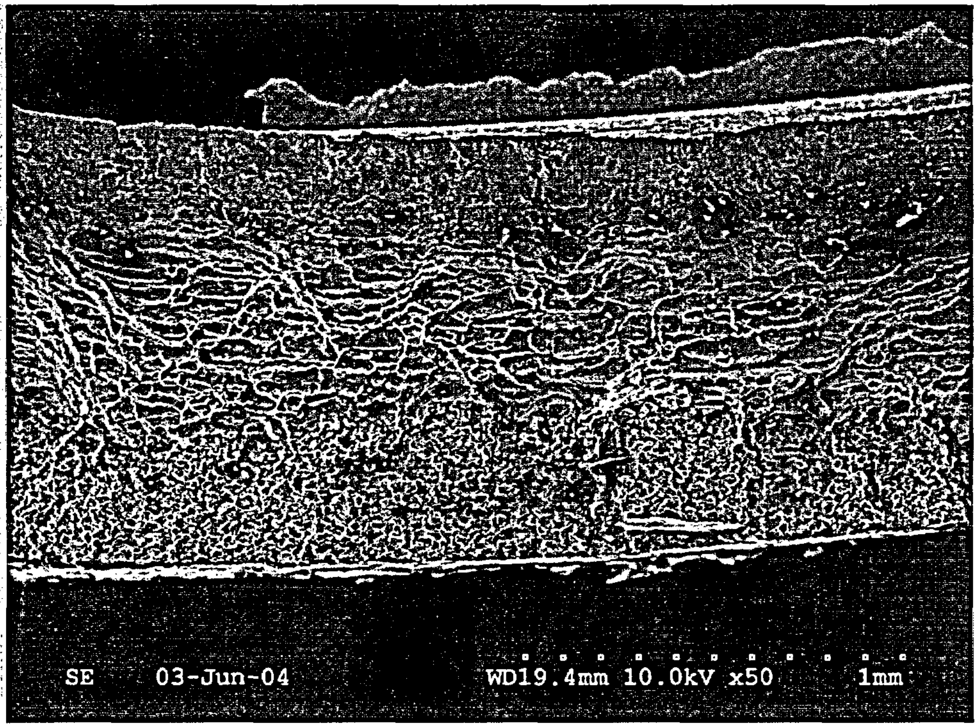

Figure 72: SE image of central region of burst rupture surface of 2H TSP. 50X

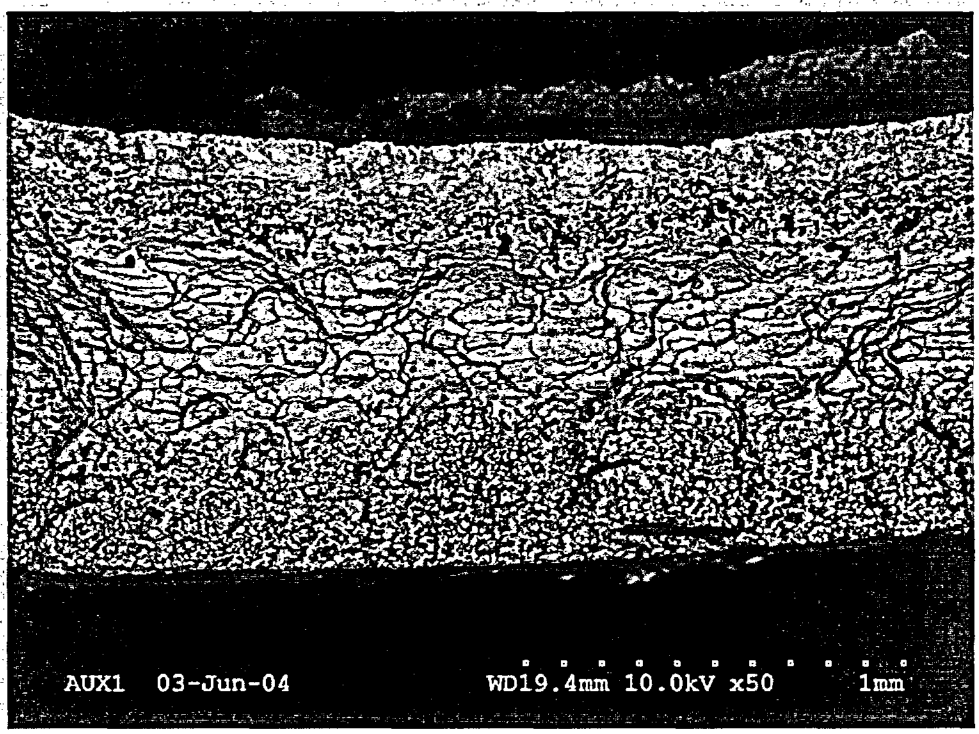

Figure 73: BSE image of central region of burst rupture surface of 2H TSP. 50X

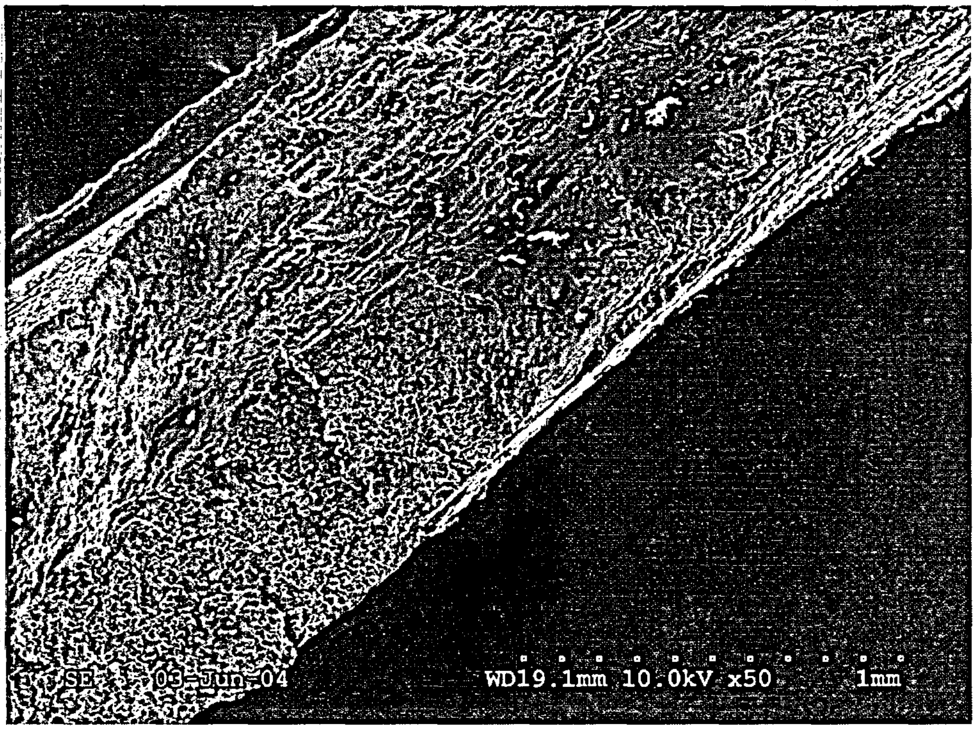

Figure 74: SE image of top edge of IGSCC on burst rupture surface of 2H TSP. 50X

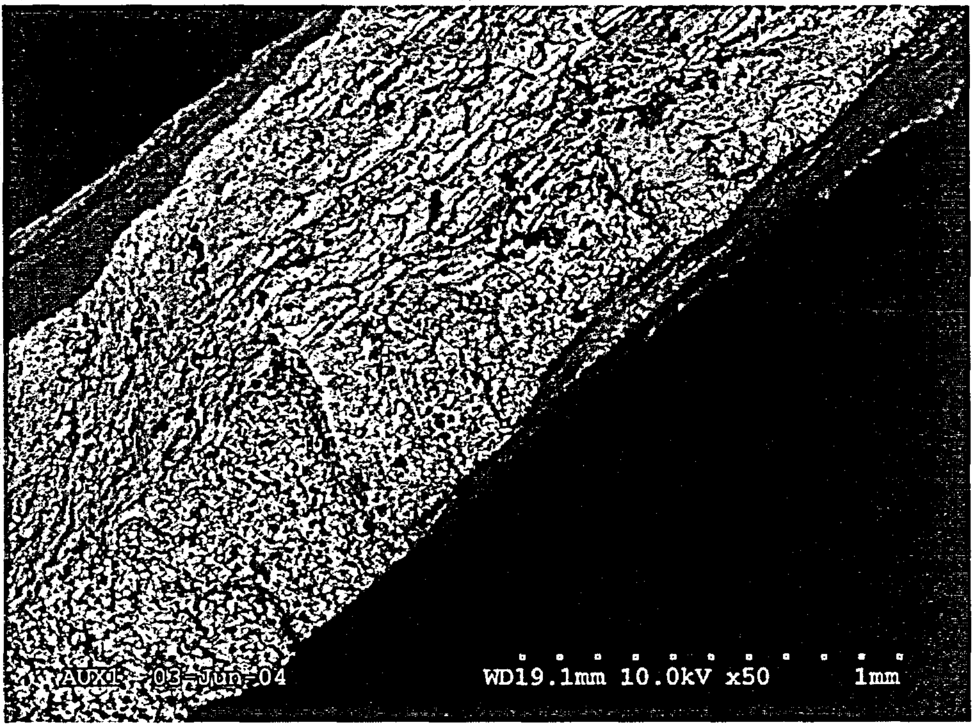

Figure 75: BSE image of top edge of IGSCC on burst rupture surface of 2H TSP. 50X

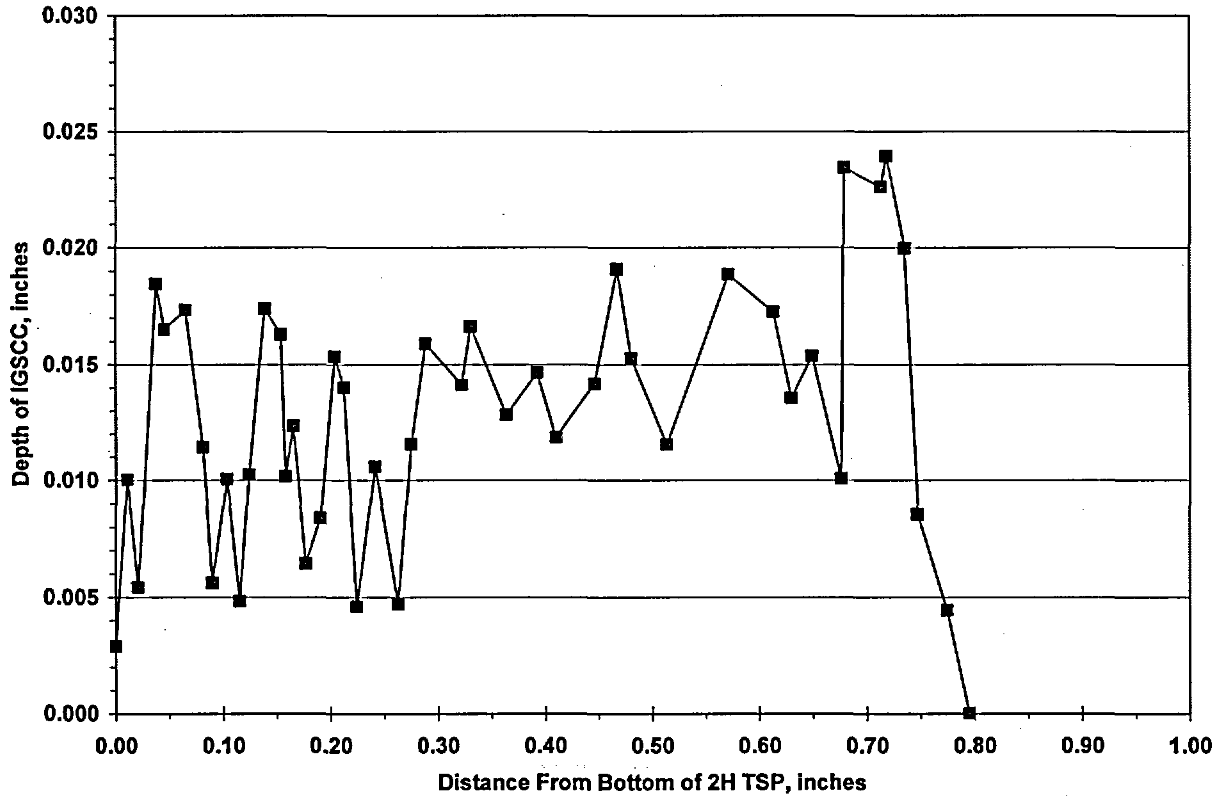

Figure 76: Plot of depth of intergranular corrosion in 2H TSP (Section R20C54-5B3)

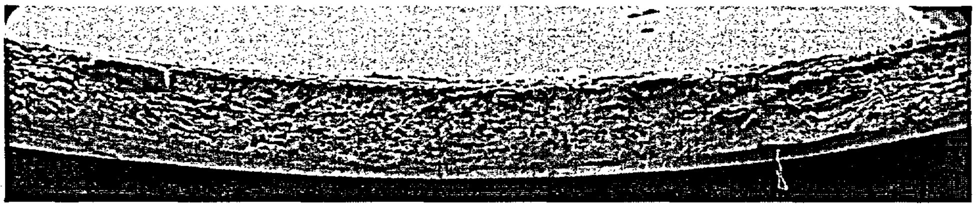

Figure 77: Free span burst rupture surface. 10X

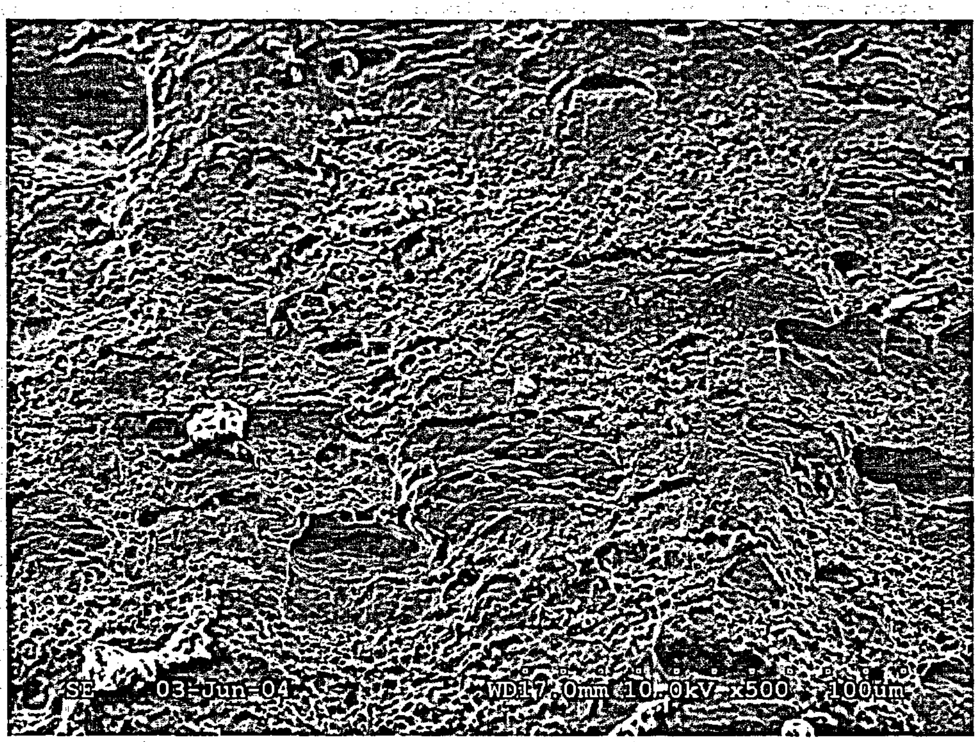

Figure 78: Typical non-corroded ductile area on free span burst rupture surface. SE image. 500X

Figure 79A: BSE image of an area on 2H burst rupture surface. 5000X

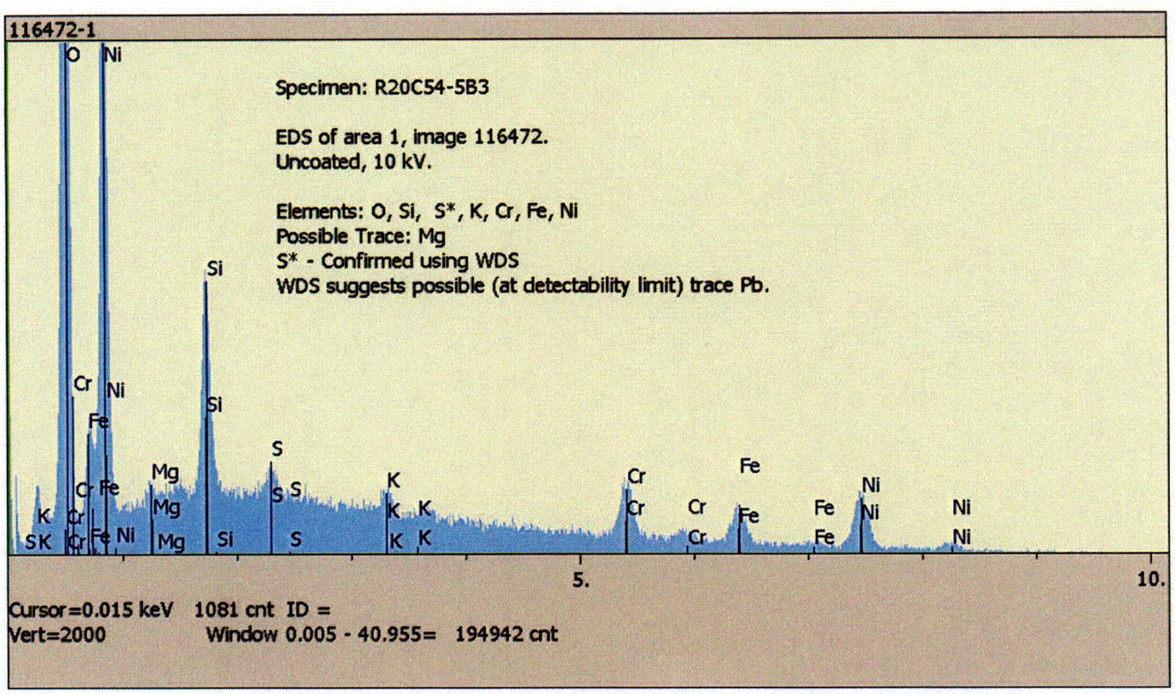

Figure 79B: EDS spectrum of area 1 in Figure 79A, showing presence of sulfur.

Figure 79: EDS analysis of area on 2H burst rupture surface.

C08

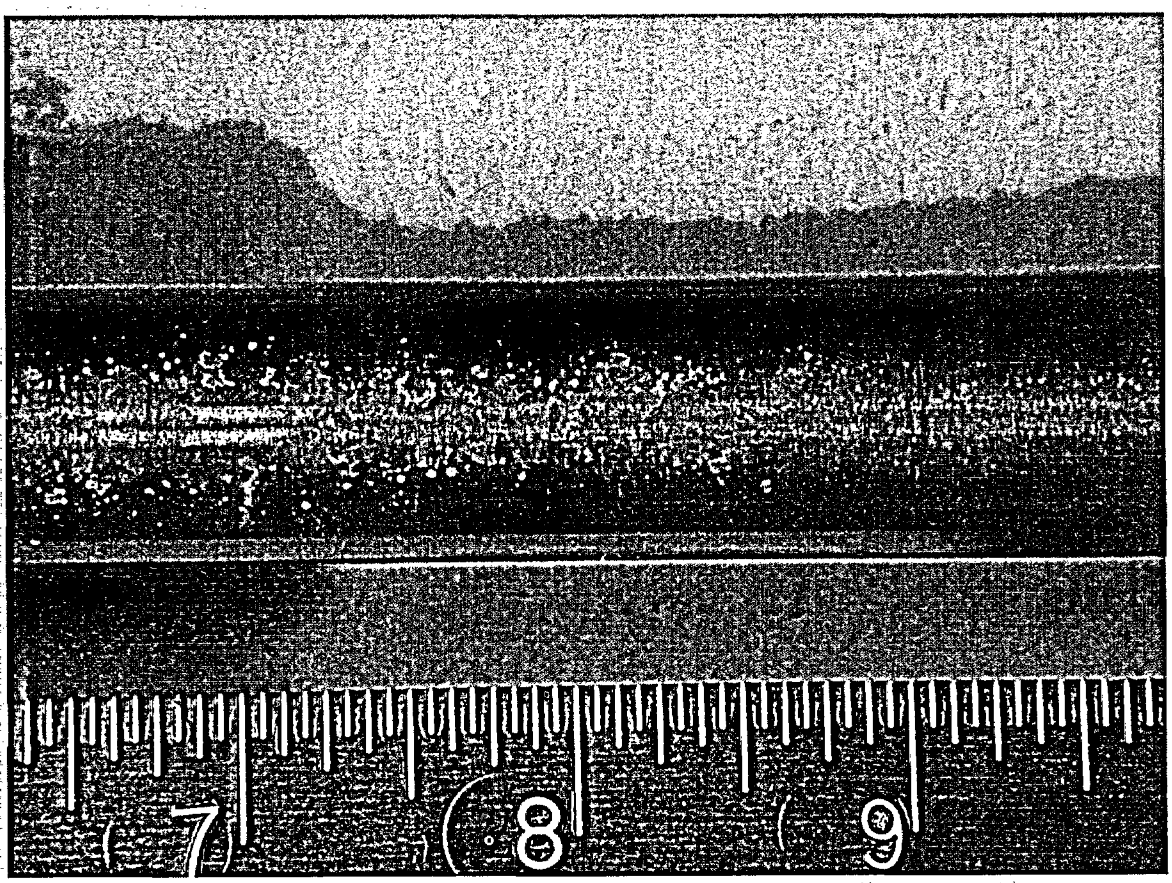

Figure 80: Typical copper colored deposits in free span areas. 1.7X

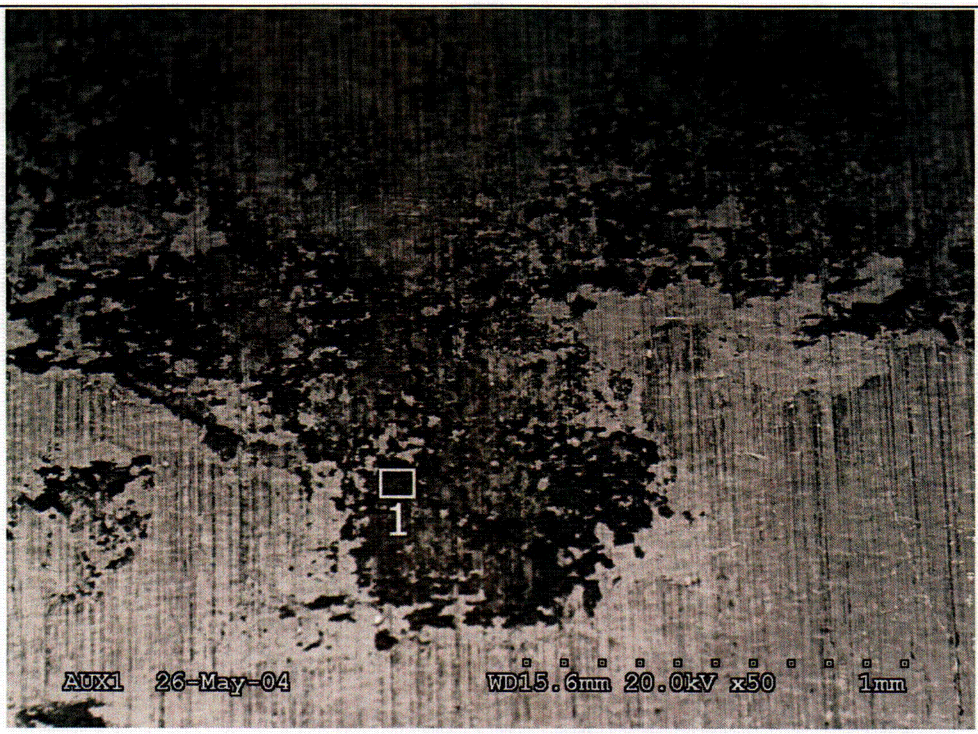

Figure 81A: BSE image of typical copper colored deposit area. 50X

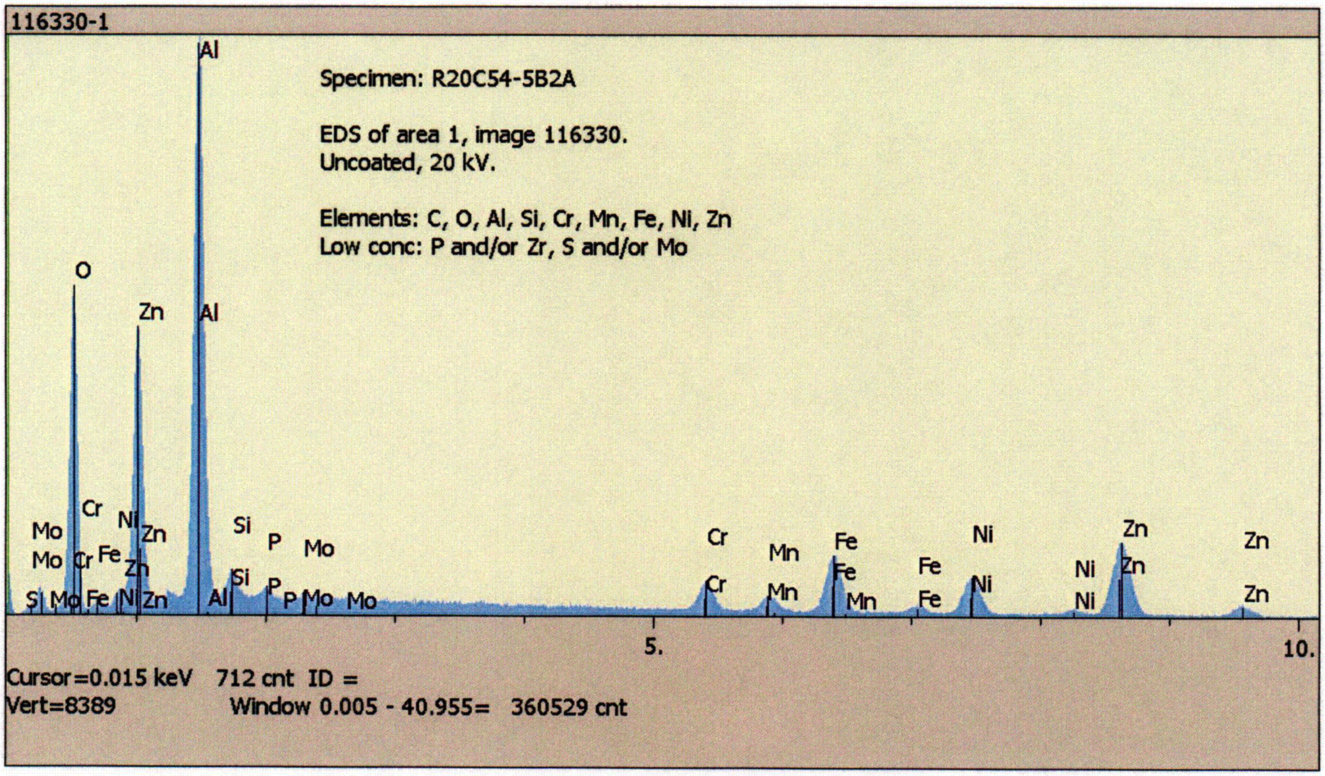

Figure 81B: EDS analysis of area 1 in Figure 74A showing Al, Zn, O.

Figure 81: SEM/EDS analysis of copper colored deposits on tube OD.

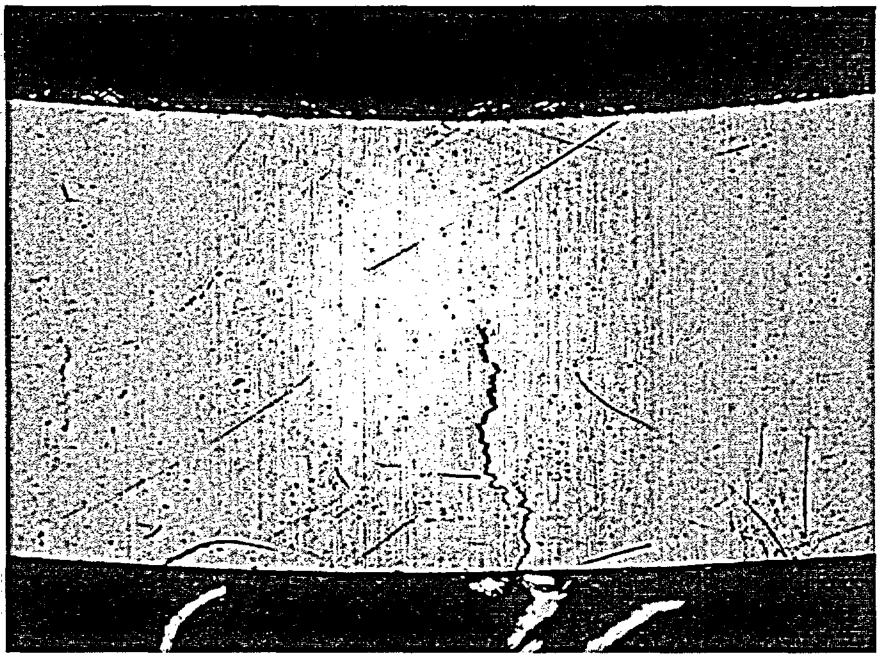

Figure 82: 53% TW indication near 298° in centerline of 1H TSP, corresponding to approximate location of secondary eddy current indication. 46X

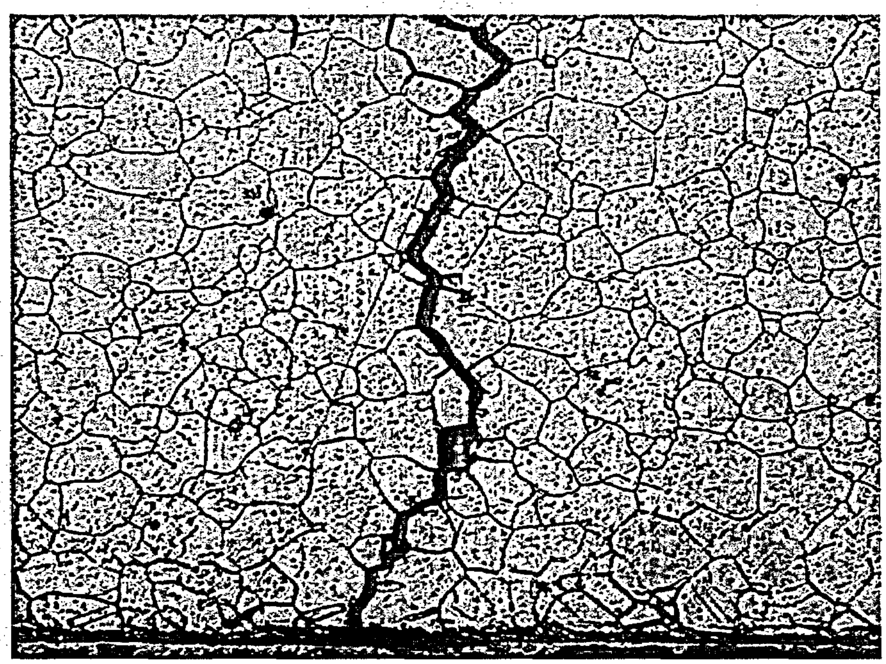

Figure 83: Etched microstructure of crack shown in Figure 82. 480X

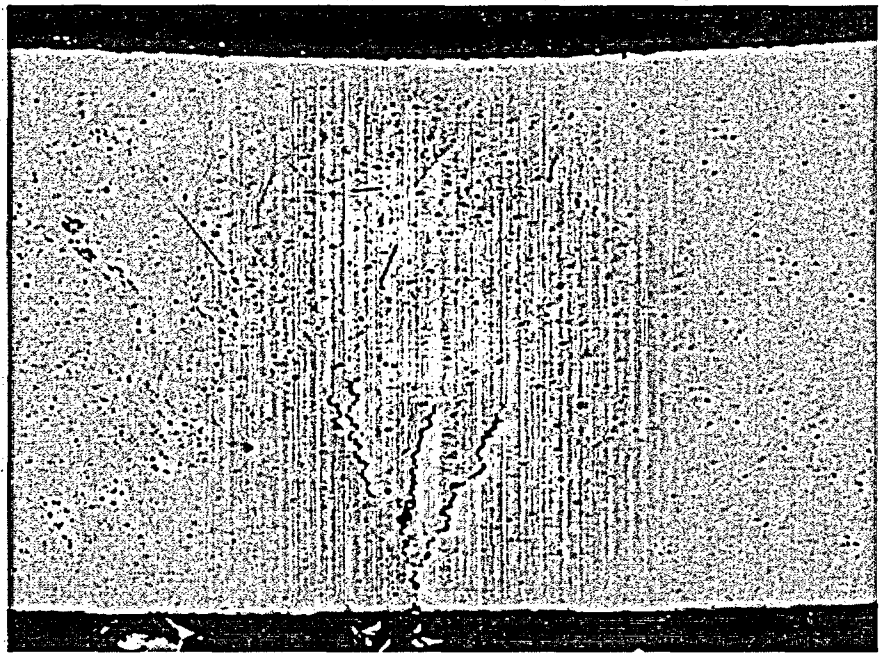

Figure 84: 40% TW indication near 330° at centerline +0.1 inches of 1H TSP, corresponding to approximate location of secondary eddy current indication. 59X

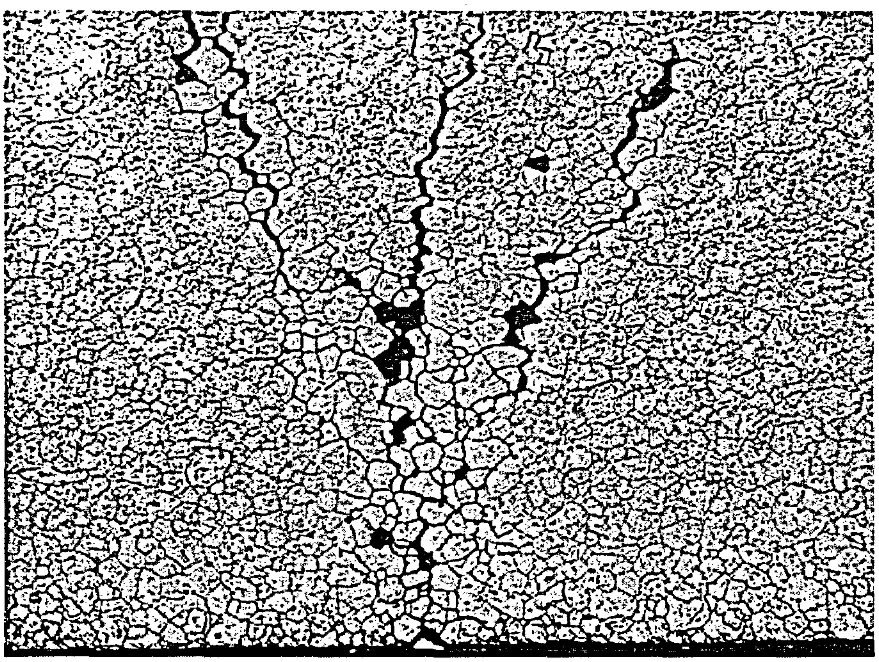

Figure 85: Etched microstructure of cracking shown in Figure 84. 175X

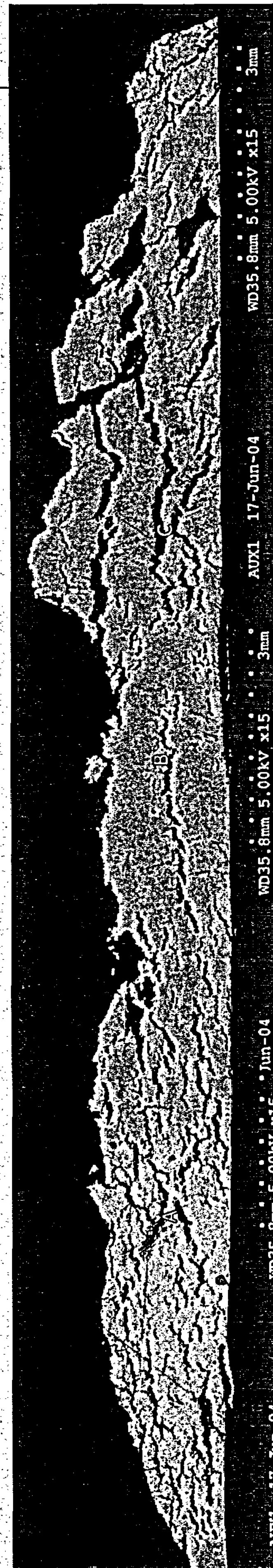

Figure 86: Overall mosaic of 5B3BB1 (first face) 11.2X

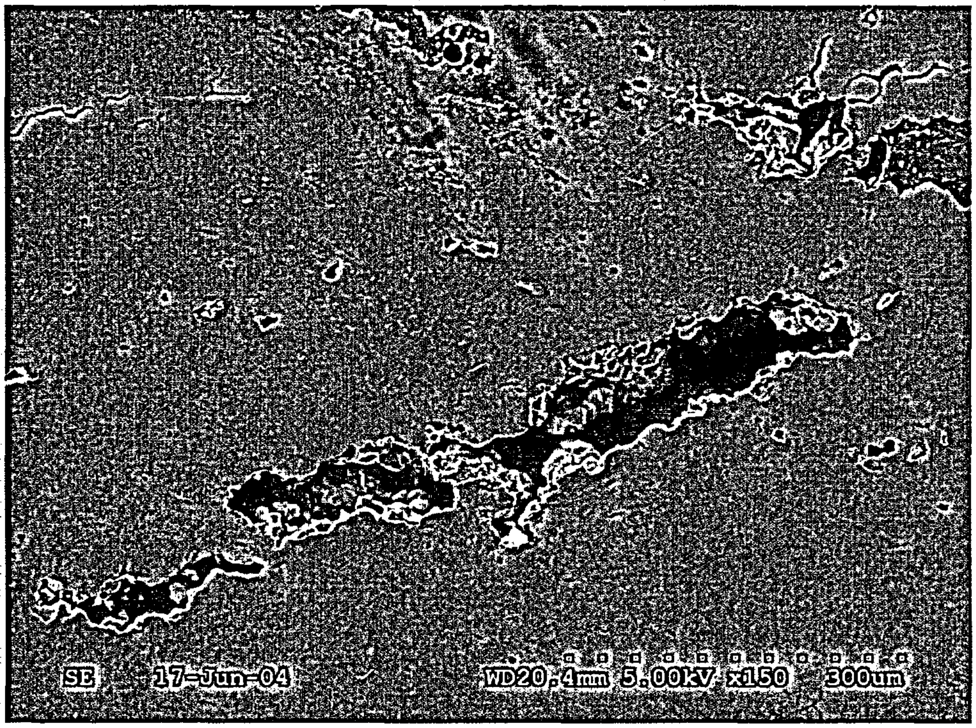

Figure 87: Area "A" in Figure 86. 146X

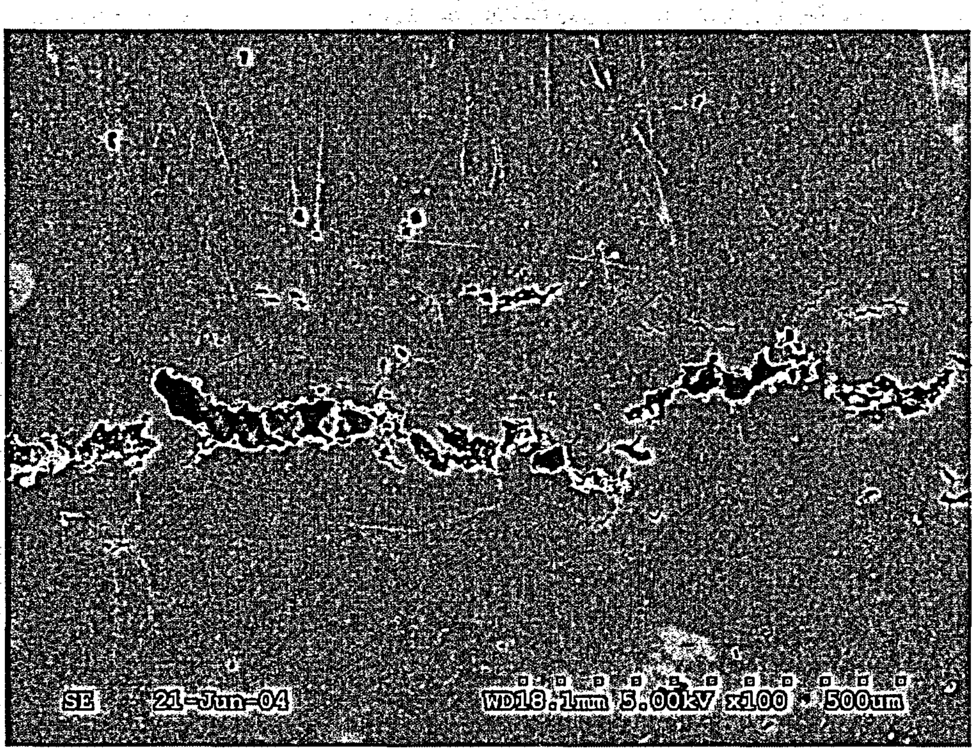

Figure 88: Area "B" in Figure 87. 99X

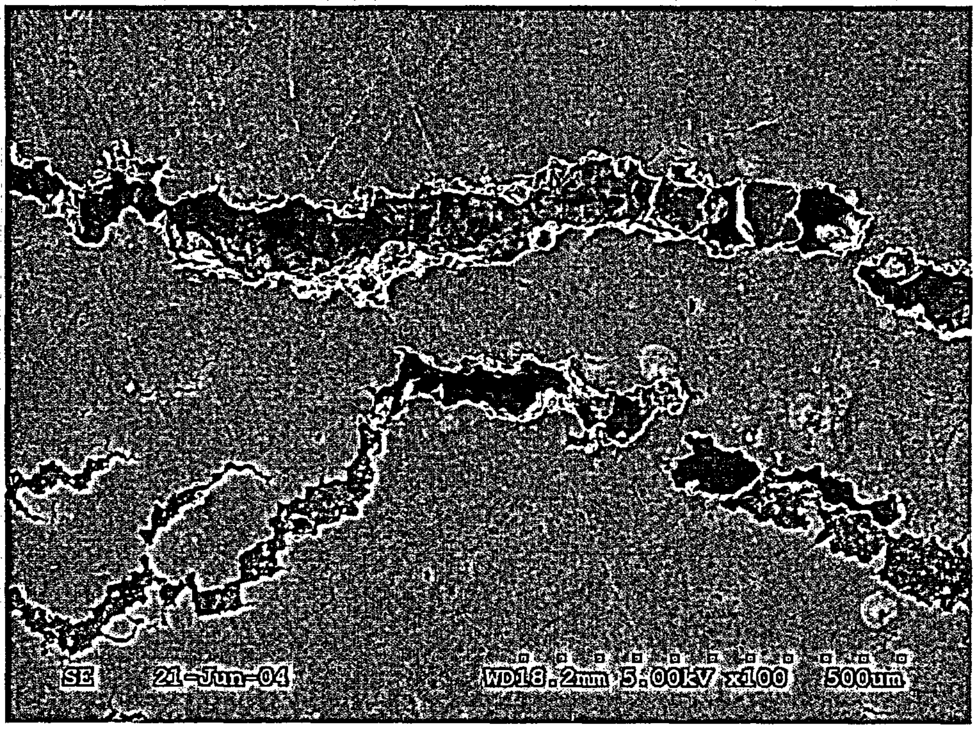

Figure 89: Area "C" in Figure 80. 99X

Figure 90: Overall mosaic of 5B3BB1 (second face) 10.6X

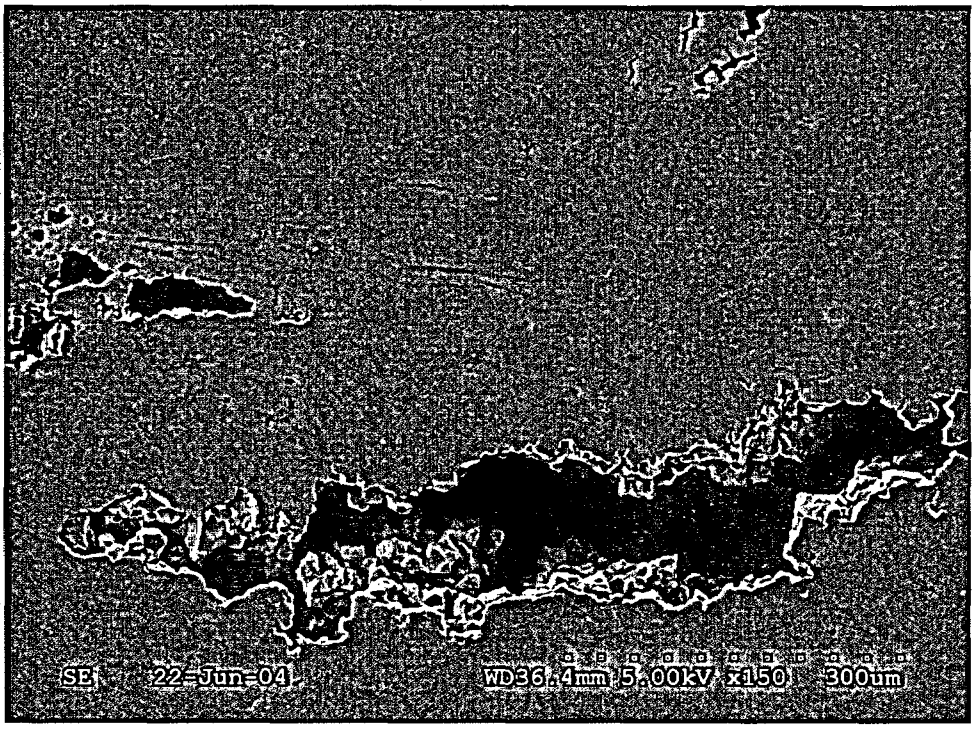

Figure 91: Area "A" in Figure 90. 146X

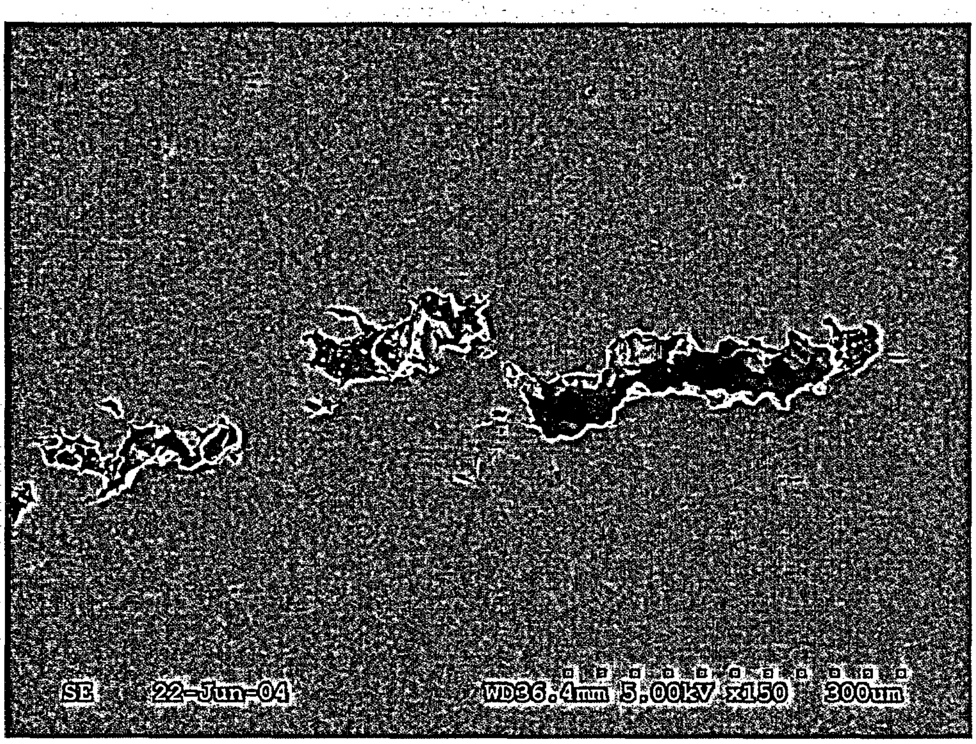

Figure 92: Area "B" in Figure 90. 146X

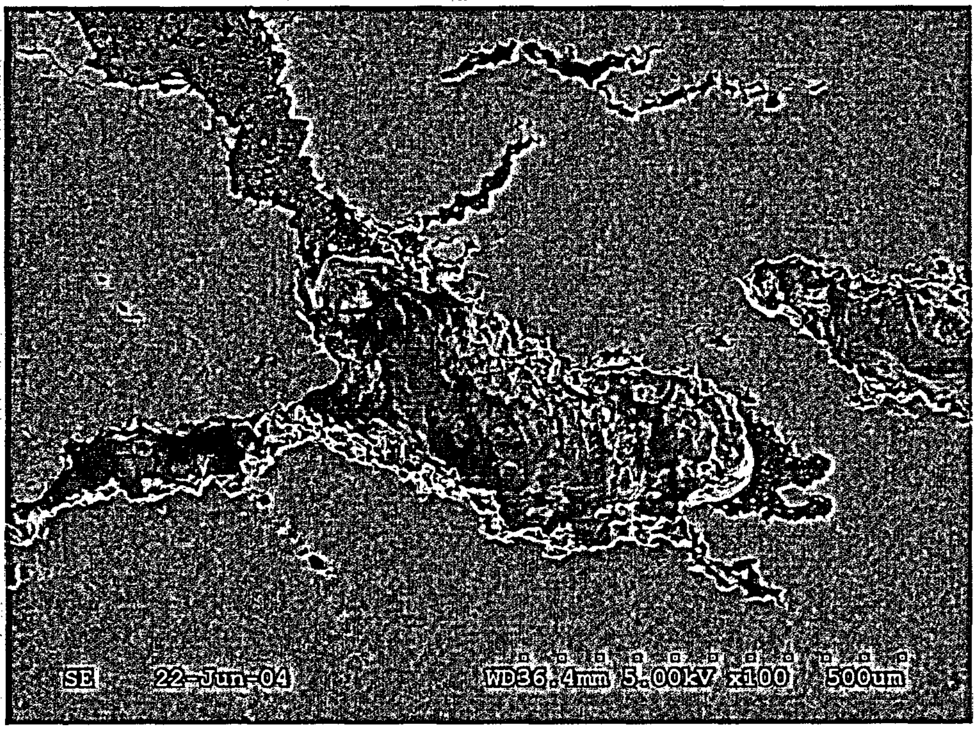

Figure 93: Area "C" in Figure 90. 99X

Figure 94: Overall mosaic of 5B3BB1 (third face) 10.0X

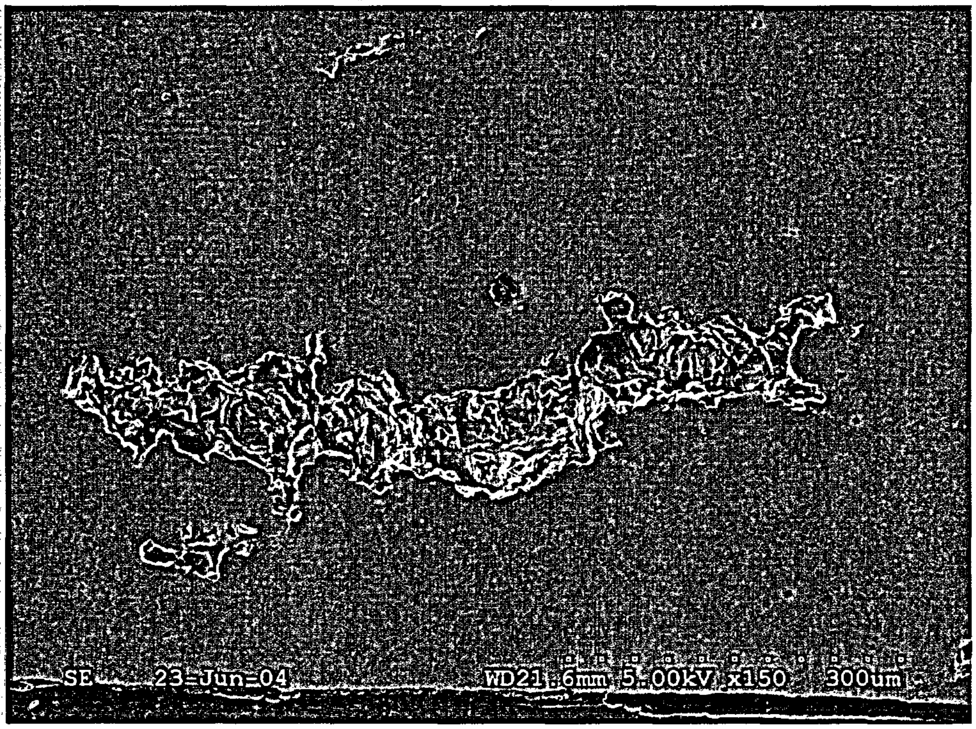

Figure 95: Area "A" in Figure 94. 146X

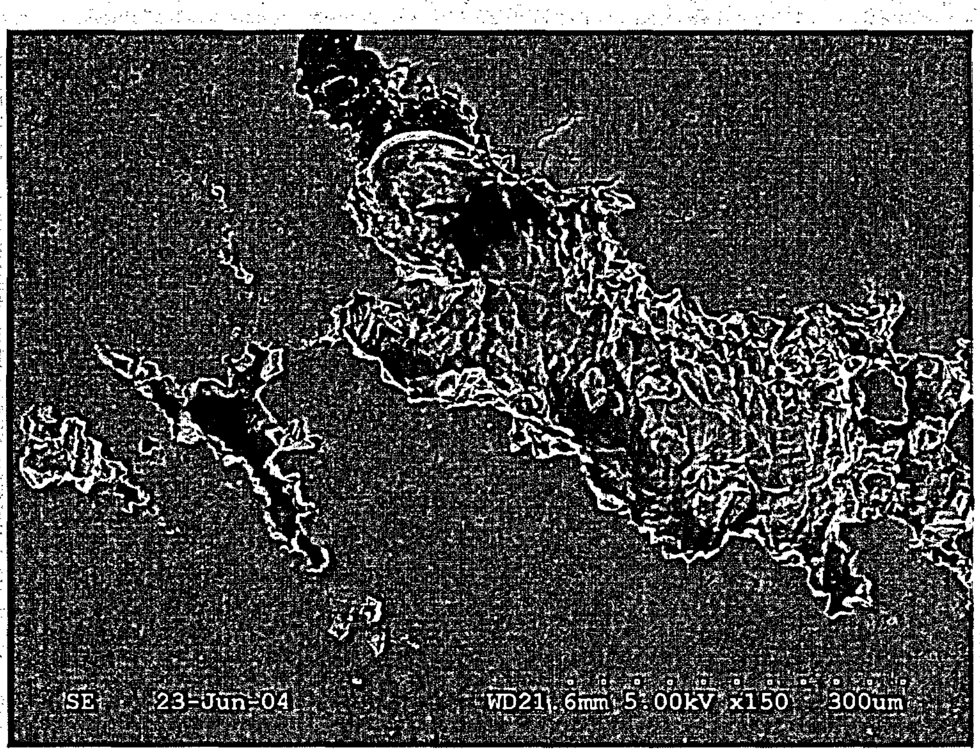

Figure 96: Area "B" in Figure 94. 146X

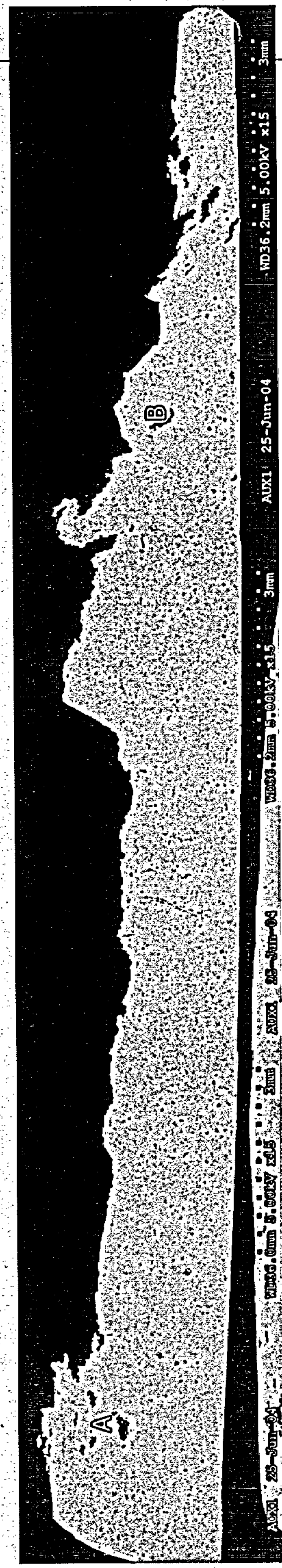

Figure 97: Overall mosaic of 5B3BB1 (fourth face) 9.9X

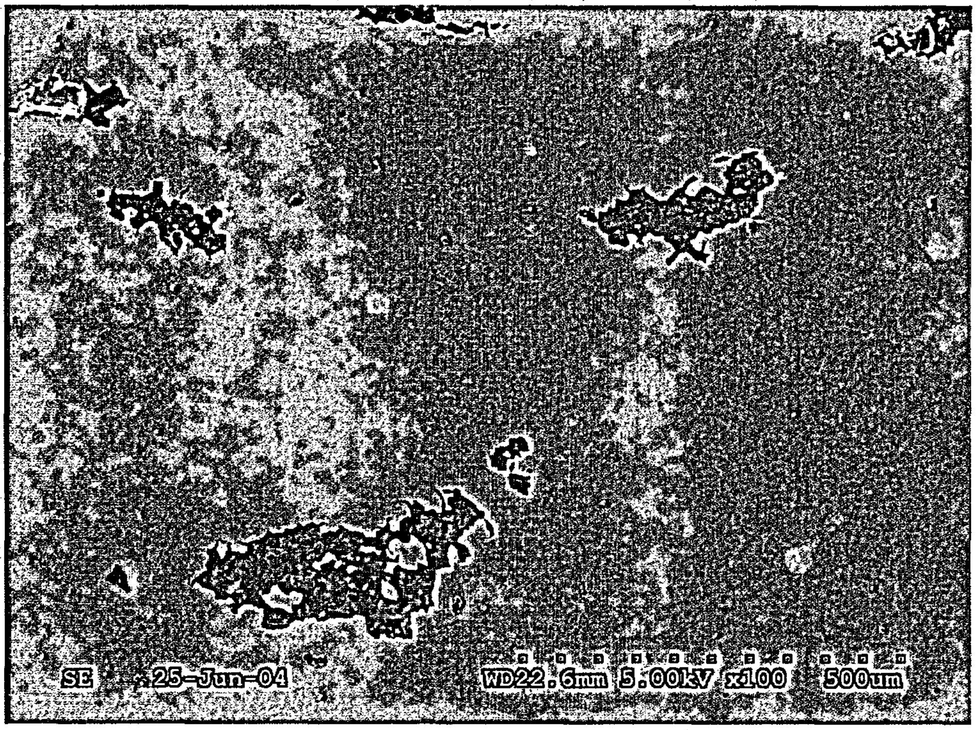

Figure 98: Area "A" in Figure 97. 99X

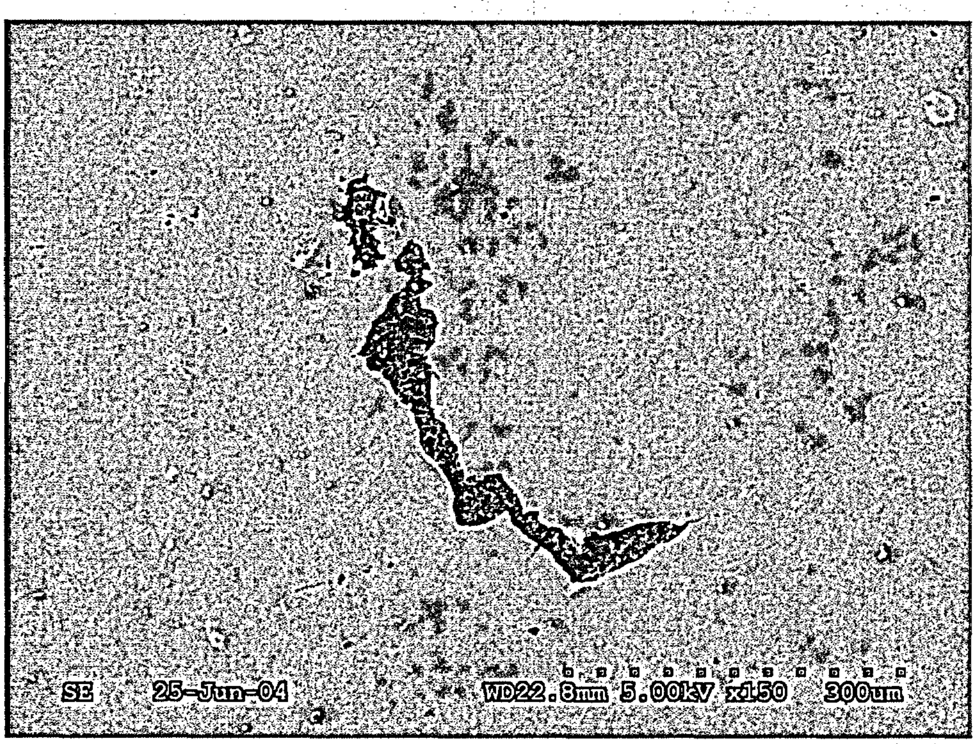

Figure 99: Area "B" in Figure 97. 146X

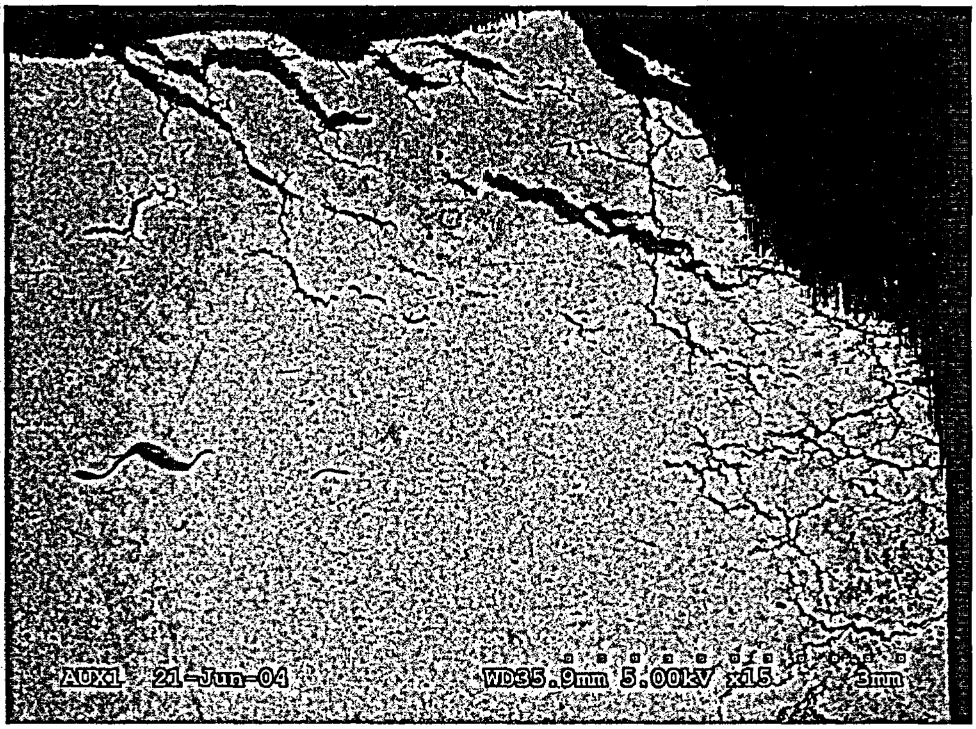

Figure 100: Corrosion area near top of 2H TSP in 5B3B2A (first face). 14.6X

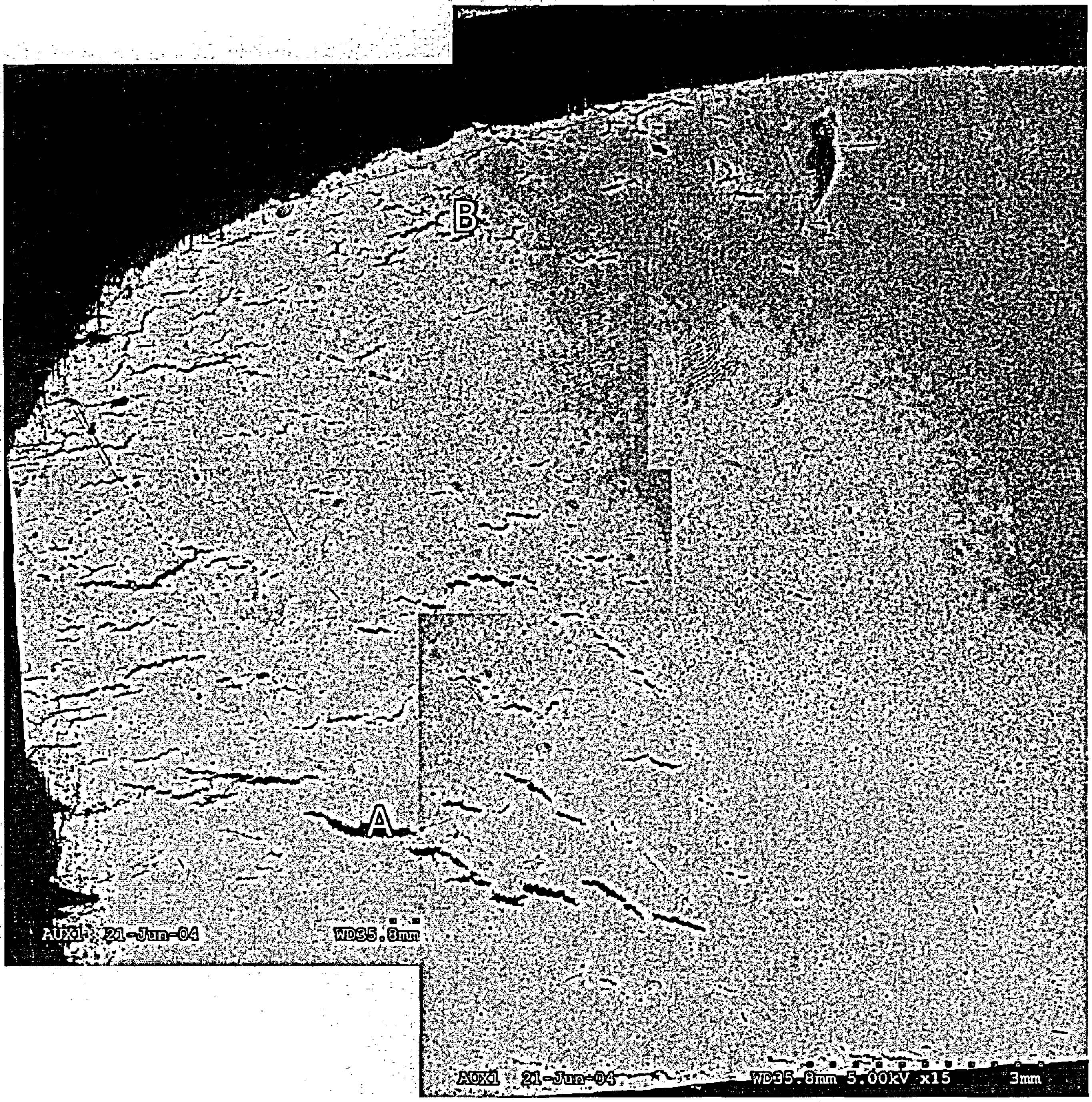

Figure 101: Overall mosaic of corrosion near bottom end of 2H TSP in 5B3B2A (first face). 12.6X

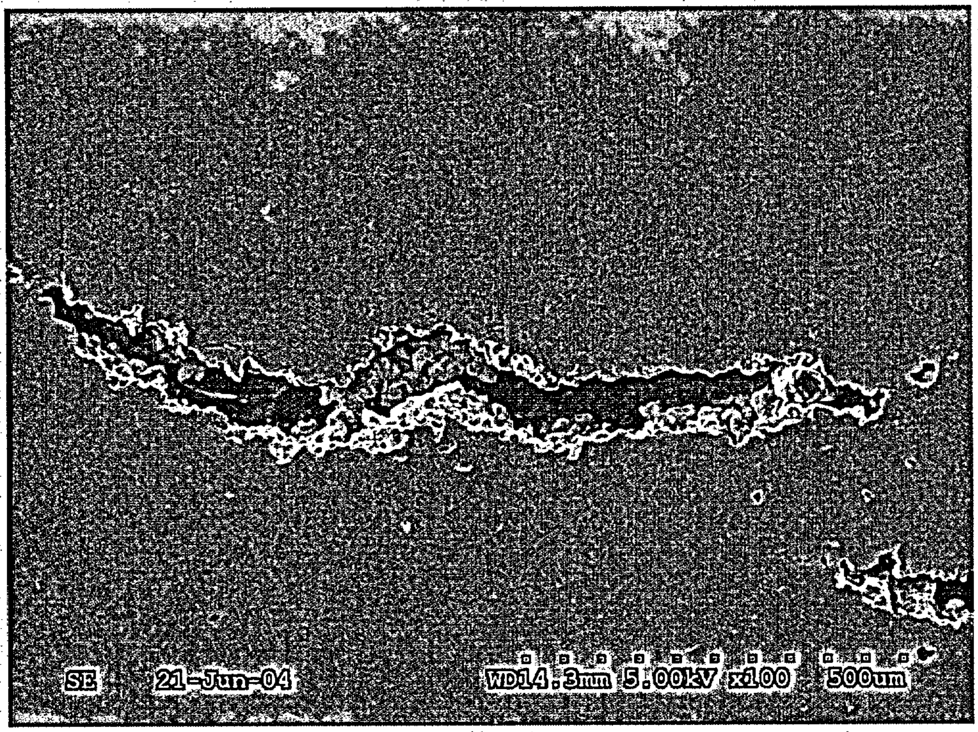

Figure 102: Area "A" in Figure 101. 99X

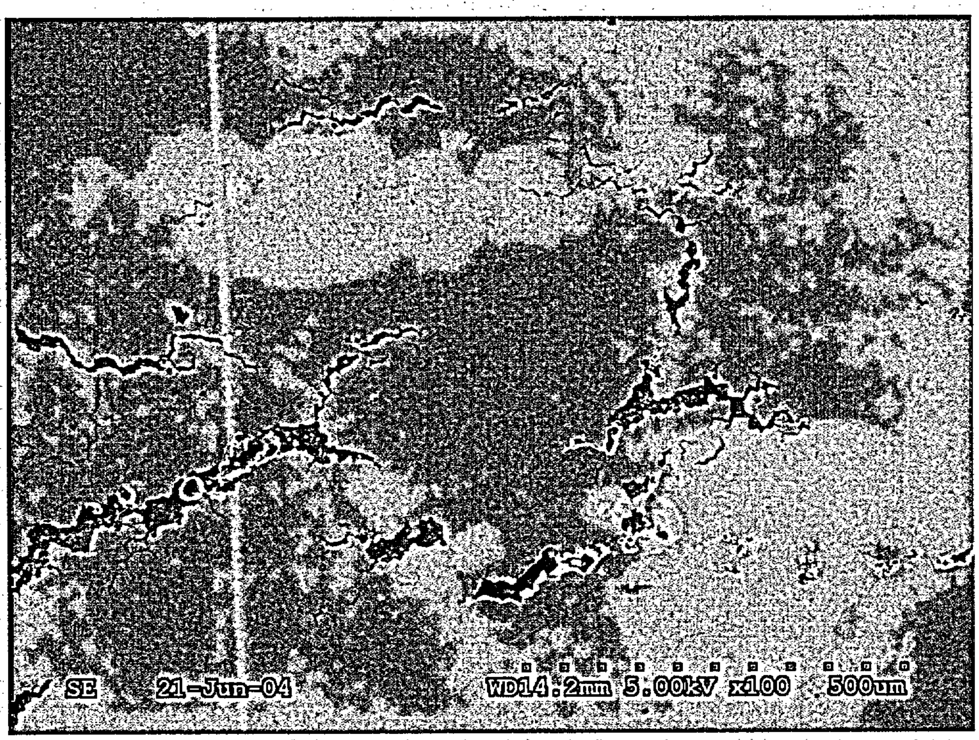

Figure 103: Area "B" in Figure 101. 99X

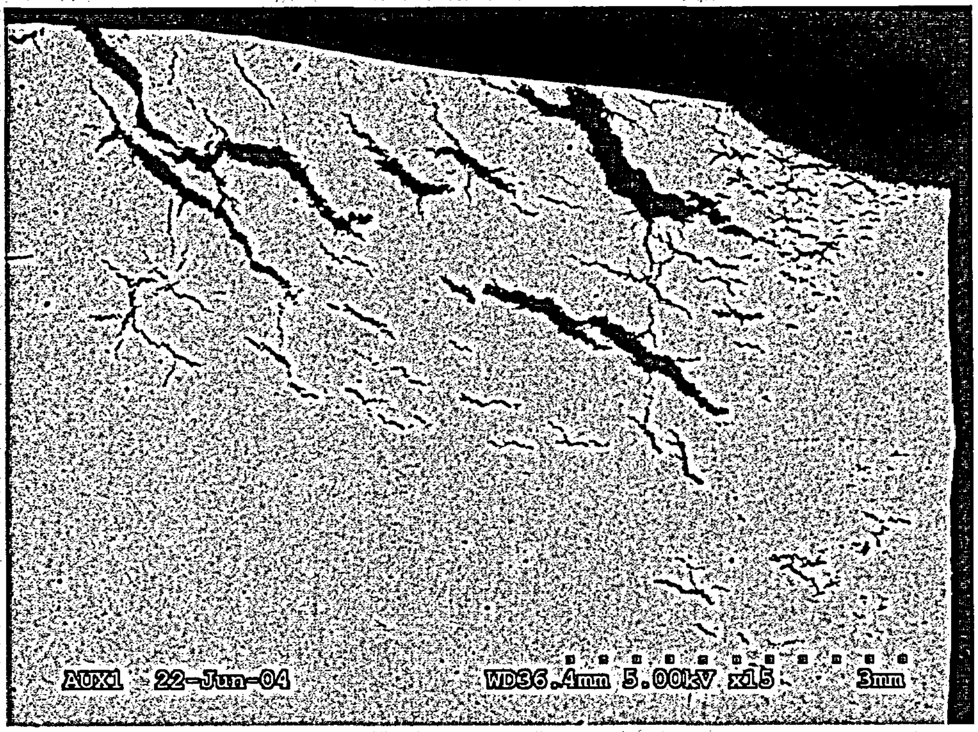

Figure 104: Corrosion area near top of 2H TSP in 5B3B2A (second face). 14.6X

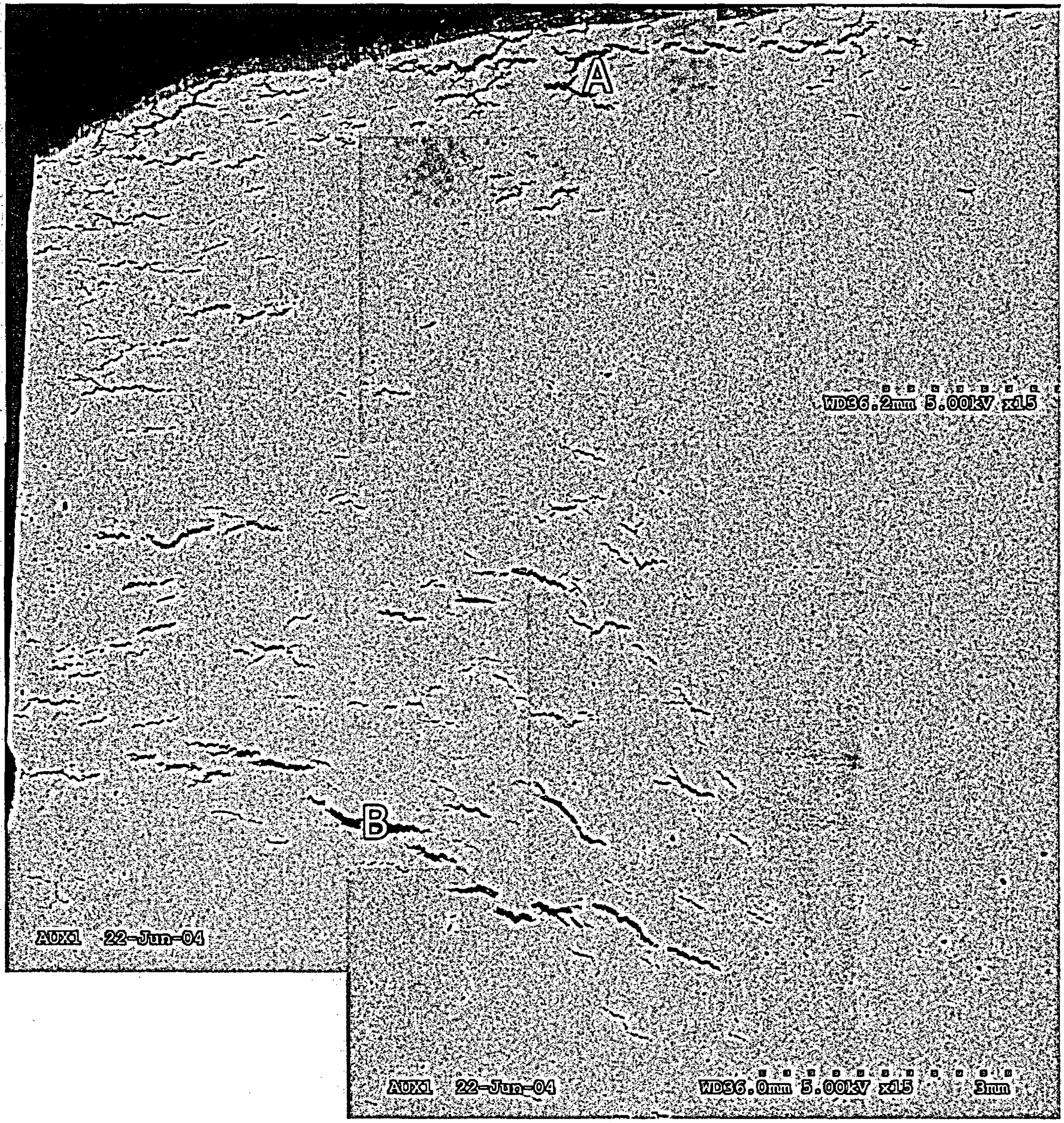

Figure 105: Overall mosaic of corrosion near bottom end of 2H TSP in 5B3B2A (second face). 13.7X

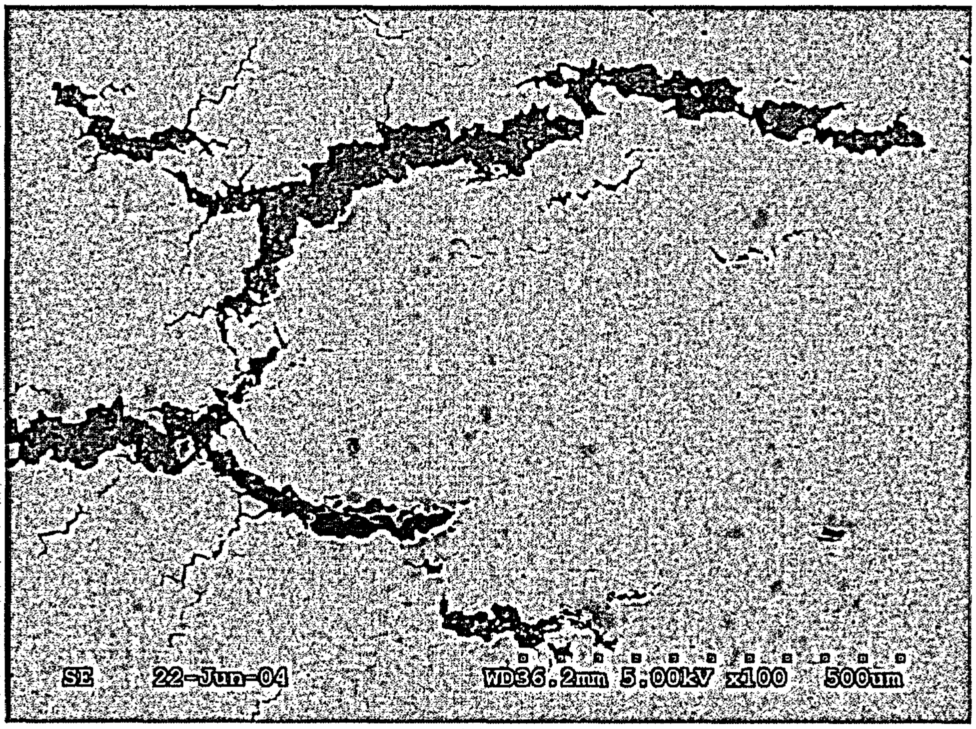

Figure 106: Area "A" in Figure 105. 99X

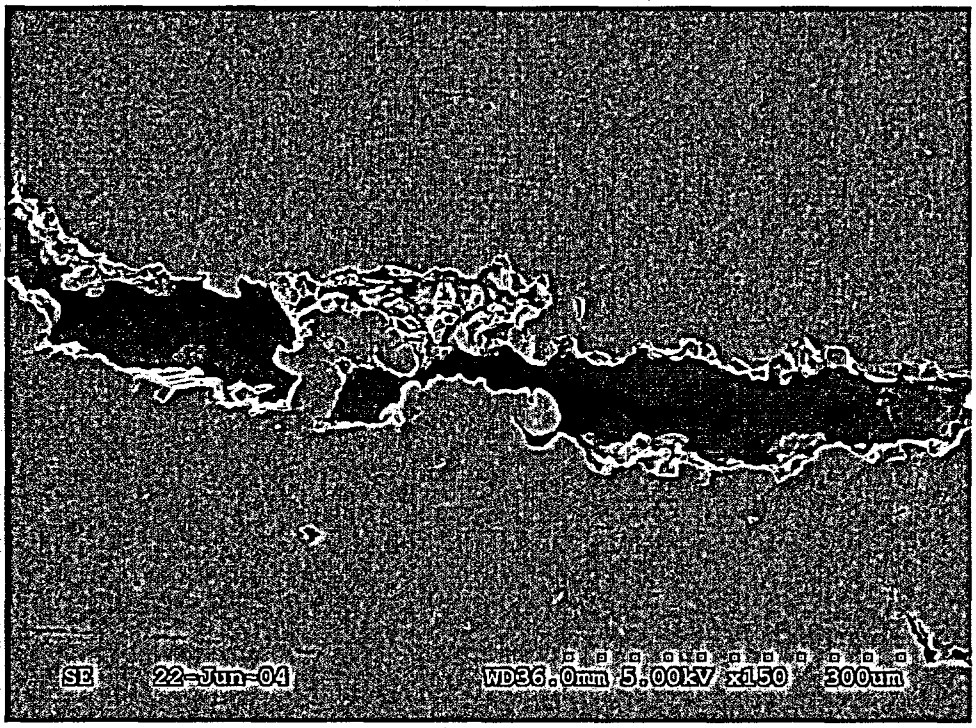

Figure 107: Area "B" in Figure 105. 146X

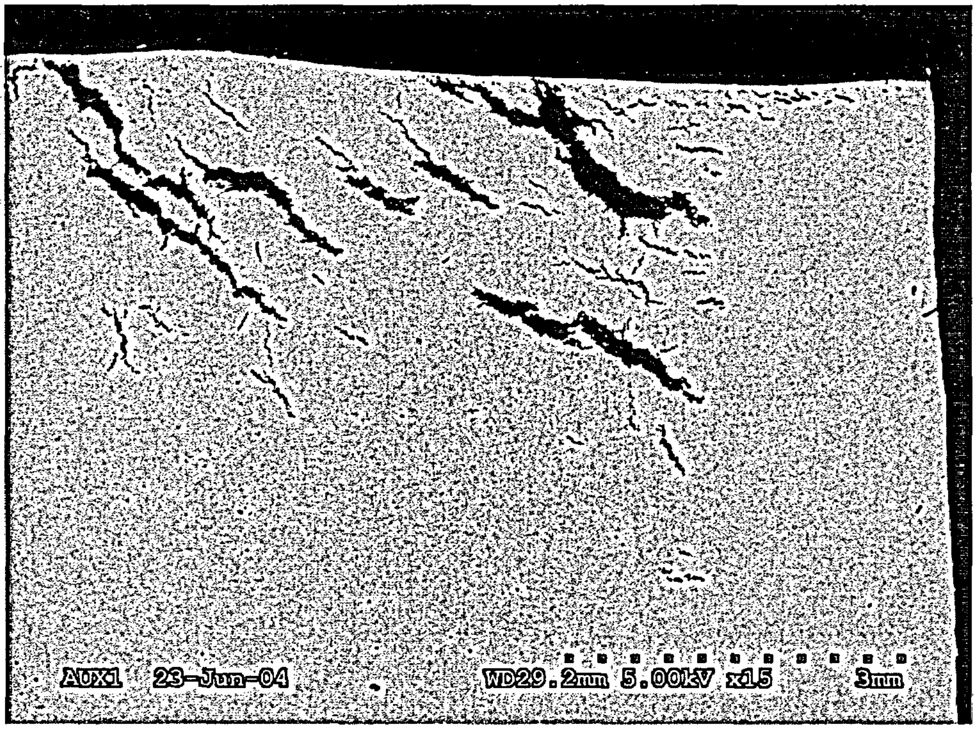

Figure 108: Corrosion area near top of 2H TSP in 5B3B2A (third face). 14.6X

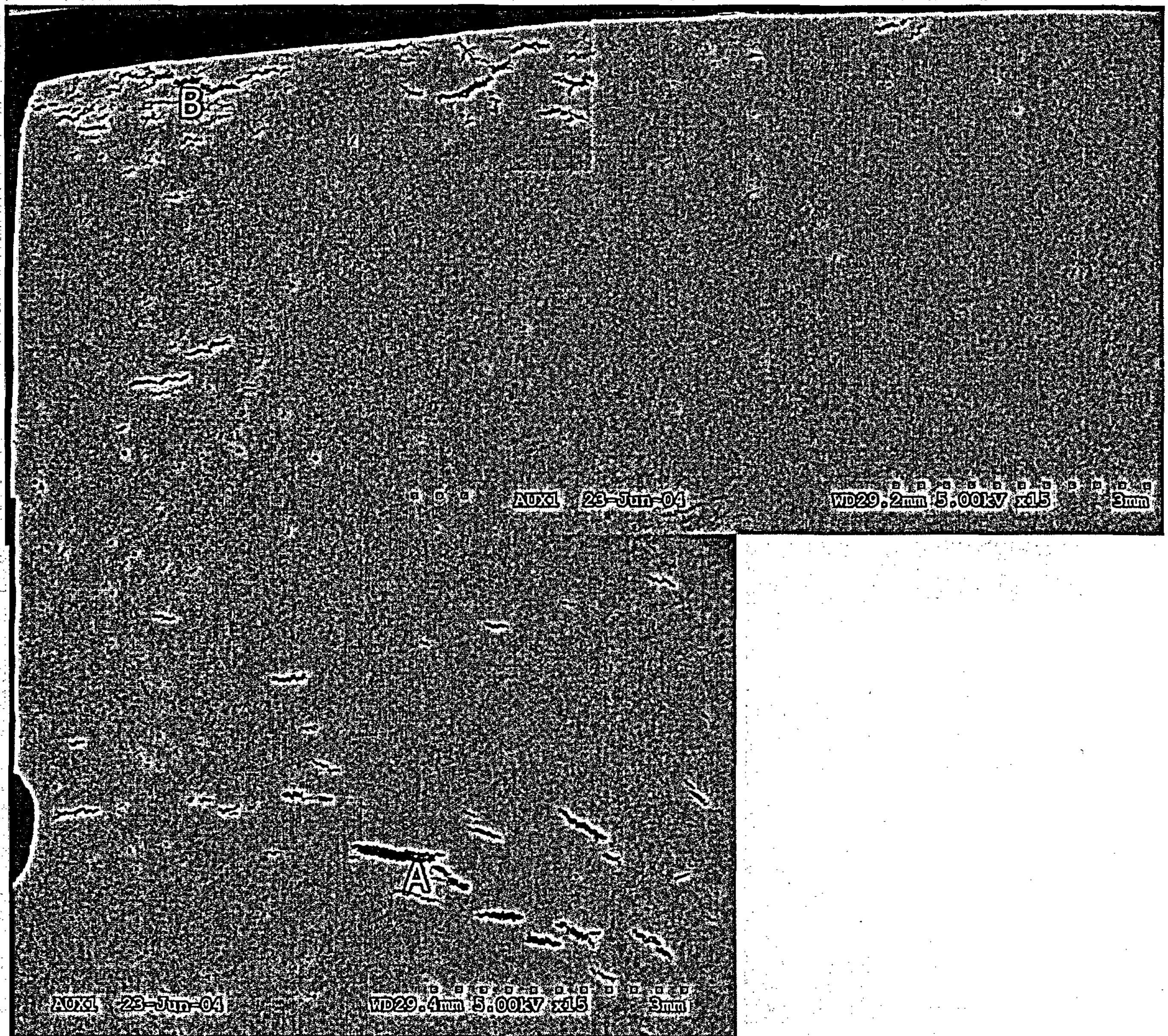

Figure 109: Overall mosaic of corrosion near bottom end of 2H TSP in 5B3B2A (third face). 12.8X

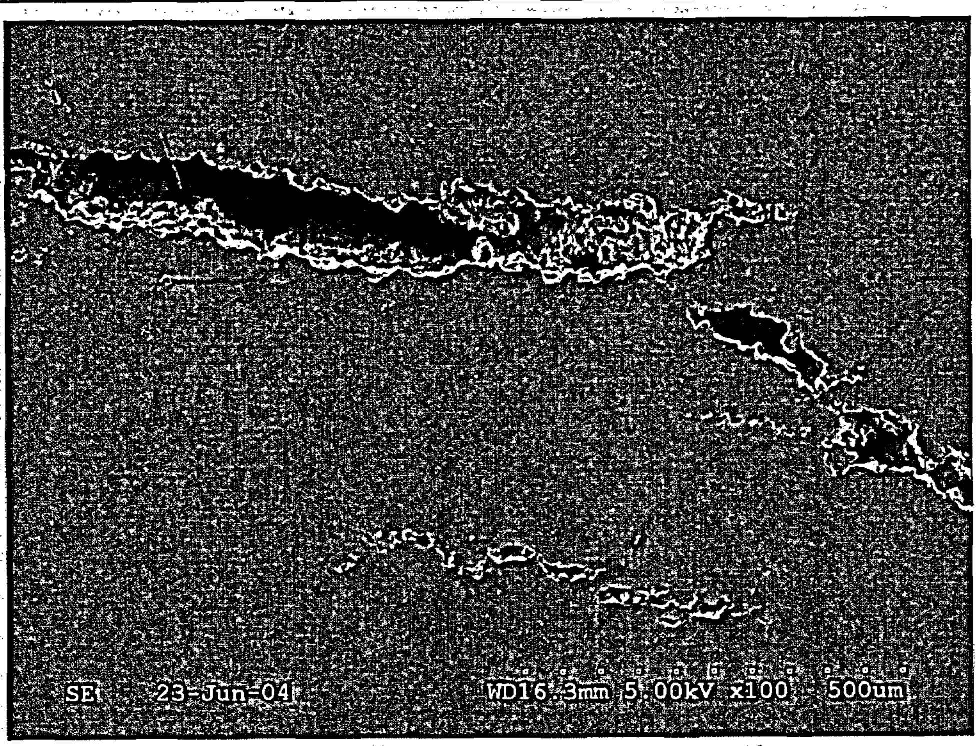

Figure 110: Area "A" in Figure 109. 99X

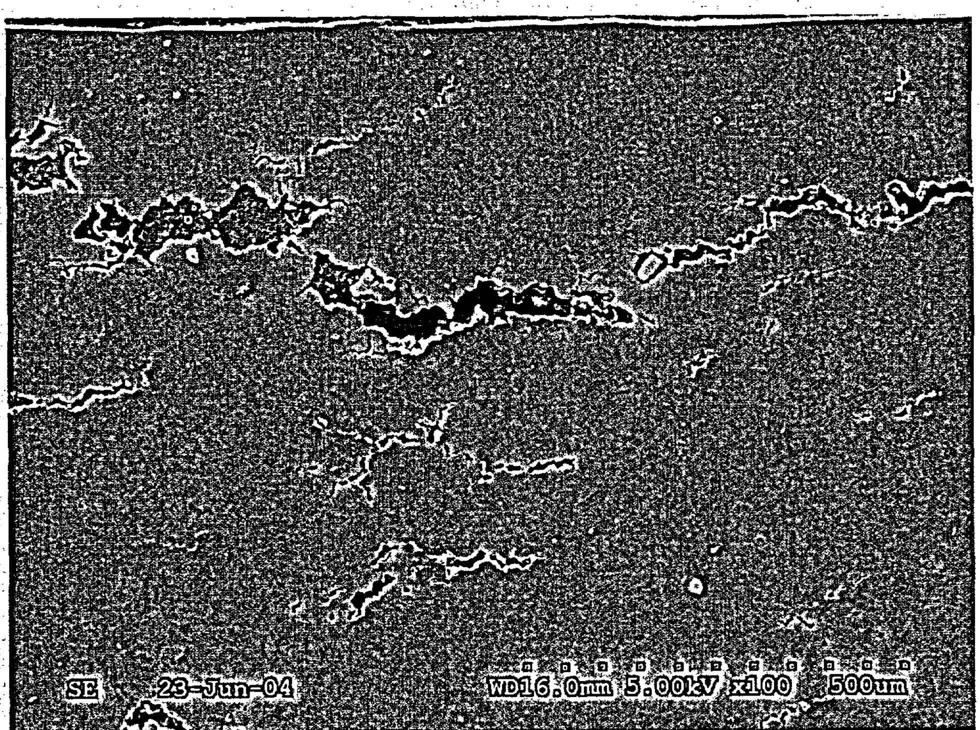

Figure 111: Area "B" in Figure 109. 99X

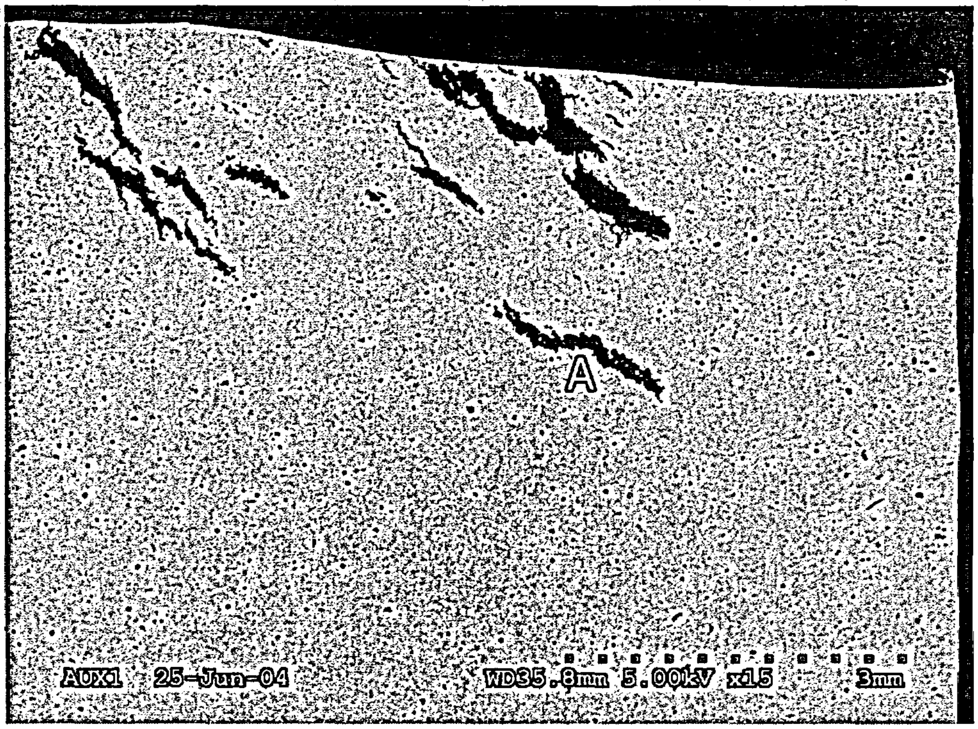

Figure 112: Corrosion area near top of 2H TSP IN 5B3B2A (fourth face). 14.6X

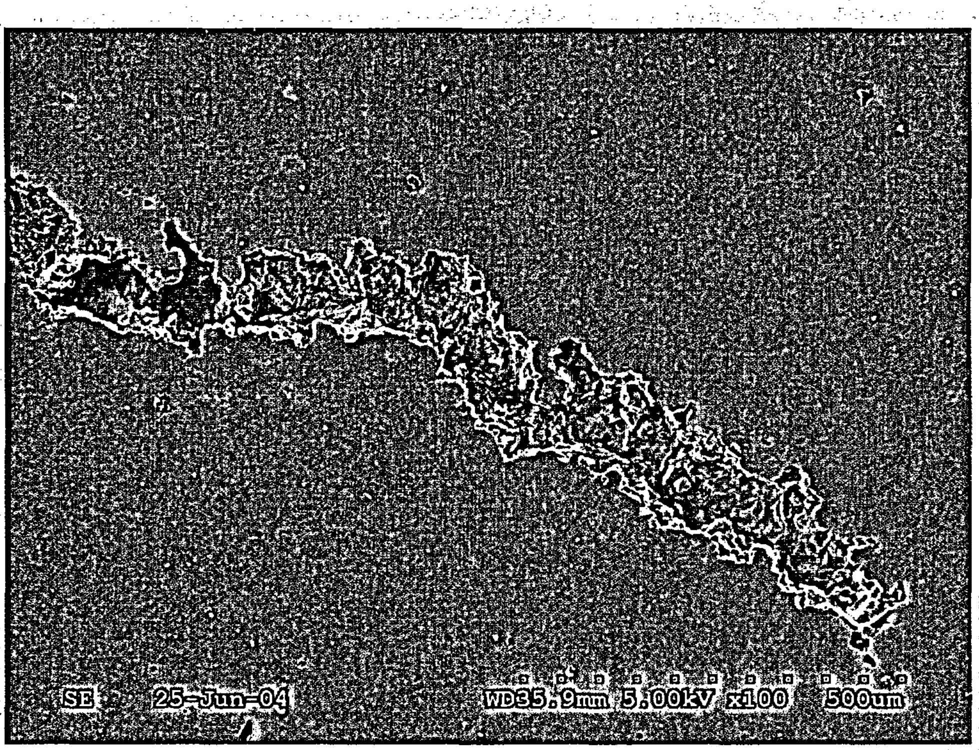

Figure 113: Area "A" in Figure 112. 99X

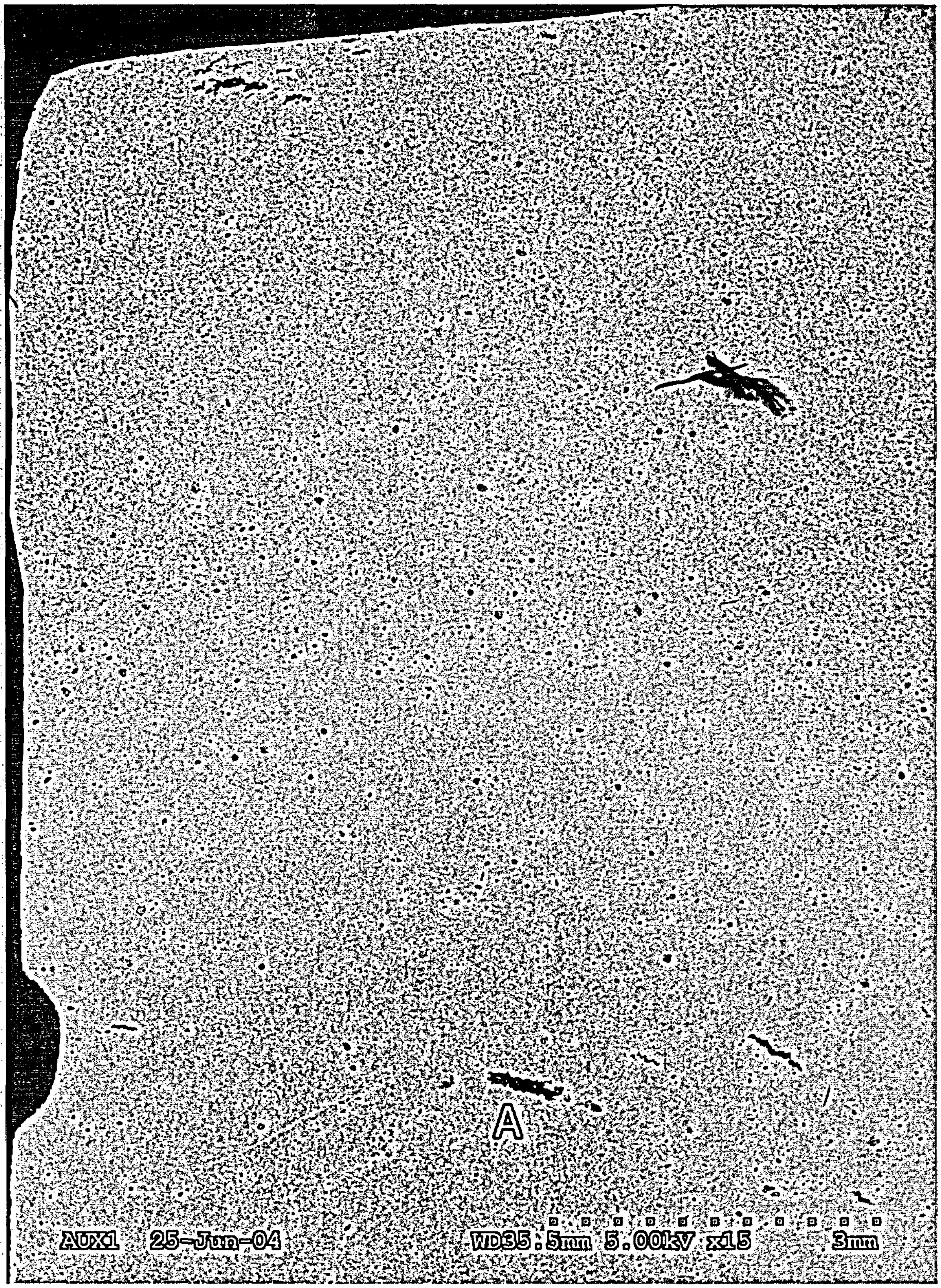

Figure 114: Overall mosaic of corrosion near bottom end of 2H TSP in 5B3B2A (fourth face). 17.5X

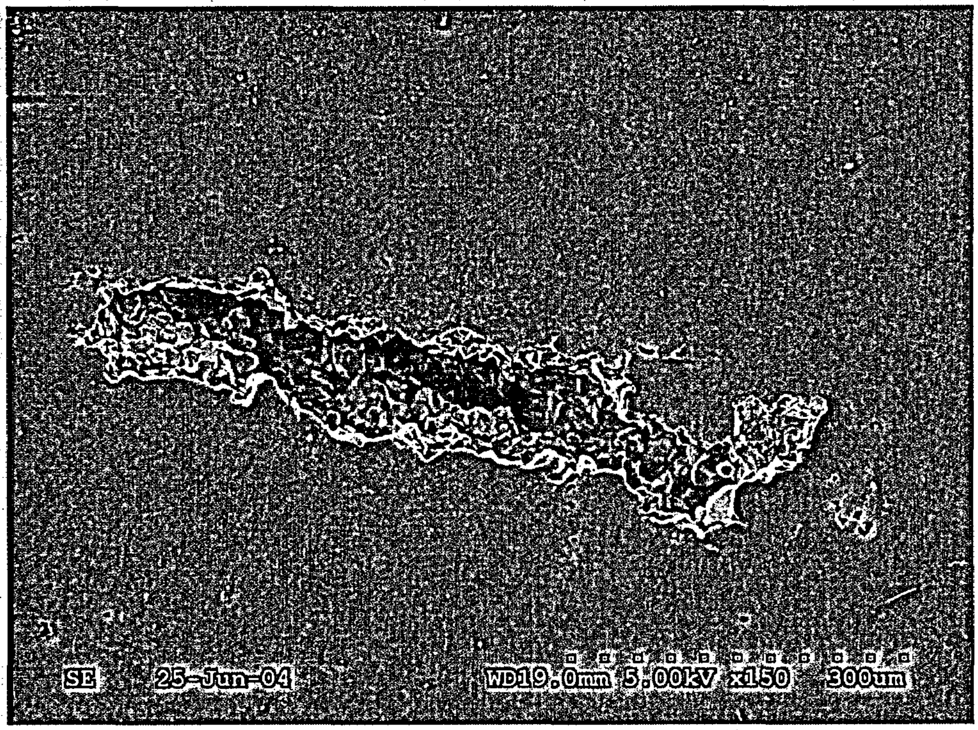

Figure 115: Area "A" in Figure 114. 146X

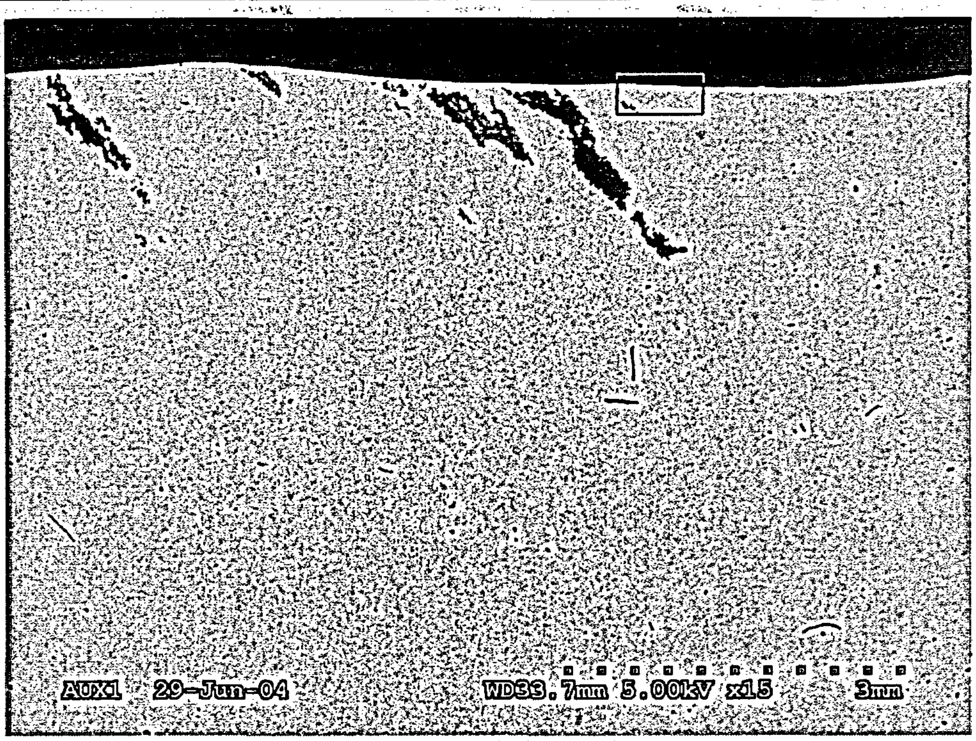

Figure 116: Corrosion area near top of 2H TSP in 5B3B2A (fifth face). 14.6X

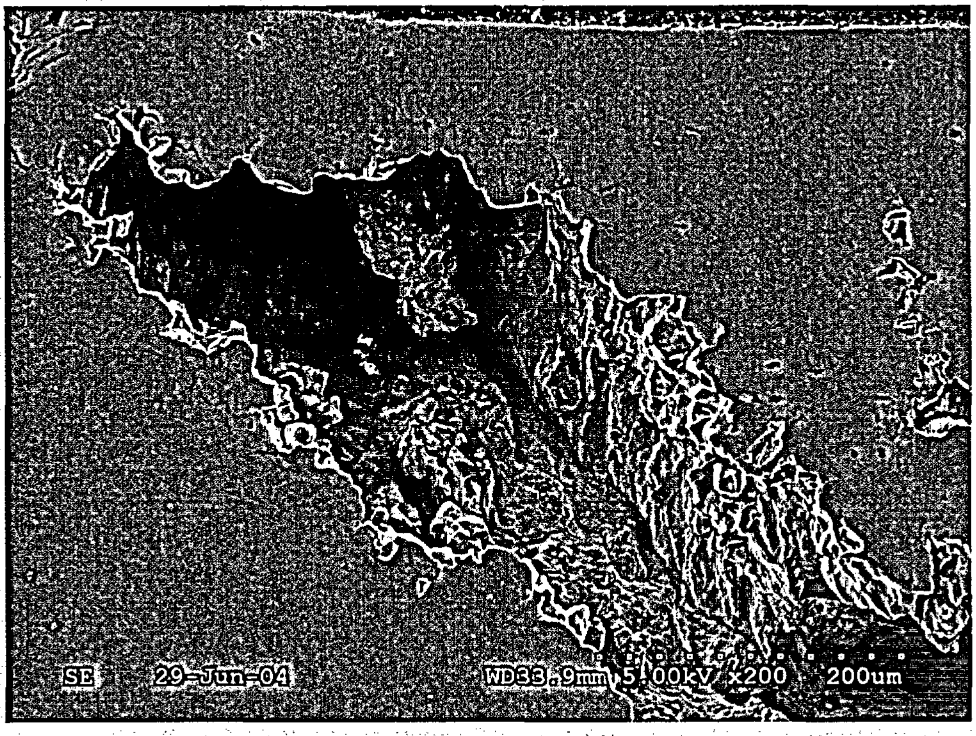

Figure 117: Detail of area shown in box in Figure 116. 198X

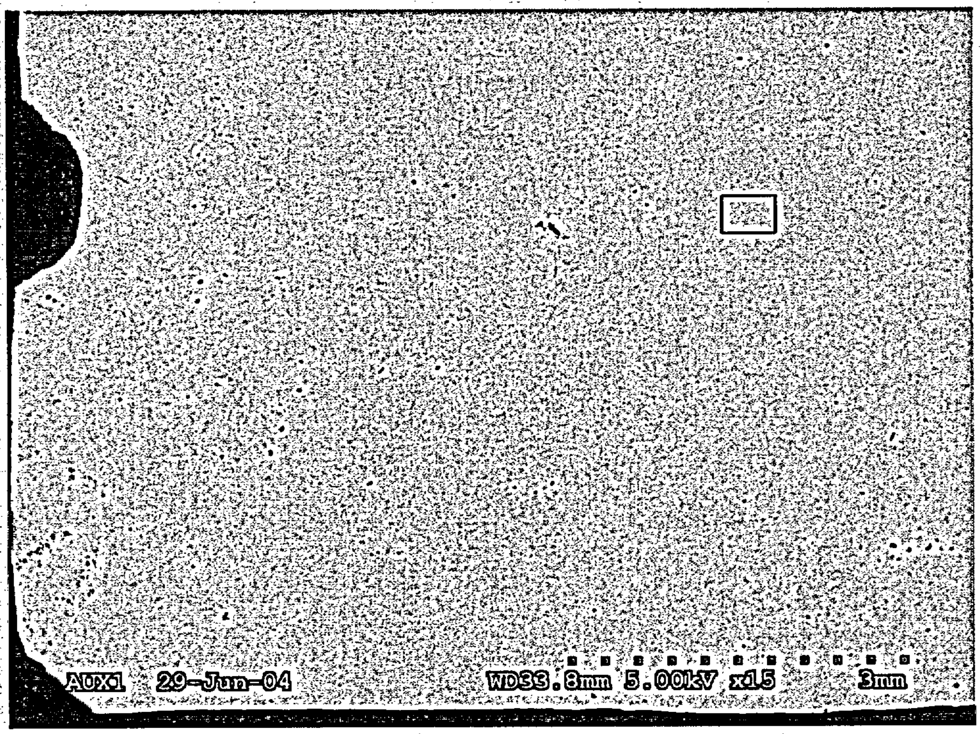

Figure 118: Bottom end of 2H TSP in 5B3B2A (fifth face). 14.6X

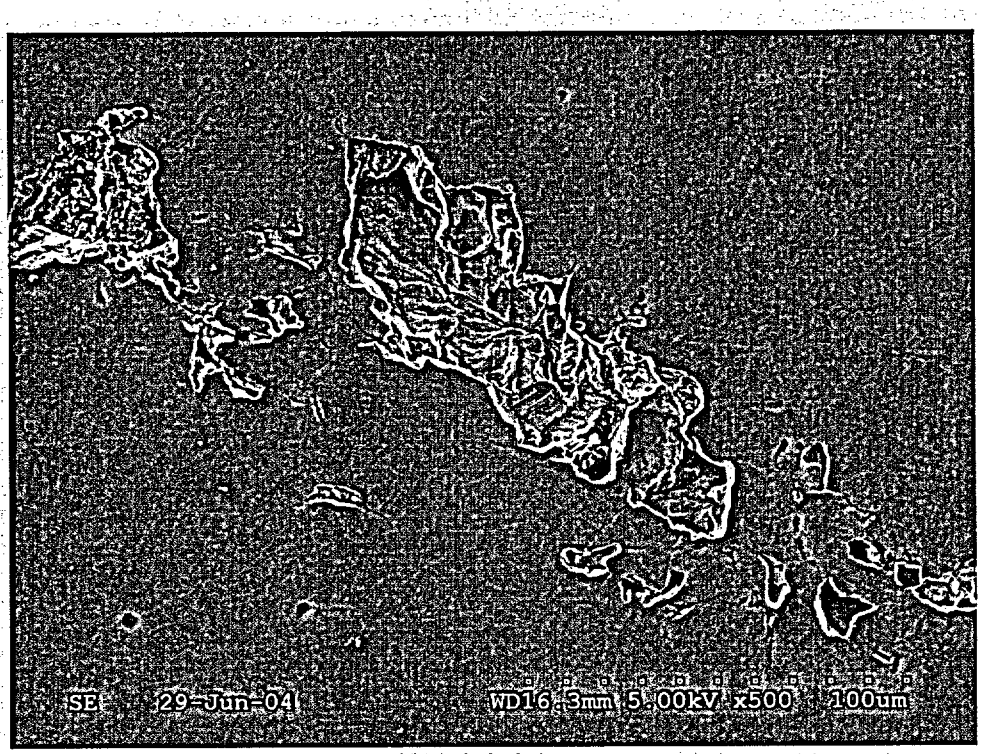

Figure 119: Detail of area shown in box in Figure 118. 496X

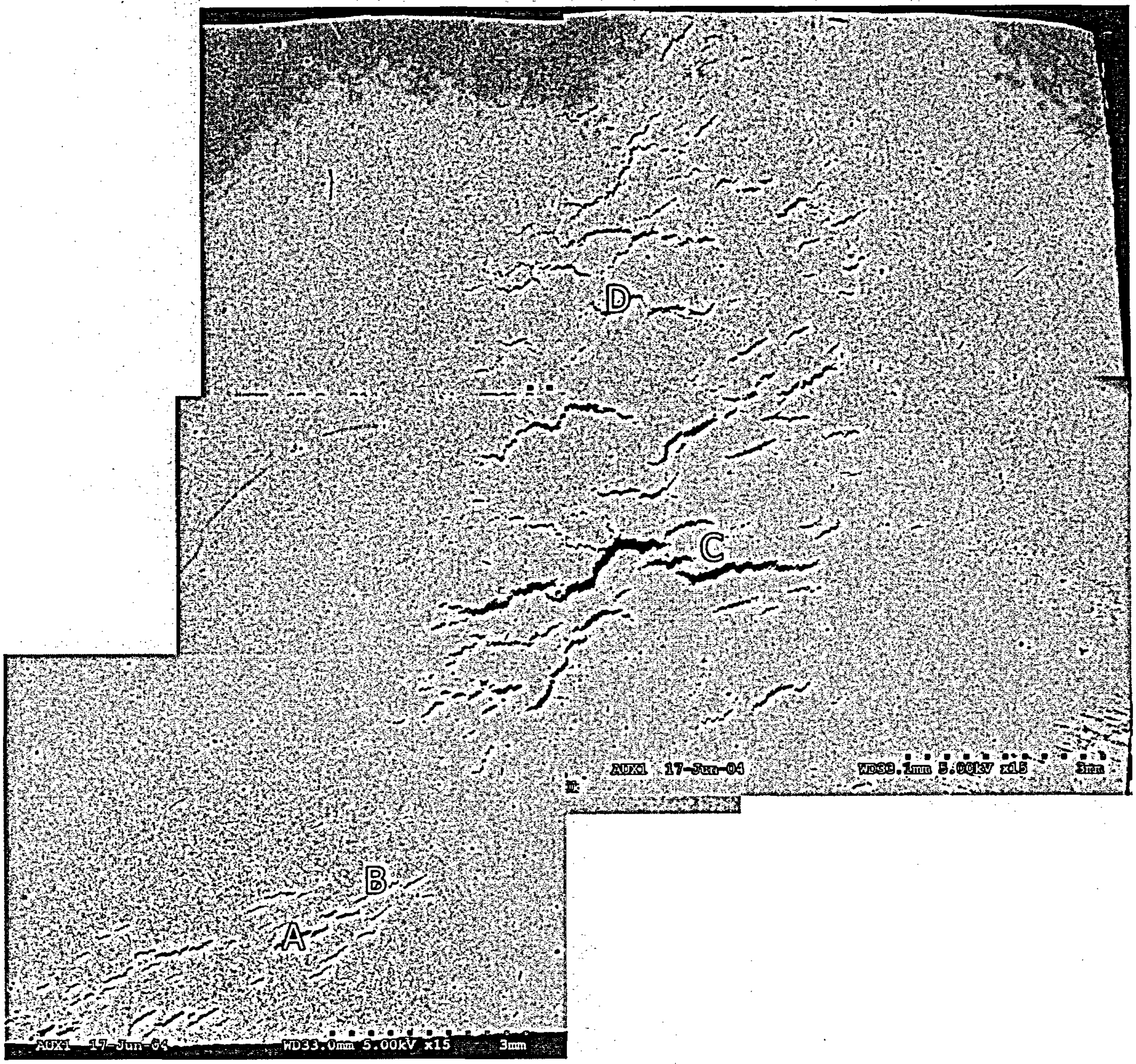

Figure 120: Overall mosaic of corrosion on 5B3B2C (first face). 10.0X

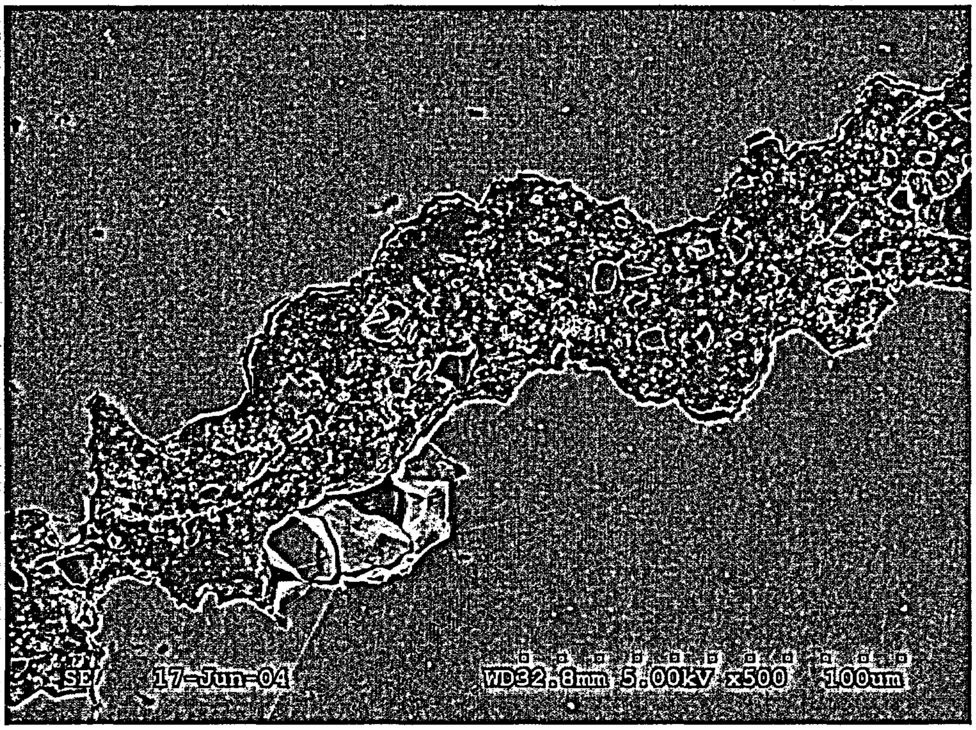

Figure 121: Area "A" in Figure 120. 492X

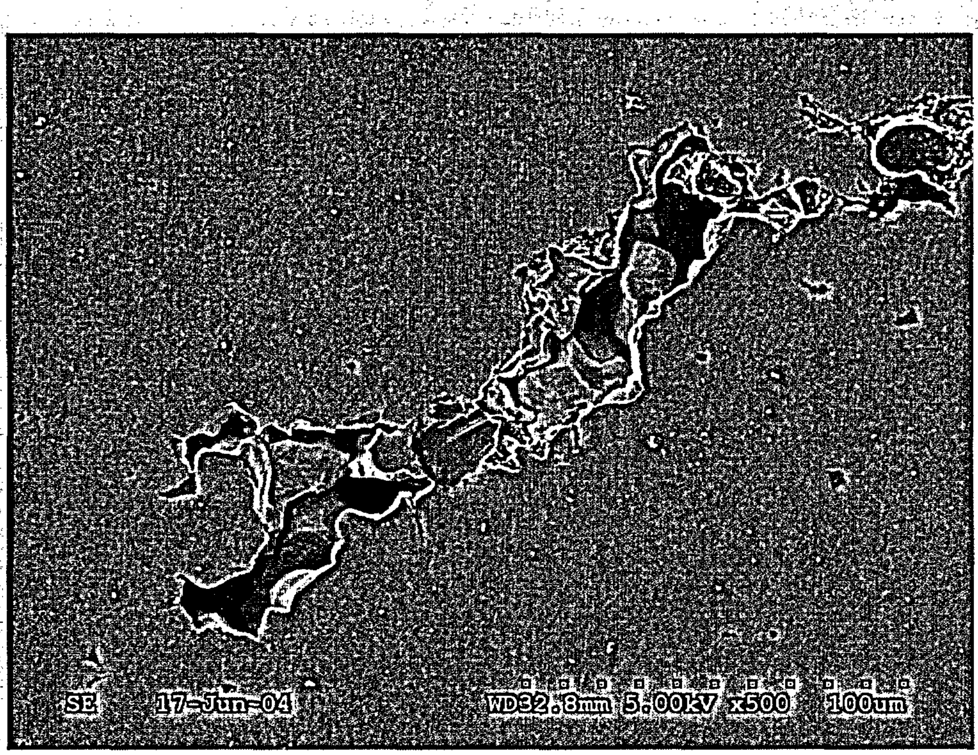

Figure 122: Area "B" in Figure 120. 492X

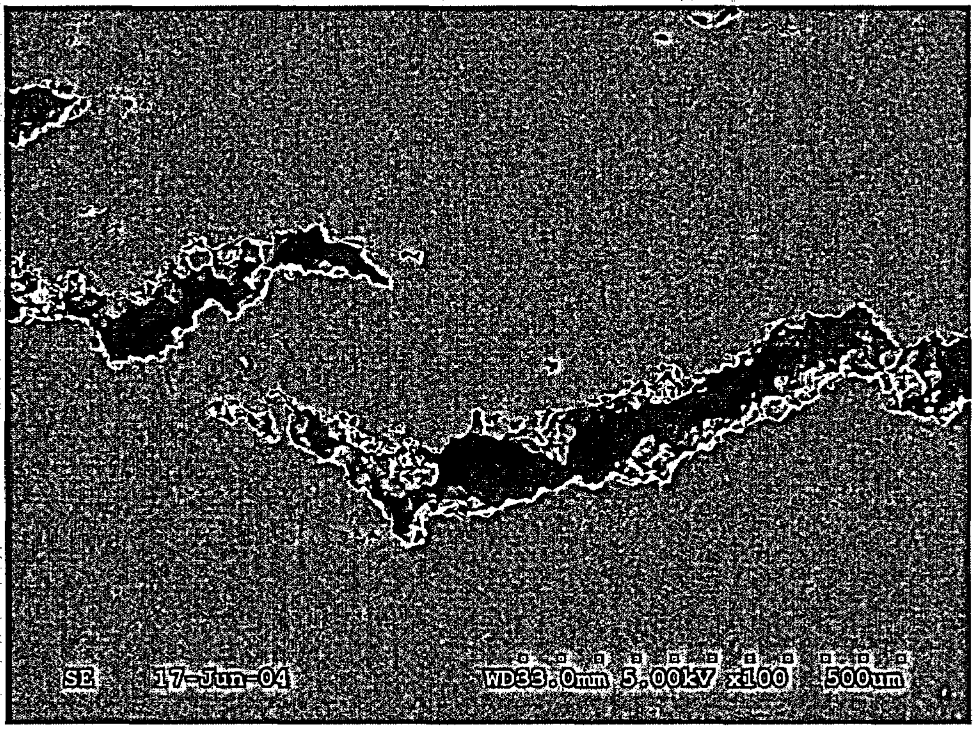

Figure 123: Area "C" in Figure 120. 99X

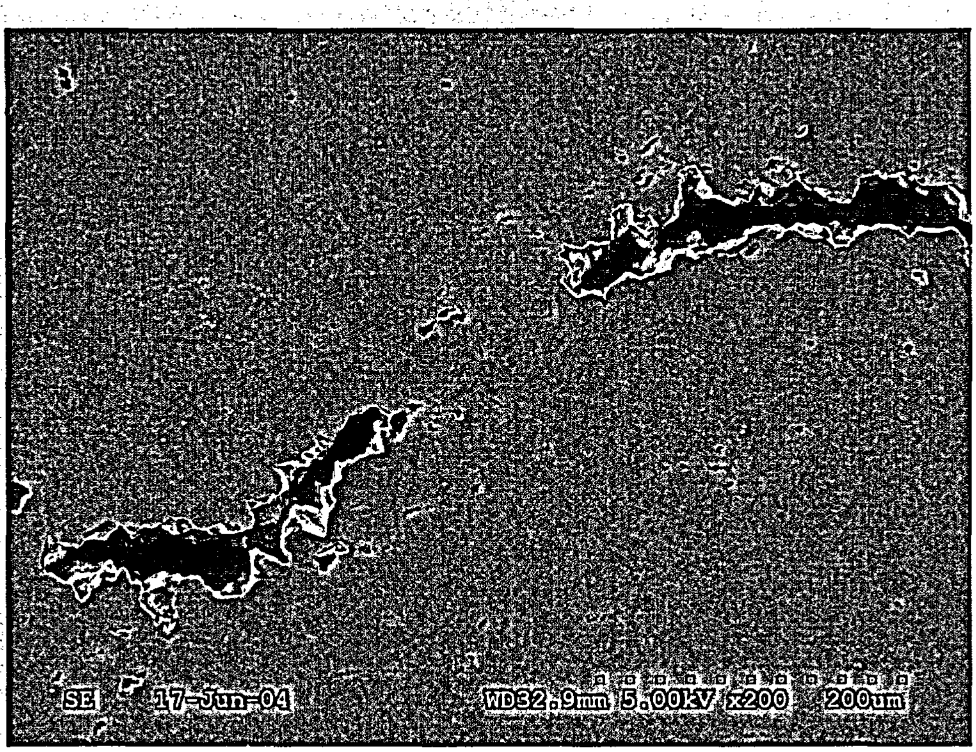

Figure 124: Area "D" in Figure 120. 199X

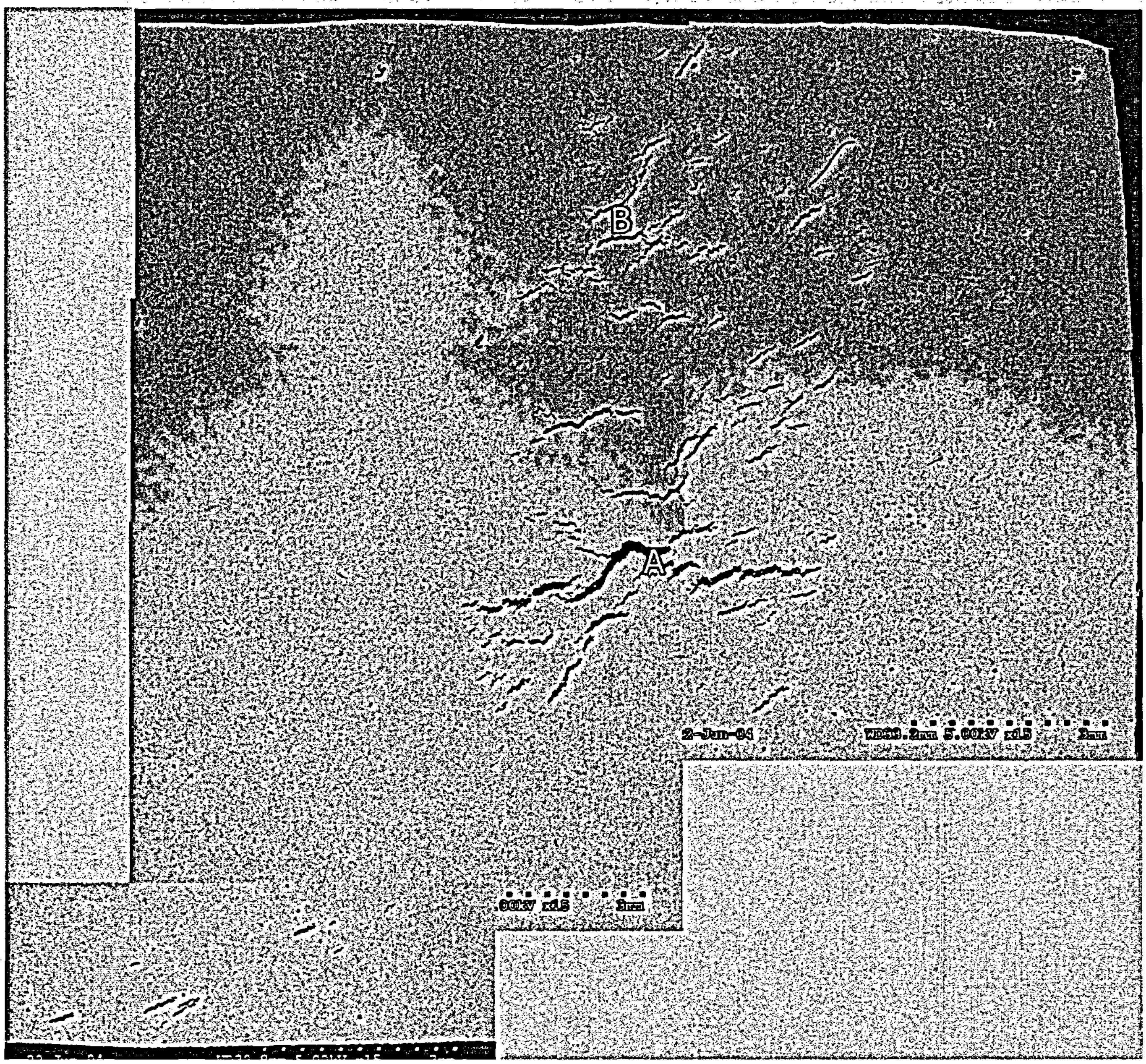

Figure 125: Overall mosaic of corrosion on 5B3B2C (second face). 9.9X

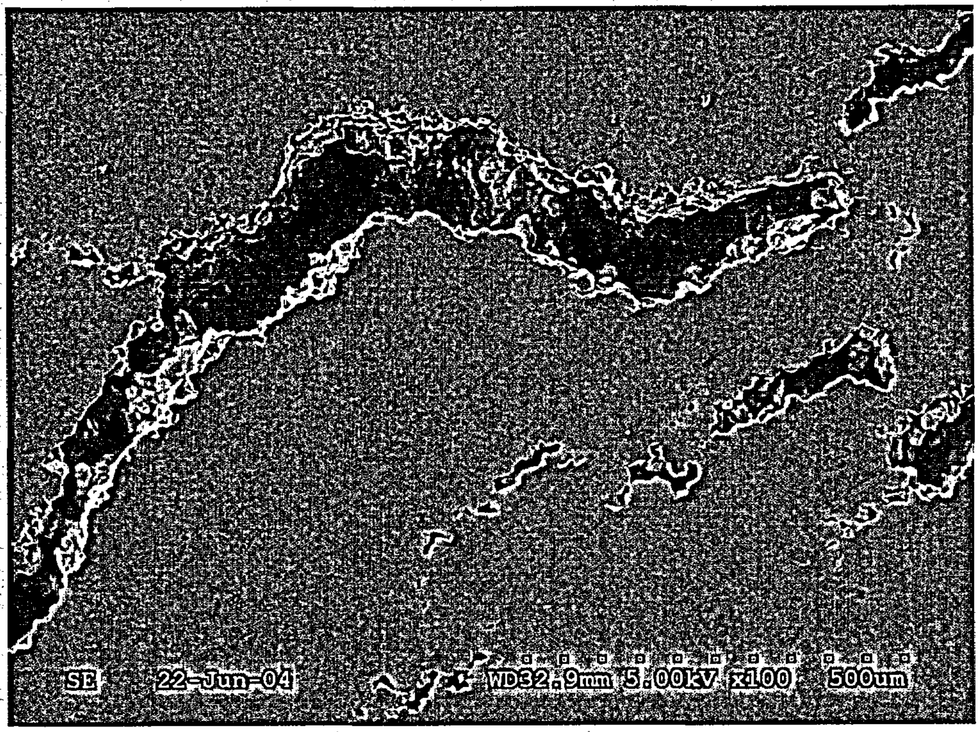

Figure 126: Area "A" in Figure 125. 99X

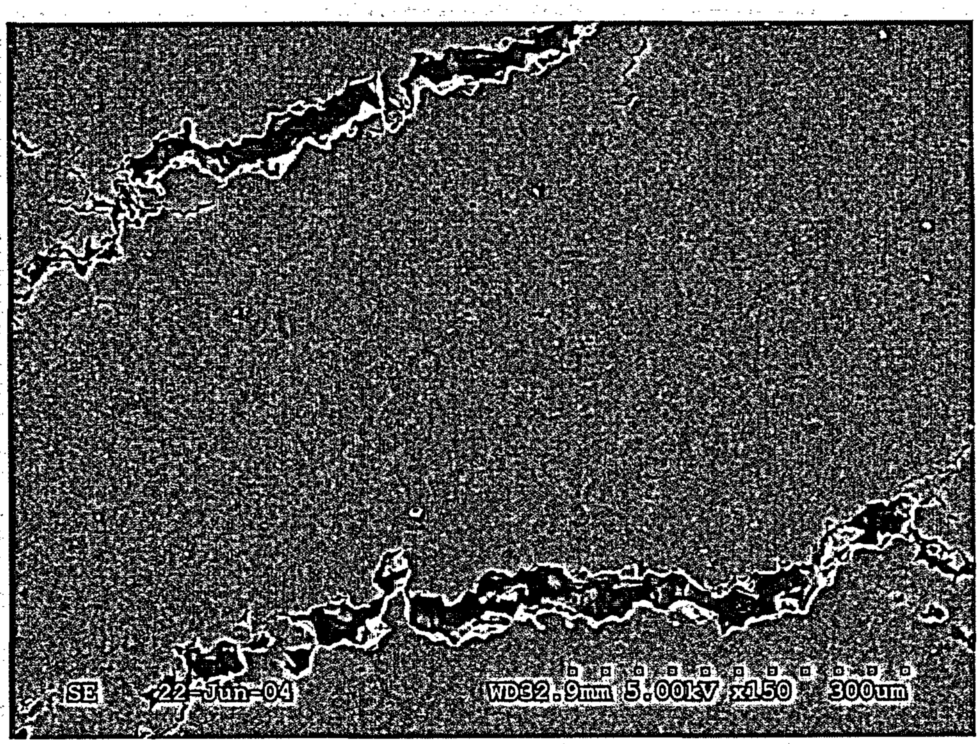

Figure 127: Area "B" in Figure 125. 146X

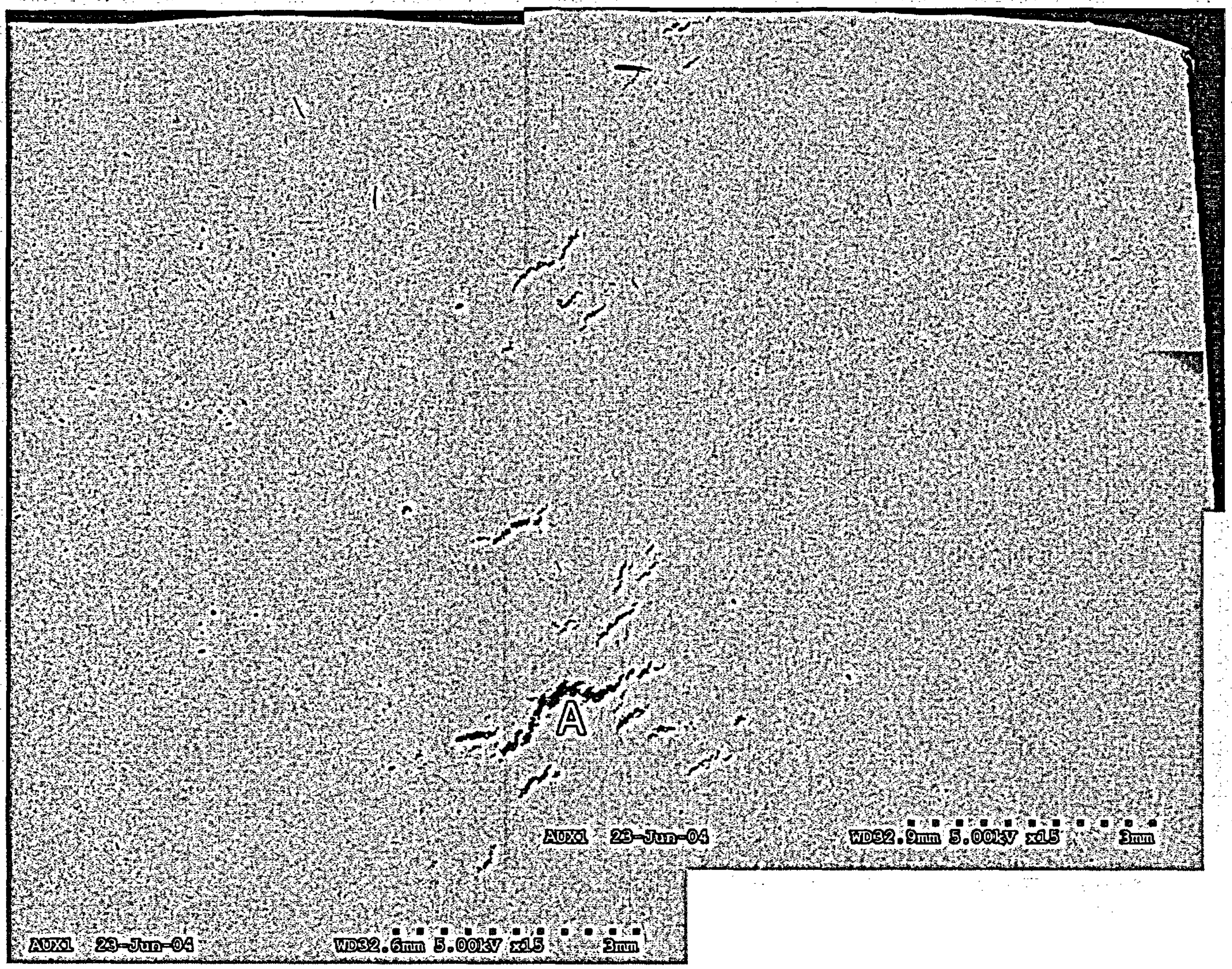

Figure 128: Overall mosaic of corrosion on 5B3B2C (third face). 11.7X

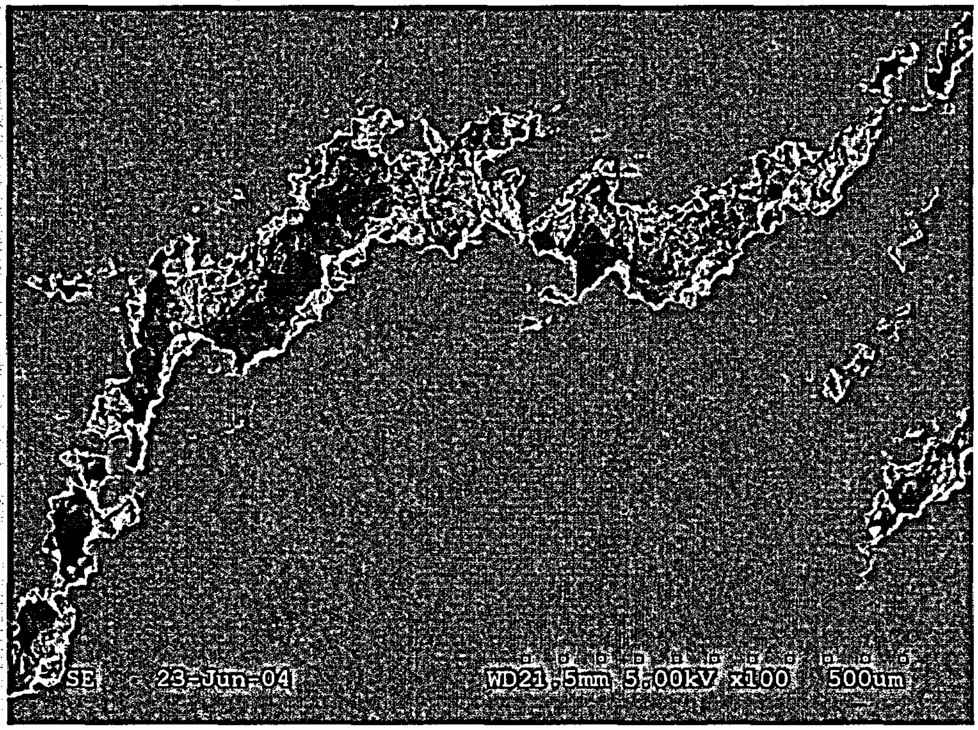

Figure 129: Area "A" in Figure 128. 99X

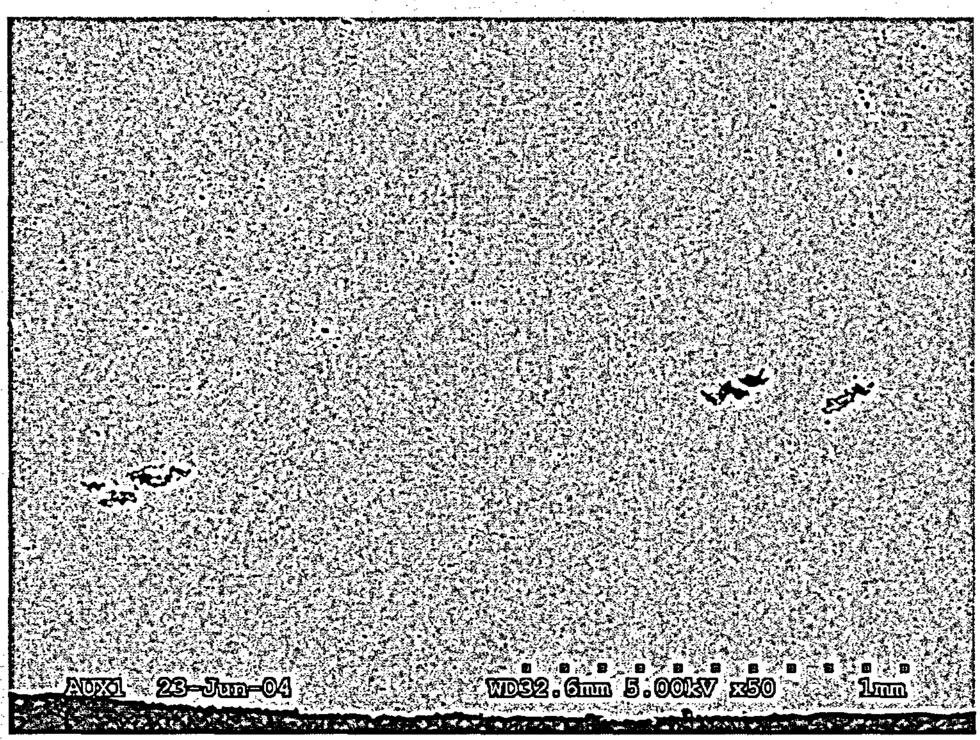

Figure 130: Last remnants of corrosion shown previously in lower left of Figure 125 (third face now). 49.6X

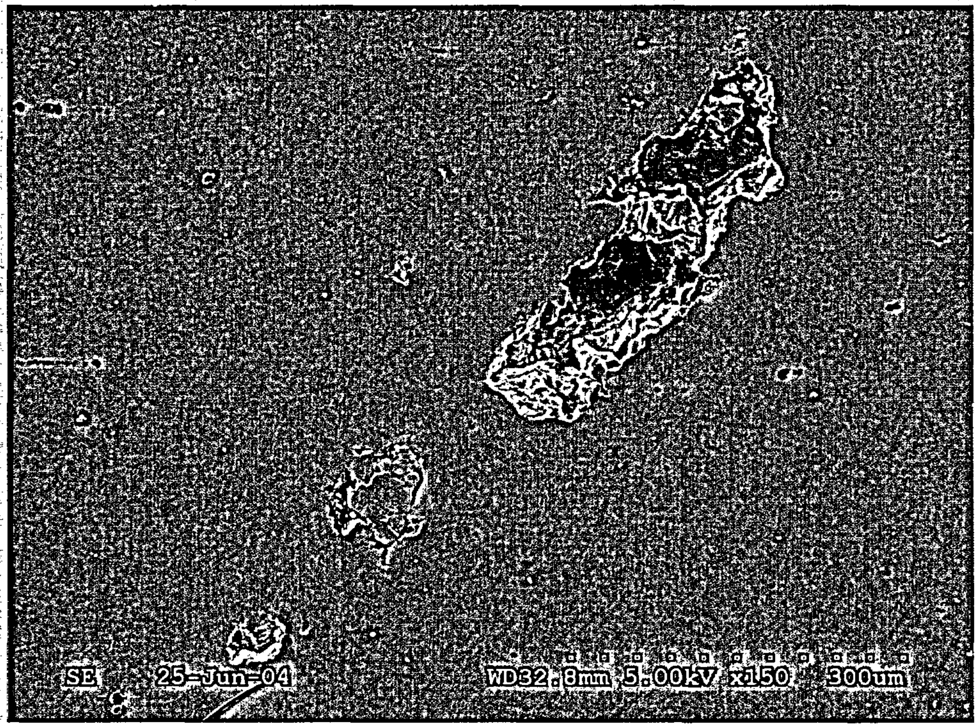

Figure 131: Last remnants of corrosion shown previously in upper portion of Figure 128 (fourth face now). 146X

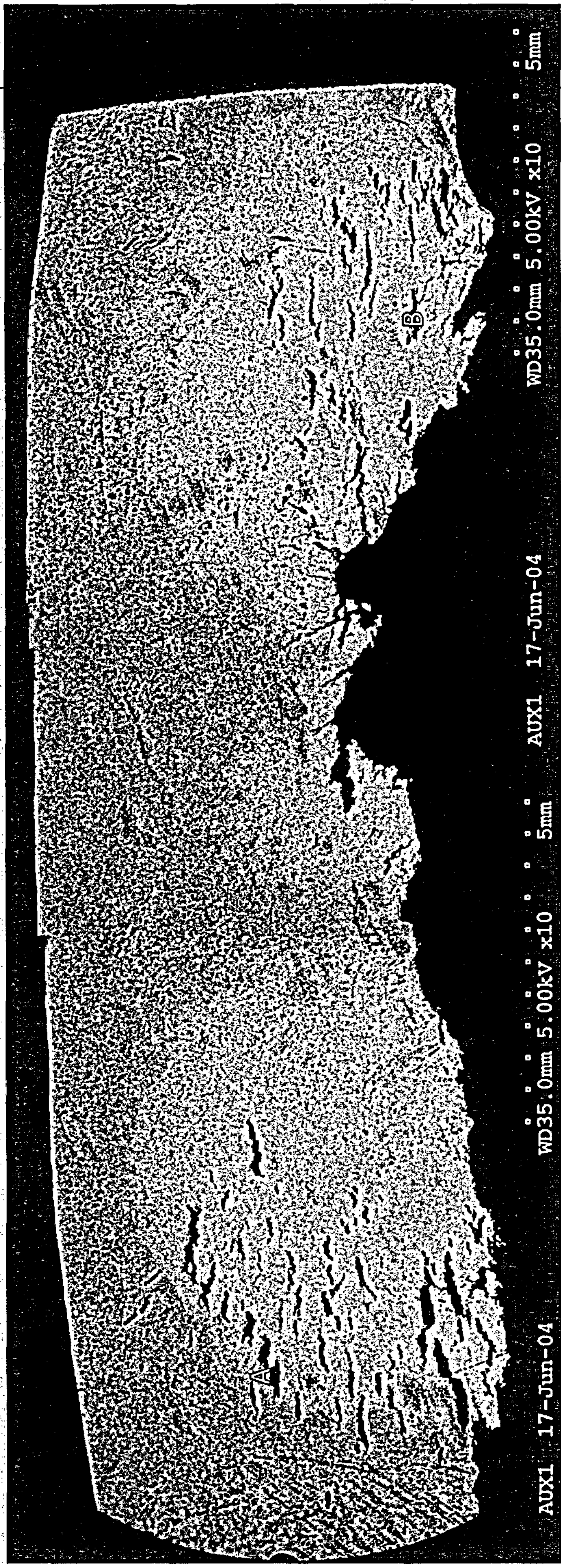

Figure 132:
Overall mosaic of 5B3B2E (first face)
10.4X

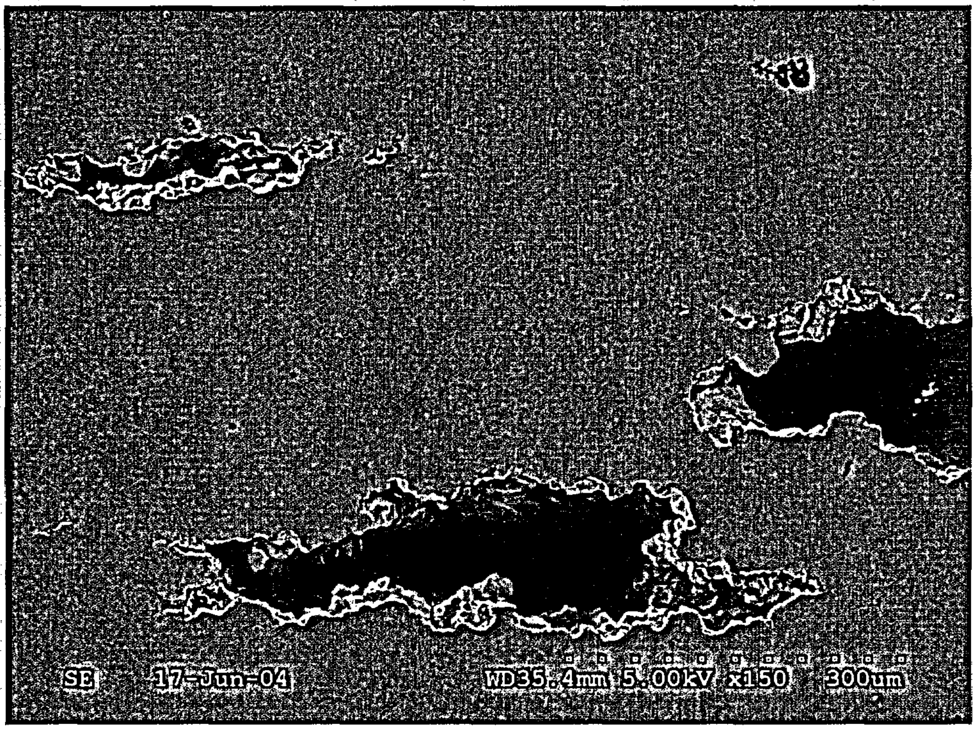

Figure 133: Area “A” in Figure 132. 146X

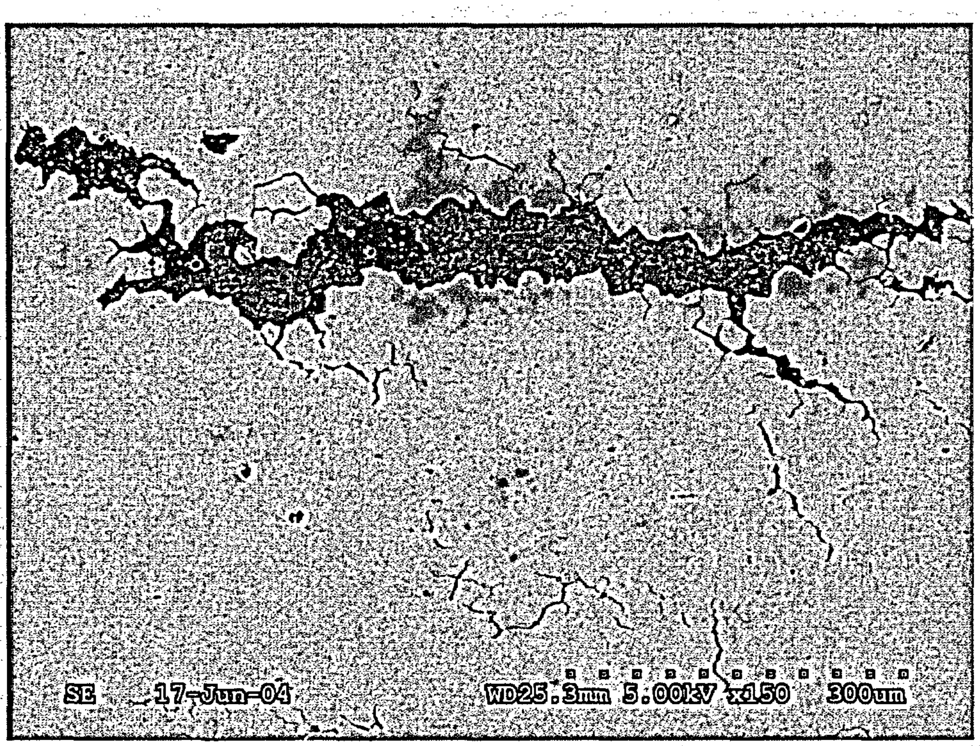

Figure 134: Area “B” in Figure 132. 146X

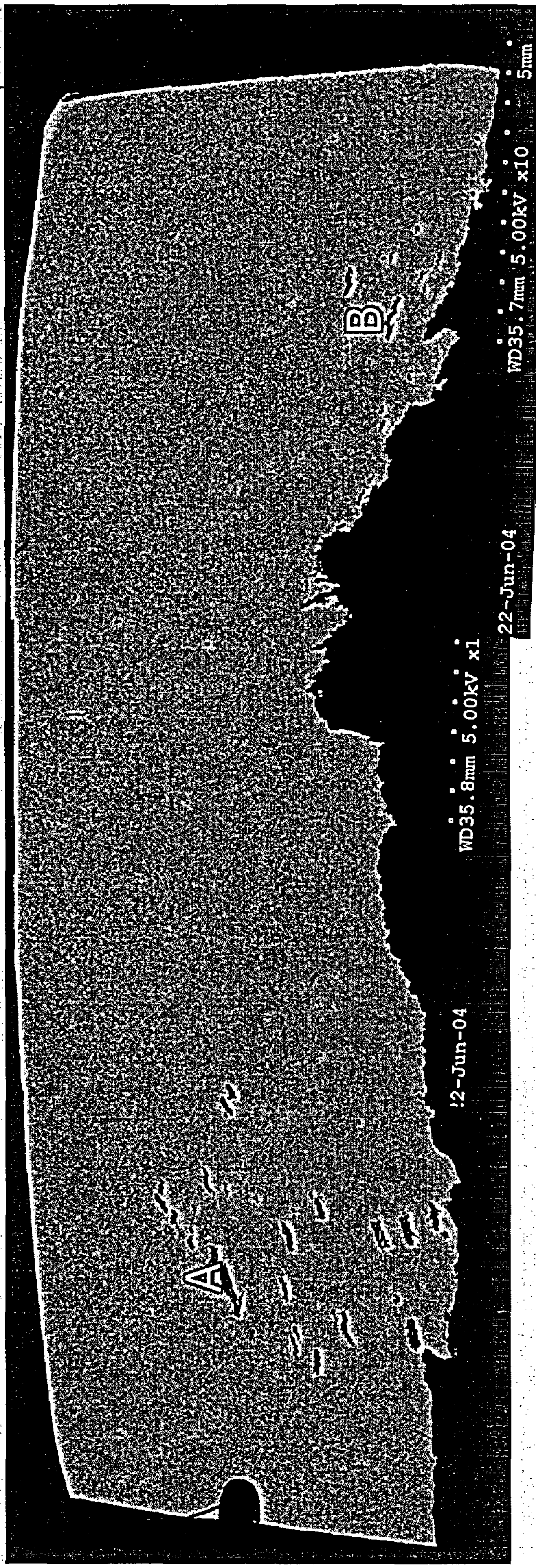

Figure 135: Overall mosaic of 5B3B2E (second face) 9.7X

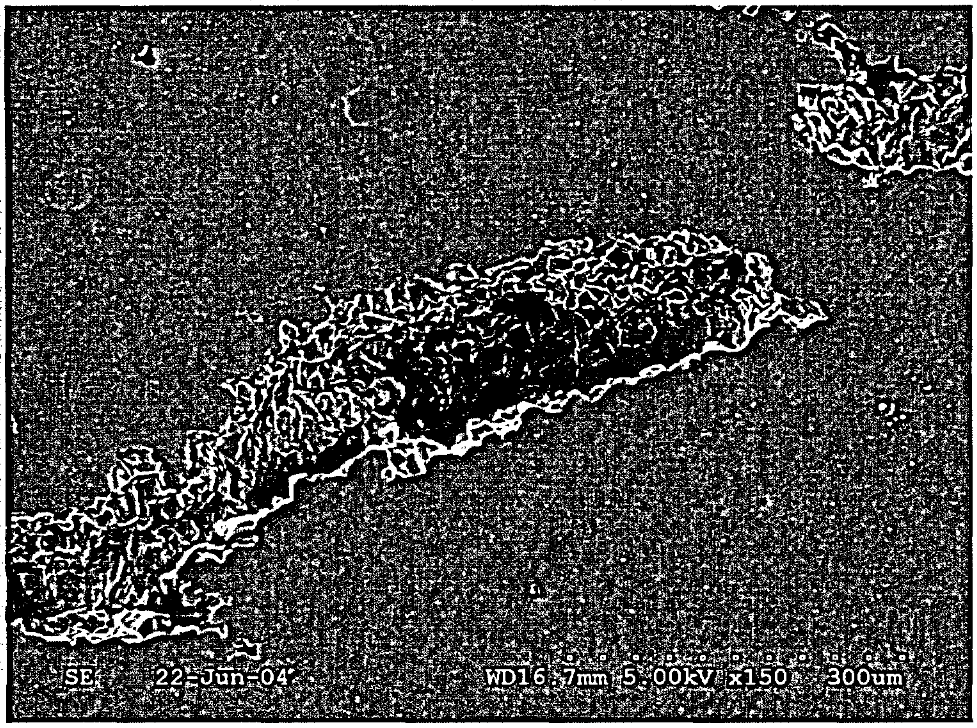

Figure 136: Area "A" in Figure 135. 146X

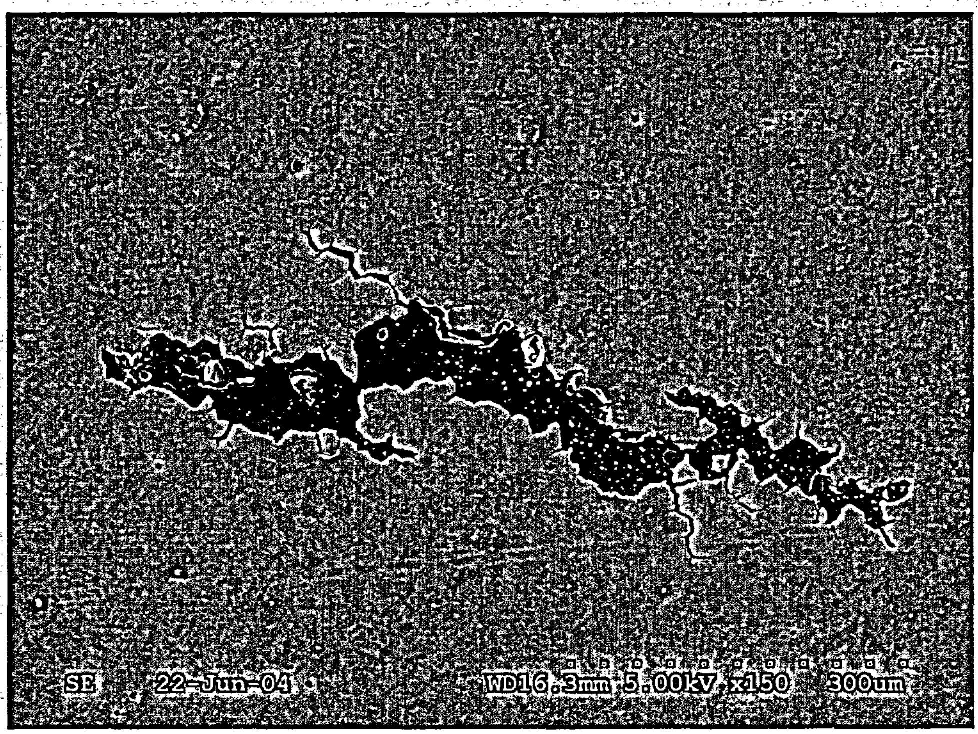

Figure 137: Area "B" in Figure 135. 146X

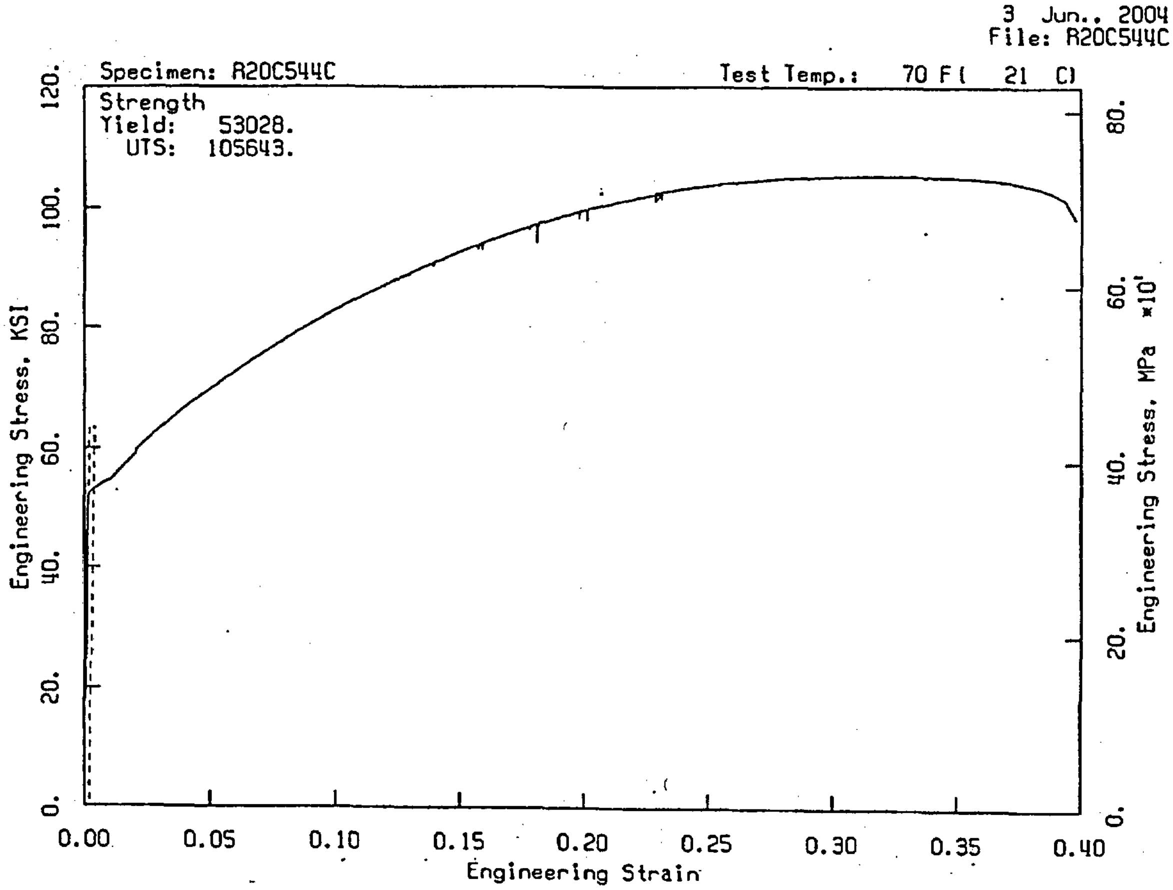

Figure 138: Engineering stress/strain curve for tensile specimen R20C54-4C

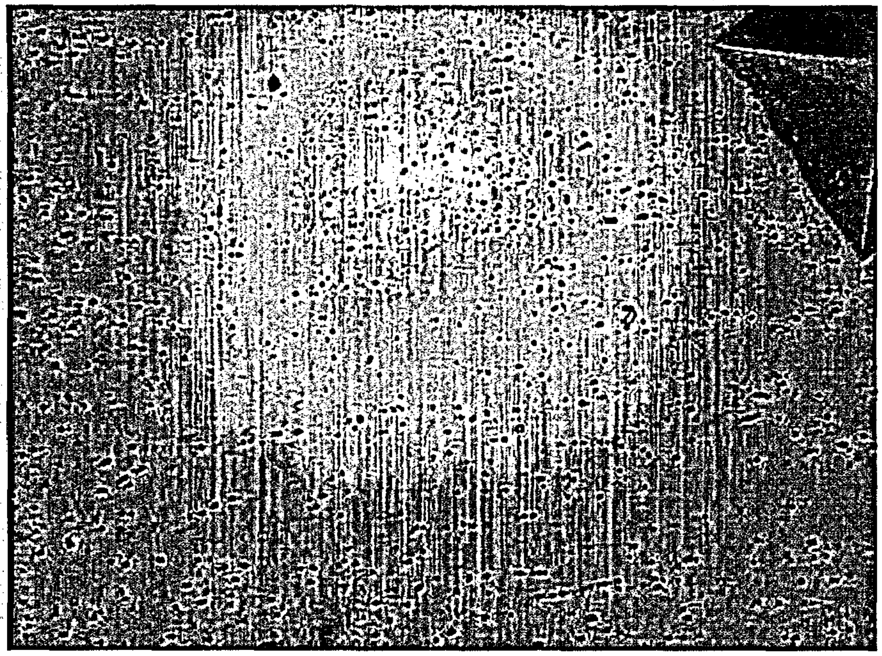

Figure 139: Typical carbide distribution in R20C54. 678X

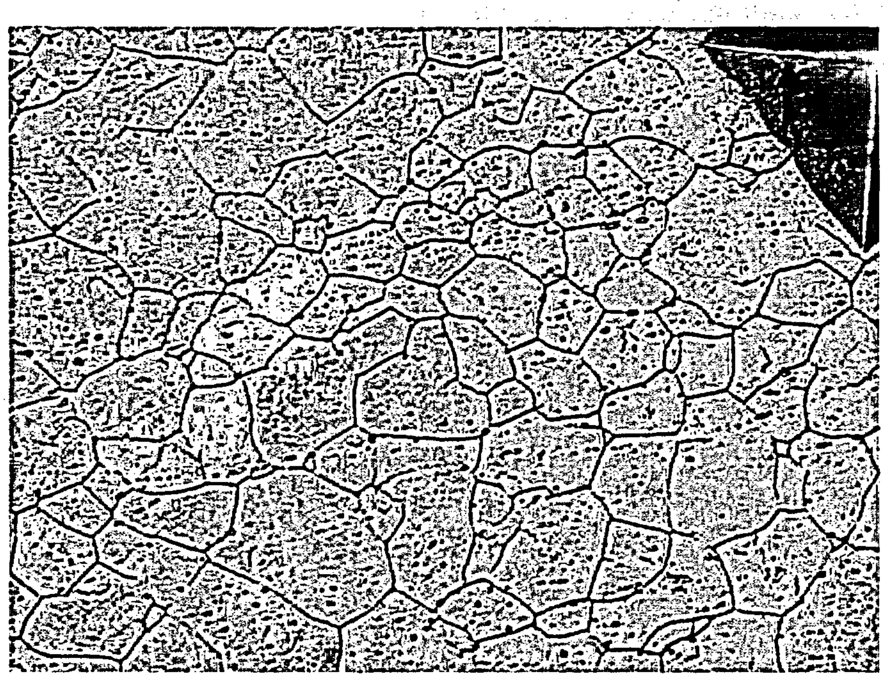

Figure 140: Typical microstructure in R20C54, corresponding to same area as Figure 80. 678X